
SLOVAK GEOLOGICAL MAGAZINE

VOLUME 9 NO 4

ISSN 1335-096X

1 C 66 b



Geological Survey of Slovak Republic, Bratislava
Dionýz Štúr Publishers

4/2003

SLOVAK GEOLOGICAL MAGAZINE

Periodical journal of Geological Survey of Slovak Republic is a quarterly presenting the results of investigation and researches in a wide range of topics:

- regional geology and geological maps
- lithology and stratigraphy
- petrology and mineralogy
- paleontology
- geochemistry and isotope geology
- geophysics and deep structure
- geology of deposits and metallogeny
- tectonics and structural geology
- hydrogeology and geothermal energy
- environmental geochemistry
- engineering geology and geotechnology
- geological factors of the environment
- petroarcheology

The journal is focused on problems of the Alpine-Carpathian region.

Editor in Chief

JOZEF HÓK

Editorial Board

INTERNAL MEMBER

Vladimír Bezák	Jaroslav Lexa
Miroslav Bielik	Karol Marsina
Dušan Bodiš	Ján Mello
Pavol Grecula	Jozef Michalík
Vladimír Hanzel	Milan Polák
Juraj Janočko	Michal Potfaj
Michal Kaličiak	Martin Radvanec
Michal Kováč	Dionýz Vass
Ján Kráľ	Anna Vozárová
	Ján Vlěko

EXTERNAL MEMBERS

Dimitros Papanikolaou	Athens
Franz Neubauer	Salzburg
Jan Veizer	Bochum
Franco Paolo Sassi	Padova
Niek Rengers	Enschede
Géza Császár	Budapest
Miloš Suk	Brno
Zdeněk Kukal	Praha
Vladica Cvetkovic	Beograd
Nestor Oszczypko	Kraków
Ján Pašava	Praha

Managing Editor: G. Šipošová

Technical Editor: G. Šipošová

Address of the publishers: Geological Survey of Slovak Republic, Mlynská dolina 1, 817 04 Bratislava, Slovakia

Printed at: ALFAPRINT Martin

Price of single issue: USD12

Ústredná geologická knižnica SR
ŠGÚDŠ

le the postage

7 04 Bratislava, SLOVAKIA

Annual subscription

© Geological Survey of Slovak Republic



3902001018503

457-

SLOVAK GEOLOGICAL MAGAZINE

VOLUME 9 NO 4

ISSN 1335-096X



Geological Survey of Slovak Republic, Bratislava
Dionýz Štúr Publishers

4/2003

Hydrothermal siderite – basemetals vein mineralization in the vicinity of Čavoj, Suchý Mts.

TOMÁŠ MIKUŠ¹, MARTIN CHOVAN², JAROSLAV PRŠEK² and TIBOR ŠLEPECKÝ³

¹Geological Institute, Slovak Academy of Sciences, Severná 5, 974 01 Banská Bystrica

²Dept. of Mineral. and Petrol., Faculty of Sciences, Comenius University, Mlynská dolina G, 842 15 Bratislava

³Progeo Ltd., Predmestská 25, 010 01 Žilina

Abstract. Detailed mineralogical and paragenetical research distinguished several stages of the hydrothermal mineralization at the Čavoj deposit. The first stage is Ni-Co assemblage in the siderite veins, with arsenopyrite, gersdorffite and NiAs₂ phase. The second is quartz-carbonate-sulphide stage with Ag-mineralization (silver, freibergite, Ag-tetrahedrite, pyrargyrite, argentite, polybasite). Tetrahedrite with high Ag content (up to 35 wt. %) is unique in the Tatric tectonic unit. The youngest stage is represented by barite mineralization with hematite.

Key words: Western Carpathians, siderite mineralization, Pb-Zn-Ag mineralization, freibergite, Ag-sulphosalts

Introduction

The first report about mining activities in the Čavoj is from years 1568–1569, however in the year 1589, mines were destroyed. Renewal of mining was in the first half of 17th century. According to archive reports in the year 1609, 60 tons of lead from Čavoj was exported to Silesia. In the year 1613 it was only 45 tons. During Rakoczy uprising, the mines were closed and since ninetieth years of 17th century the baron Schmidegg reopen mines. Čavoj and Valaská Belá mines were reopen in the 1724, but in the 1746 following bad results mining activities were stopped. Mining company from Banská Štiavnica repurchased Čavoj deposit in the 1783. However, the unprofitable exploitation was stopped in the 1795 (Holec, 1968). In period 1941–1944 were rejected 270 m in the Eleonora adit (Mikoláš et al., 1993).

Čillík & Polák in Slávik et al. (1967) described mineralization in the Čavoj. Ore mineralization occurs in tiny ore veins in the crystalline schists. Veins generally have direction SW-NE with steep dip to SE and thickness up to 2 m. Two generations of minerals were distinguished by Kantor (1977): older – quartz, calcite, barite, siderite and younger – galena, sphalerite, pyrite and arsenopyrite. Šlepecký et al. (1992) described from the Čavoj deposit gersdorffite and Ag minerals as: Ag-tetrahedrite, freibergite, argentite, polybasite, stephanite, pyrargyrite and native silver.

Variscan age of Pb-Zn mineralization supports lead isotopes investigations: 240–250 Ma (Kantor & Rybár, 1964) (sample of galena from Temeš), 240–270 Ma (Černyšev et al., 1984) (sample of galena from Čavoj - Mendel adit).

Sulphur isotopic composition of barite is $\delta^{34}\text{S} = +23.7\text{‰}$ (Kantor, 1977). Repčok et al. (1993) provided isotopic

analyses of oxygen and carbon in calcite (Čavoj, Baniská and Geschenk localities): $\delta^{13}\text{C}_{\text{PDB}}$ from -5.44 to -8.79‰ , $\delta^{18}\text{O}_{\text{SMOW}}$ from $+14.68$ to $+20.48\text{‰}$.

After expansive drill-hole prospecting, reserves were calculated and ores were classified to rank P1 and Z3 (Mikoláš et al., 1995).

Low attention of mineralogists was paid to mineralization at the Čavoj deposit. No publication in periodical mineralogical magazines was published up to this time; results of mineralogical – geochemical investigations could be found in manuscripts and proceedings. During our mineralogical study we have reconstructed development of mineralization and correctly determined minerals by microprobe analysis.

Methods of study

Samples for mineralogical study were taken from old dumps in the vicinity of Čavoj village. A Carl Zeiss Jena – Jenapol microscope was used for microscopic studies. Sulphides and sulphoarsenides were analysed by a wave-dispersion (WDS) electron microprobe and photographed by back-scattered electron (BSE) at Faculty of Natural Sciences, Comenius University Bratislava; using a JEOL JXA 840A probe under following conditions: 20kV, 15nA, beam diameter 2–5 μm , standards – arsenopyrite, pyrite, sphalerite, cinnabar, chalcopyrite, GaAs, Fe, Ni, Co, Sb, Cu, Cd, MnO.

Ag minerals and Ag-tetrahedrites were analysed in the Geologisk Institut University of Kobenhagen in Denmark; using a JEOL SUPERPROBE 733 probe under following conditions: 15kV, 10nA, beam diameter 5 μm , standards – Sb₂Se₃, Ag, Cu₃As₄ for Ag minerals and 20kV, 20nA, standards ZnS, HgS, Ag, CdS, Cu₃As₄, Cu₃SbS₄, CuFeS₂ for tetrahedrite.

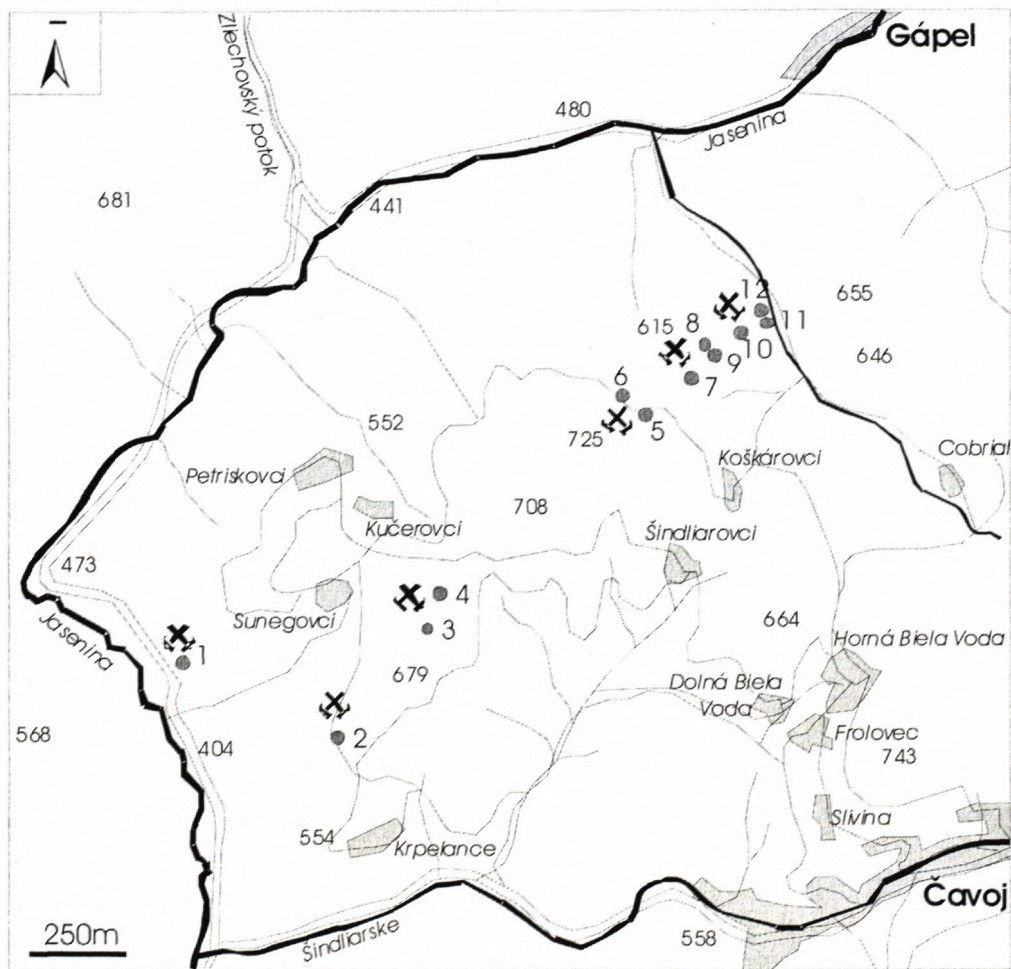
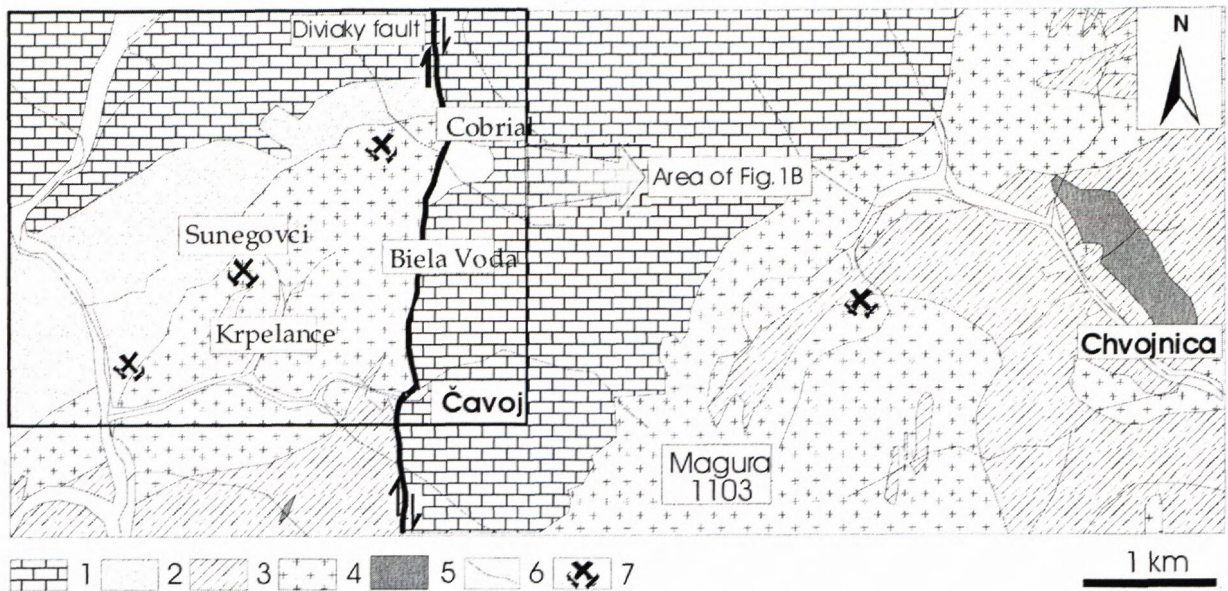


Fig. 1A: Schematic geological map of vicinity of Čavoj (according to Mahel', 1985). 1 - undivided Mesozoic (Křížna nappe and sedimentary Mesozoic cover), 2 - quartz biotitic paragneisses, 3 - ribbed migmatites and migmatized micaschists, 4 - leucocratic granites, biotitic granites, granodiorites and quartz diorites, 5 - amphibolites, 6 - quaternary delluvial and alluvial sediments, 7 - old mine entrances.

Fig. 1B: Schematic sketch of mining field between Čavoj and Gápel' with names of old adits and shafts: 1) Strieborná adit, 2) Alte adit, 3) Geschenk shaft, 4) Pingové pole field, 5) Ferdinand shaft, 6) Mendel adit, 7) Trojičná shaft, 8) Nepomuk adit, 9) Kormendi adit, 10) Jozef adit, 11) Eleonóra adit, 12) Kaiser adit.

Carbonates were analysed by an energy-dispersion (EDS) KEVEX at Geological Survey of Slovak Republic Bratislava, using a JEOL SUPERPROBE 733.

Geological settings and ore mineralization

The Pb-Zn-Ag deposit Čavojs is located in the Suchý Mts. The crystalline complexes of the Suchý Mts. are separated from Malá Magura Mts. by the Paleogene Diviaky fault (Fig. 1A). The crystalline core of the Suchý Mts. is mainly composed of granitoid rocks, paragneisses and migmatite complexes. The metamorphic rocks correspond to high-grade paragneisses. Granitic rocks (tonalites, granodiorites, granites) belong to the S-type group (Hovorka & Fejdi, 1983).

The age of granitoidic rocks from the Suchý and Malá Magura Mts. was determined by Rb-Sr isochron at 393 ± 6 Ma (Kráľ et al., 1987). Variscan tectonogenesis is dominant in both cores. The Alpine restructuring of the crystalline complex is relatively poor and did not change the older tectonic pattern substantially (Maheľ, 1985). P-T-X parameters of metamorphic processes indicate differences in their progressive and retrogressive metamorphic evolution in the crystalline cores of Suchý and Malá Magura Mts. The metamorphic temperatures and pressures are as follows: Suchý Mts: $540 - 560^\circ / 4 - 5$ Kbar, $X_{H_2O} = 0.6 - 0.8$, Malá Magura Mts: $620-640^\circ / 4.5 - 5.5$ Kbar, $X_{H_2O} = 0.8-1.0$ (Dyda, 1994).

Investigated hydrothermal siderite - basemetal (Pb-Zn-Ag) mineralization occurrences are situated 2 km NW and from the village Čavojs between settlements Krpeľanci, Sunegovci, Kučerovci, Šindliarovci and Koškároveci in the crystalline complex of the Suchý Mts (Fig. 1B). Mining field generally has direction NE-SW, length approximately 3.25 km and width in average about 50 m. It is situated in biotitic gneisses, paragneisses, granodiorites, granites, ribbed migmatites and migmatized paragneisses. Veins of pegmatites 50 cm thick are often situated in the migmatites. Samples were taken from old dumps shafts and adits Strieborná, Alte, Geschenk, Pingové pole, Ferdinand, Mendel, Trojičná, Jozef, Nepomuk, Eleonóra (Fig. 1B).

Mineralogy

Ore minerals

Acanthite is relatively rare on the Pingové pole locality. It forms anhedral grains and admixtures within galena large up to 0.05 mm in size (Fig. 2). Its characteristic feature is instability under the reflected polarised light (corrosion and colour changes). *Acanthite* is one of the youngest sulphide minerals at the deposit. WDS analyses are presented in Table 1 and in Fig. 3.

Arsenopyrite occurs commonly in the form of euhedral grains in large up to 1 mm in size or in form of impregnations in quartz I, mainly at the Jozef locality. It sometimes forms anhedral aggregates. *Arsenopyrite* occurs with pyrite I and pyrrhotite. Euhedral crystals are

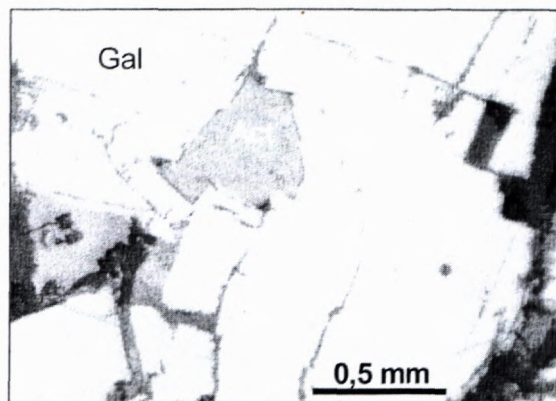


Fig. 2 Anhedral grains of acanthite (Act) up to 0.05 mm in galena (Gal). Reflected polarized light.

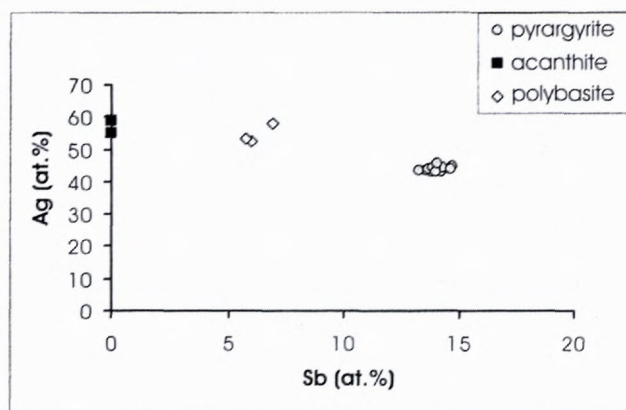


Fig. 3. The relationship between Ag and Sb content in the Ag sulphides and sulphosalts from the Čavojs deposit.

often crushed and cracks are filled by chalcopyrite, galena and sphalerite.

Bourbonite is rare at the Jozef and Eleonóra localities. *Bourbonite* forms anhedral aggregates up to 0.02 mm in size. At the Jozef locality, it occurs with arsenopyrite and replace chalcopyrite I. On the Eleonóra locality *bournonite* occurs with galena. *Bourbonite* was identify by microscopic study by its greyish white colour with a distinct blue tint and very rare was observed weak anisotropy on twin lamellae.

Galena is one of the major sulphide minerals at the Čavojs deposit. It is usually medium to fine-grained, rarely forms individual crystals up to 0.5 cm in diameter. *Galena* creates veins in the quartz and carbonates up to few cm in thick. It accompanies sphalerite. *Galena* replaces chalcopyrite and is replaced by tetrahedrite and pyrite II. The fissures are often filled by Ag-sulphosalts and sulphides (Fig. 2). Secondary minerals from the grain-margins and through fissures corrode galena.

Gersdorffite is very abundant at the Jozef locality. It forms aggregates of euhedral crystals or impregnations in the quartz I and in the siderite. It occurs with arsenopyrite and pyrite I, replacing these minerals. Other association is with tetrahedrite, chalcopyrite and sphalerite. *Gersdorffite* create atolls structures with galena and rarely forms ske-

leton aggregates (Fig. 4). Gersdorffite is heterogeneous and is oscillatory zoned (Fig. 5). Content of As and S is changing in the zones. The black zones have the highest content of S, while the lightest phase with diameter 10 μm (Fig. 6) correspond to NiAs_2 . It is possible that it is one of these minerals: *rammelsbergite*, *pararammelsbergite* or *krutovite*. WDS analyses are presented in Table 2 (Fig. 7).

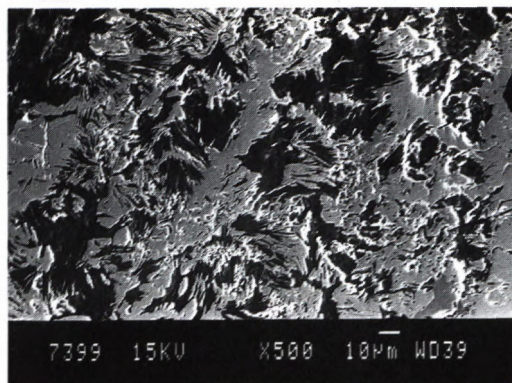


Fig. 4. Skeleton aggregates of gersdorffite. SEM-BEI.

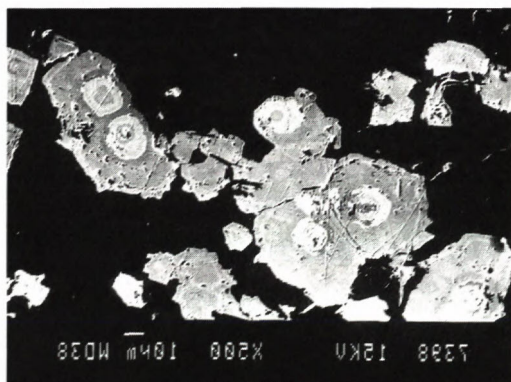


Fig. 5. Oscillatory zoned gersdorffite crystals with changing content of As and S. The black zones have the highest content of S, while the lightest zones have the highest As content. SEM-BEI.

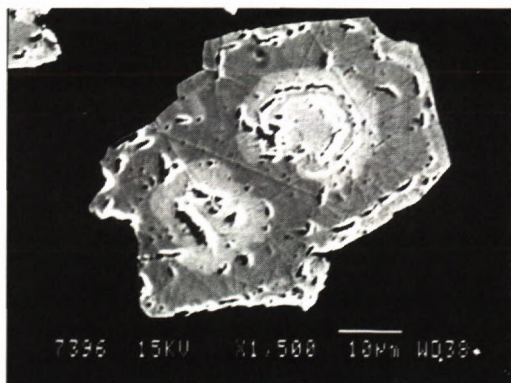


Fig. 6. Detailed view of gersdorffite grain. Darkest zones correspond to gersdorffite; white zones correspond to NiAs_2 phase. SEM-BEI.

Gold was found only exclusively at the Strieborná locality in the form of anhedral grain (0.0X mm) in the quartz vein. It occurs in the fragments of quartz, that cements veins of secondary Pb minerals in the galena. Its position within the succession scheme is uncertain.

Hematite is relatively rare and occurs at the Ferdinand locality in the barite. Hematite forms lamellar crystals up to 1 mm in size. It occurs in association with barite and replaces pyrite III and barite. The youngest mineral assemblage is consisting of hematite with barite and pyrite III. Hematite was identified by microscopic study. It has grey-white colour with a bluish tint and deep-red internal reflections.

Chalcopyrite is abundant at the all localities in the Čavoj deposit. It forms anhedral grains in two different associations and generations:

1. as inclusions in sphalerite up to 100 μm in size forming blebs, dots, minute particles and vermicular structures in intimate chalcopyrite-sphalerite intergrowth.

2. in association with carbonate, pyrite I, galena or tetrahedrite.

Veins of chalcopyrite penetrate tetrahedrite and sphalerite and replace galena from margins. Furthermore, chalcopyrite replaces gersdorffite.

Marcasite is relatively abundant at the locality Baniská in the quartz I in the form of lamellar crystals up to 2 mm in size. It occurs with pyrite I and is replaced by quartz II. Its relation to other ore minerals is unclear. Marcasite was identified by optical properties. It has yellowish white colour and strong white bireflectance with brownish tint. Its anisotropy is strong with blue and green-yellow colour.

Native silver occurs only exclusively at the localities Strieborná and Geschenk. It forms admixtures, inclusions and veins (up to 10 μm) in the galena. Its relation to other ore minerals is unclear. WDS analyses are given in Table 1.

Pyrrargyrite is abundant mineral at the localities in the Čavoj deposit. It forms dark-red anhedral aggregates (up to 0.5 cm) in the quartz and galena. Pyrrargyrite occurs with galena and tetrahedrite. Fissures in galena are often filled by pyrrargyrite (Fig. 8). Together with other Ag sulphosalts and sulphides, it is one of the youngest minerals at the deposit. WDS analyses are given in Table 3, and their plot in Fig. 3. In reflected polarized light it has bluish grey colour with strong anisotropy masked by intense carmine-red internal reflections.

Polybasite is rare and it forms anhedral grains and admixtures in the galena (up to 0.2 mm) (Fig. 9). Fissures in galena are filled by polybasite. WDS analyses are in Table 1 and their plot in Fig. 3. In reflected polarized light it has grey colour with a greenish tint. The anisotropy is very weak. A deep-red internal reflections are nearly always visible.

Pyrite is very abundant in silicified hydrothermal alteration zones in wallrock and also in hydrothermal veins. It forms euhedral crystals up to 3 mm in size. Pyrite occurs in several generations:

1. pyrite I forms euhedral grains and impregnations in the quartz and carbonates. Euhedral crystals are some-

Table 1. Representative electron microprobe analyses of ore minerals from the Čavoj deposit

	*	1	2	3	4	5	6	7
wt. %	Cu	0.57	2.53	0.03	1.63	0.01	0.01	
	S	16.43	18.11	13.49	15.26	0.47	0.01	
	As	0.10	0.02	-	-	0.07	0.01	
	Ag	81.22	79.12	0.01	70.74	95.59	102.5	
	Sb	0.01	0.01	0.01	8.56	0.01	0.01	
	Se	0.02	0.01	-	-	0.01	0.01	
	Fe	-	-	0.01	0.01	-	-	
	Pb	-	-	86.24	0.47	-	-	
Bi	-	-	0.01	0.01	-	-		
	Σ	98.36	99.80	99.80	96.12	96.68	96.16	102.6
at. %	Cu	0.70	2.97	0.06	2.16	2.08	0.02	0.02
	S	40.16	42.20	50.22	39.45	38.69	1.63	0.03
	As	0.10	0.02	-	-	-	0.10	0.01
	Ag	59.01	54.79	0.01	52.26	53.31	98.23	99.89
	Sb	0.01	0.01	0.01	6.01	5.76	0.01	0.01
	Se	0.02	0.01	-	-	-	0.01	0.04
	Fe	-	-	0.02	0.01	0.01	-	-
	Pb	-	-	49.68	0.09	0.18	-	-
Bi	-	-	0.01	0.00	0.00	-	-	

* 1, 2 – acanthite, 3 – galena, 4, 5 – polybasite, 6, 7 – native silver

Table 2. Representative electron microprobe analyses of gersdorffite (1-8) and NiAs₂ phase (9-15) from the Čavoj deposit.

Jozef adit															
wt. %	1	2	3	4	5	6	7	8	9	10	11	12	13	14	15
Ni	27.96	28.34	27.97	28.76	28.64	28.06	29.00	28.89	23.42	22.56	23.48	23.47	23.12	21.67	21.67
As	53.84	50.34	49.34	52.28	51.61	54.48	52.91	52.26	67.44	68.96	66.63	66.16	66.31	68.02	67.57
S	11.96	13.58	14.94	13.43	13.86	11.55	12.59	13.00	3.36	4.26	4.84	5.10	4.04	4.31	4.55
Co	2.85	3.05	3.17	3.33	3.32	2.87	2.91	2.90	3.10	3.44	3.51	3.51	3.69	3.53	3.53
Fe	2.21	2.77	2.41	2.60	2.59	2.22	2.13	2.12	1.33	1.74	1.77	1.77	1.60	1.72	1.72
Cu	0.15	0.56	0.56	0.46	0.46	0.15	0.25	0.25	0.10	0.30	0.08	0.08	0.09	0.14	0.14
Σ	98.97	98.65	98.39	100.87	100.47	99.32	99.79	99.41	98.74	101.26	100.32	100.09	98.86	99.40	99.18
at. %															
Ni	28.72	28.59	27.91	28.53	28.38	28.86	29.33	29.18	26.92	25.09	26.09	26.06	26.30	24.53	24.51
As	43.34	39.80	38.59	40.64	40.08	43.91	41.93	41.37	60.75	60.09	58.02	57.55	59.09	60.35	59.90
S	22.50	25.08	27.30	24.39	25.14	21.76	23.31	24.05	7.06	8.66	9.85	10.36	8.41	8.94	9.42
Co	2.92	3.07	3.15	3.30	3.28	2.94	2.94	2.92	3.55	3.81	3.89	3.88	4.18	3.98	3.98
Fe	2.39	2.94	2.53	2.72	2.70	2.40	2.27	2.25	1.61	2.04	2.07	2.07	1.92	2.05	2.05
Cu	0.14	0.52	0.52	0.42	0.42	0.14	0.23	0.23	0.11	0.30	0.08	0.08	0.10	0.15	0.15

Table 3. Representative electron microprobe analyses of pyrargyrite from the Čavoj deposit.

		Eleonóra adit		Strieborná adit		Eleonóra adit							
		1	2	3	4	5	6	7	8	9	10	11	12
wt. %	Cu	0.07	0.01	0.01	0.18	0.21	0.16	0.09	0.10	0.21	0.16	0.42	0.01
	S	17.58	17.77	16.97	16.90	17.11	16.77	17.21	16.29	17.73	16.79	17.87	16.49
	As	0.49	0.02	0.08	0.01	0.13	0.01	0.04	0.01	0.01	0.01	0.09	0.08
	Ag	60.59	59.70	60.61	60.68	60.20	60.93	61.28	60.71	60.17	60.09	61.39	62.45
	Sb	21.40	22.46	22.72	22.19	21.74	21.57	21.66	22.61	22.10	22.68	21.15	21.83
	Se	0.01	0.01	0.01	0.04	0.03	0.06	0.01	0.07	0.01	0.01	0.01	0.01
	Σ	100.15	99.98	100.4	100.0	99.41	99.51	100.25	99.79	100.23	99.82	100.29	100.87
at. %	Cu	0.09	0.01	0.01	0.22	0.26	0.20	0.11	0.12	0.25	0.20	0.51	0.01
	S	42.39	42.88	41.38	41.33	41.83	41.24	41.78	40.35	42.67	41.21	42.62	40.37
	As	0.51	0.02	0.08	0.01	0.14	0.01	0.04	0.01	0.01	0.09	0.07	0.08
	Ag	43.42	42.81	43.93	44.11	43.75	44.53	44.21	44.69	43.04	43.83	43.51	45.44
	Sb	13.59	14.27	14.59	14.29	14.00	13.97	13.85	14.75	14.01	14.66	13.28	14.07
	Se	0.01	0.01	0.01	0.04	0.03	0.06	0.01	0.07	0.01	0.01	0.01	0.01

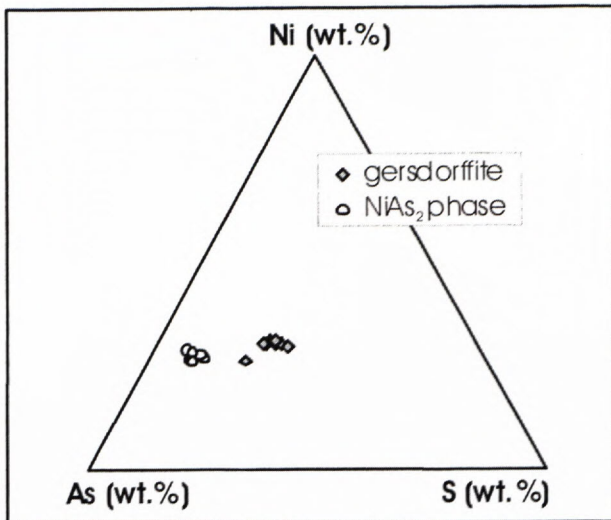


Fig. 7. The ternary diagram of WDS electron microanalyses of gersdorffite and NiAs₂ phase from Čavoj.

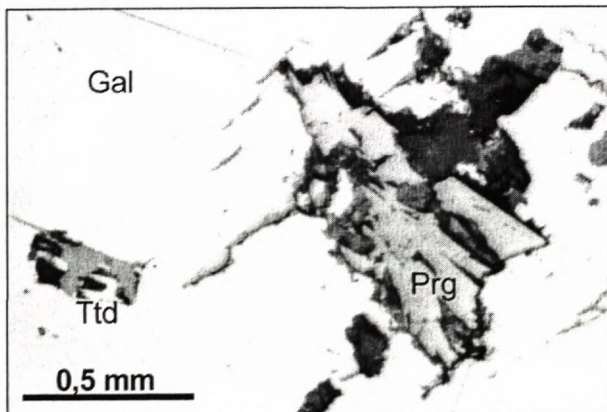


Fig. 8. Anhedral grain of pyrargyrite (Prg) and tetrahedrite (Ttd) in galena (Gal). Reflected polarized light.

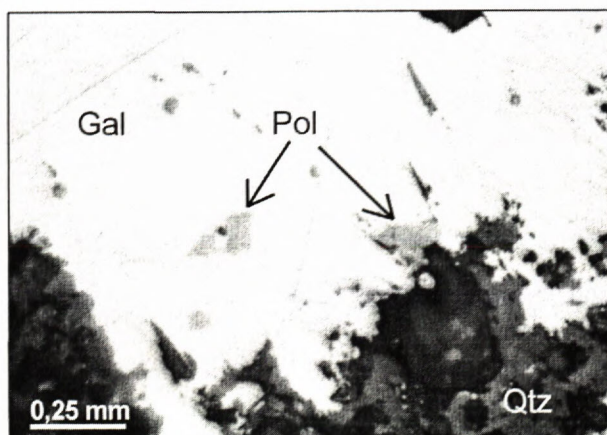


Fig. 9. Anhedral grains of polybasite (Pol) in galena (Gal). Reflected polarized light.

times crushed. Fissures are filled by secondary Fe-minerals. Pyrite I occurs in association with arsenopyrite, gersdorffite and marcasite. Sphalerite, galena and chalcopryrite intensive replace pyrite I from grain margins.

2. pyrite II occurs in form of tiny grains (up to 0.5 mm). Sphalerite, galena and chalcopryrite are replaced by pyrite II.

3. pyrite III is associated with barite and hematite.

Pyrrhotite was sporadically found at the Strieborná adit locality. Pyrrhotite forms anhedral grains in quartz I. It is replaced by galena and sphalerite. Pyrrhotite was identifying by microscopic properties: its colour is cream with a faint pinkish brown tint. It tarnishes slowly on air. Bireflectance is very distinct – brownish creamy. Anisotropy is very strong with yellow-grey, greenish grey or greyish blue colour.

Sphalerite is the prevailing ore mineral together with galena. It forms veins several cm thick, rarely 30 cm, in the quartz and carbonate at locality Eleonóra adit. In this locality, sphalerite occurs in two generations. The older sphalerite I has red-brown colour and is impregnated by pyrite. Younger sphalerite II is dark and it forms veins in the older one. Sphalerite II is enclosed by galena. Sphalerite is mostly replaced by galena and often contains chalcopryrite inclusions and admixtures. Sphalerite with „chalcopryrite disease” is enriched in Fe (3.59 wt. %, Table 4). Sphalerite is penetrated by chalcopryrite and tetrahedrite. Sphalerite is from the grain-margins and through fissures intensely corroded by secondary minerals. WDS analyses of sphalerite are given in Table 4.

Stephanite? occurs only rarely in the form of tiny, mostly anhedral grains in association with galena. It was identified only on the base of the optical properties: its colour is grey with pinkish tint. Bireflectance is weak, but distinct: grey with a brownish pink tint.

Tetrahedrite and Freibergite are relatively abundant in the all studied localities. Tetrahedrites from the Čavoj deposit have the high content of Ag (Fig. 10). Two types of „tetrahedrites” were distinguished. The 1st type - Ag-tetrahedrite contains 8.63-12.51 wt. % Ag (Table 5). The 2nd type - freibergite contains up to 35.52 wt. % Ag (Table 6). Both types occur with galena, sphalerite, chalcopryrite and Ag sulphosalts. Tetrahedrites are younger than sphalerite and galena. The contents of As and Sb range 0.44-2.94 wt. % and 24.05-26.96 wt. %, respectively. Relation Fe-Zn shows complementary substitution. In reflected polarized light they have grey colour, tetrahedrite with olive tint and freibergite with faint yellowish brown tint.

Gangue minerals

Barite forms veins, lenses and tabular crystals up to 4 cm in diameter. The colour of barite is white, pink and brownish. It occurs together with calcite, quartz III, hematite and pyrite III. Barite was identified on the base of the optical properties.

Carbonates are very abundant in the Čavoj deposit. Carbonate I - *siderite* (Fig. 11) occurs with quartz I, arsenopyrite, pyrite, and gersdorffite. Siderite replaces quartz I and it is heterogeneous. Carbonate II - *Fe-dolomite* (Fig. 11), occurs with carbonate III - *calcite* (Fig. 11). *Fe-dolomite* and *calcite* are associated with

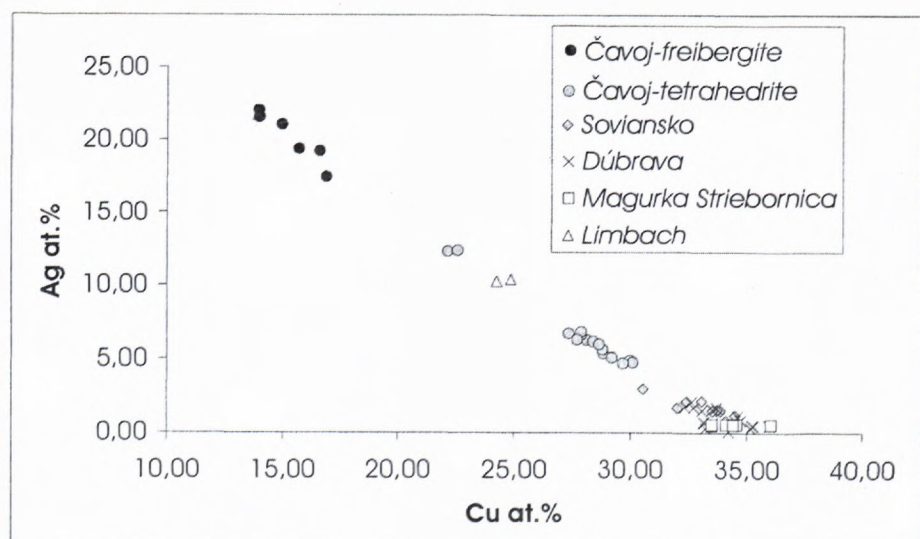
Table 4. Representative electron microprobe analyses of sphalerite from the Čavoj deposit.

Pingy shafts		Eleonóra adit							Alte adit			
		1	2	3	4	5	6	7	8	9	10	11
wt. %	Zn	63.20	68.96	69.36	67.80	64.71	65.27	63.81	68.13	66.96	66.73	66.85
	Cu	0.12	0.07	0.09	0.07	0.23	0.13	0.05	0.00	0.00	0.13	0.01
	Fe	3.59	0.82	0.68	0.51	0.75	0.88	0.72	1.48	1.47	1.42	1.49
	Mn	0.08	0.00	0.00	0.00	0.00	0.06	0.11	0.03	0.03	0.00	0.14
	Hg	0.10	0.17	0.00	0.16	0.03	0.00	0.04	0.04	0.04	0.05	0.18
	S	35.32	30.55	29.98	30.31	34.78	33.58	34.68	30.88	30.63	31.77	31.31
	Cd	0.46	0.20	0.11	0.19	0.14	0.21	0.16	0.15	0.14	0.23	0.22
	Σ	102.8	100.7	100.2	99.34	100.6	100.1	99.56	100.7	99.28	100.3	100.2
at. %	Zn	45.17	52.06	52.78	51.84	47.29	48.31	47.04	51.24	51.01	50.01	50.35
	Cu	0.09	0.06	0.07	0.06	0.17	0.10	0.04	0.00	0.00	0.10	0.01
	Fe	3.01	0.73	0.60	0.73	0.64	0.77	0.62	1.31	1.31	1.24	1.32
	Mn	0.07	0.00	0.00	0.00	0.00	0.06	0.09	0.03	0.03	0.00	0.12
	Hg	0.02	0.04	0.00	0.04	0.01	0.00	0.01	0.01	0.01	0.01	0.04
	S	51.46	47.02	46.51	47.25	51.82	50.68	52.13	47.35	47.57	48.53	48.06
	Cd	0.19	0.09	0.05	0.09	0.06	0.09	0.07	0.06	0.06	0.10	0.10

Table 5. Representative electron microprobe analyses of Ag-tetrahedrite from the Čavoj deposit.

Jozef adit													
		1	2	3	4	5	6	7	8	9	10	11	12
wt. %	Fe	3.42	3.65	3.41	3.85	3.28	3.73	3.39	3.26	3.58	3.59	3.55	3.41
	S	24.4	24.27	24.25	24.91	24.03	24.98	23.88	24.1	23.81	23.89	24.26	23.75
	Cu	31.18	30.36	30.09	32.3	29.97	32.32	30.2	30.78	32.14	32.29	32.04	30.42
	Sb	25.26	25.82	26.21	22.75	26.26	23.06	27.26	27.9	25.62	25.7	25.85	27.76
	As	2.34	1.3	1.29	4.14	1.25	3.8	0.33	0.18	1.59	1.61	1.75	0.08
	Cd	0.11	0.22	0.18	0.13	0.2	0.14	0.16	0.18	0.21	0.18	0.06	0.18
	Hg	0.01	0.05	0.27	0.01	0.01	0.01	0.47	0.01	0.01	0.06	0.2	0.01
	Bi	0.29	0.45	0.19	0.28	0.68	0.41	0.21	0.14	0.6	0.08	0.36	0.45
	Zn	3.68	3.8	3.76	3.46	3.85	3.65	3.68	3.87	3.62	3.62	3.69	3.76
	Ag	9.88	11.56	12.2	9.58	12.51	9.56	11.17	10.26	8.91	8.68	8.63	10.82
	Σ	100.72	101.48	101.84	101.42	102.04	101.66	100.56	100.67	100.09	99.7	100.39	100.64
	Fe	3.60	3.85	3.60	3.96	3.47	3.83	3.63	3.47	3.80	3.81	3.74	3.65
	S	44.72	44.55	44.55	44.64	44.29	44.72	44.50	44.67	44.02	44.14	44.52	44.33
	Cu	28.83	28.12	27.89	29.20	27.87	29.19	28.39	28.79	29.98	30.10	29.66	28.64

Fig.10. The relationship between Ag and Cu content in the tetrahedrites from Čavoj in comparison with Ag-tetrahedrites from the Tatric tectonic unit. Limbach - Andráš et al. (1990), Soviansko - Luptáková (1999), Dúbrava - Chovan et al. (1998), Magurka-Striebornica - Chovan et al. (1995).



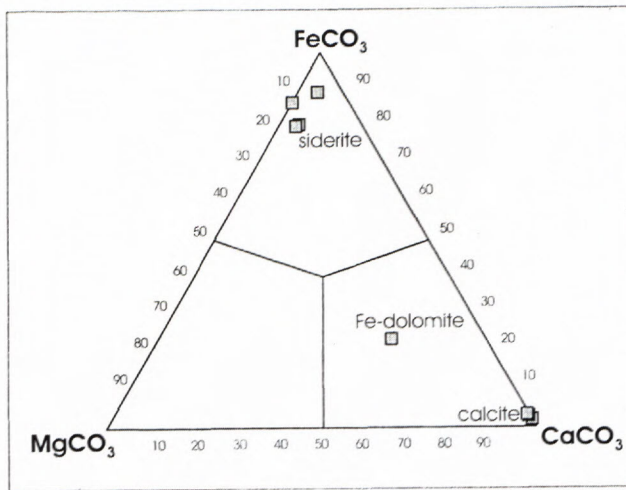


Fig. 11. The ternary diagram of EDS electron microprobe analyses of carbonates from the Čavoj deposit.

	I	II	III	IV
Stages	Quartz-siderite	Quartz-carbonate-sulphide	Barite	Secondary minerals
quartz	—	—	—	—
siderite	—	—	—	—
pyrite	—	—	—	—
arsenopyrite	—	—	—	—
gersdorffite	—	—	—	—
NiAs ₂	—	—	—	—
marcasite	—	—	—	—
pyrrhotite	—	—	—	—
Fe-dolomite	—	—	—	—
calcite	—	—	—	—
sphalerite	—	—	—	—
chalcopyrite	—	—	—	—
galena	—	—	—	—
tetrahedrite	—	—	—	—
freibergite	—	—	—	—
bourmonite	—	—	—	—
pyrargyrite	—	—	—	—
argentite	—	—	—	—
stephanite	—	—	—	—
polybasite	—	—	—	—
native silver	—	—	—	—
barite	—	—	—	—
hematite	—	—	—	—
Pb sec. min.	—	—	—	—
Cu sec. min.	—	—	—	—

Fig. 12. Paragenetic sequence of the Čavoj deposit.

quartz II, III and other younger sulphide minerals (sphalerite, galena, tetrahedrite, chalcopyrite and Ag-sulphosalts). Galena often fills cavities and fissures in *Fe-dolomite*. *Fe-dolomite* and *calcite* are homogeneous. The chemical composition of carbonates is listed in Table 7.

Quartz is prevailing gangue mineral in the Čavoj. It occurs in three generations. Quartz I occurs with arsenopyrite, pyrite I, gersdorffite, pyrrhotite and marcasite. It is usually white, mainly massive. Quartz I is replaced by carbonates. Quartz II is milky-white, coarse-grained to massive. It is associated with carbonates II and III and intensely replaces quartz I. It occurs together with sphalerite, galena and Ag-sulphosalts. Quartz III occurs together with barite, calcite, hematite and pyrite III.

Development of mineralization

The following mineralization stages were distinguished at localities with base-metal mineralization in the vicinity of Čavoj (Fig. 12). The first mineral assemblage forms veins few cm thick in hydrothermally altered rocks. Siderite is prevailing gangue mineral; quartz is less common. Aggregates of arsenopyrite and pyrite are often. Ni-Co minerals are close with siderite. Other minerals are relatively rare.

The second mineral assemblage forms veins up to 30 cm, composed of milky-quartz and carbonates with sphalerite and galena. Ag-minerals are accompanied by galena. Sphalerite locally forms accumulations up to 25 cm in size.

The third mineral assemblage forms veins up to 10 cm in size.

Discussion

We consider mineralization at the Čavoj locality as carbonate-sulphide, which belongs to the siderite type of mineralization. This type is described from many localities in Tatric, Veporic and Gemeric tectonic Units of Western Carpathians.

Development of mineralization is similar to that in Spišsko Gemerské Rudohorie Mts. (Varček, 1976; Grecula (ed.), 1995), and Nízke Tatry Mts. (Ozdín & Chovan, 1999; Pršek & Chovan, 2001).

Siderite is one from the oldest minerals. Its chemical composition is characteristic by low content of Mg, whereas Ca and mainly Mn contents are increased. High content of Mn is characteristic also for siderite from Bacúch locality (Veporic Unit) (Pršek & Chovan, 2001).

As-Ni mineralization is younger than siderite. Main mineral is gersdorffite, which proceeded sometimes to Ni diarsenides similarly at another occurrences of siderite mineralization in Western Carpathians (Halahyová-Andrusovová, 1972; Chovan et al., (eds.) 1994; Ozdín & Chovan, 1999 and others).

Quartz-carbonate-sulphide mineralization is younger than siderite; carbonate is mainly represented by *Fe-dolomite* and *calcite*. Galena prevails over sphalerite and tetrahedrite in sulphide mineral assemblage. In that case, with these amounts of specific sulphide minerals, mineralization at the Čavoj locality could be compared with Bruchatý grúnik occurrence (Ozdín & Chovan, 1999) or Soviánsko deposit (Luptáková et al., 2001). However, chalcopyrite or tetrahedrite prevails; galena is rare in Spišsko-Gemerské Rudohorie Mts. (Grecula (ed.), 1995). Chalcopyrite prevails and galena is abundant at the Bacúch locality in Northern Veporic (Pršek & Chovan, 2001). Tetrahedrite and chalcopyrite prevail; galena is presented rarely in the Vyšná Boca area (Ozdín & Chovan, 1999).

Barite, as a youngest mineral is usually presented at the prevalence of localities of siderite mineralization.

Occurrence of freibergite, Ag-tetrahedrite and other Ag sulphosalts is characteristic for Čavoj locality. Silver minerals in abundant amounts were not found at any other

locality of siderite mineralization in Western Carpathians. Tetrahedrite with $Ag \geq 4$ in the M^+ position in the tetrahedrite formula $M^{2+}_2M^{3+}_{10}M^{3+}_4S_{13}$ is considered to freibergite (Mozgova & Tsepin, 1983). Freibergite from Čavojs has more than 5 apfu of Ag. Silver rich tetrahedrite occurs on several other localities in the crystalline basement at the Western Carpathians. Tetrahedrite from the Bruchatý grúnik (Nízke Tatry Mts.) locality has content up to 7.79 wt. % Ag (Ozdín & Chovan, 1999). Tetrahedrite contains 5.65 wt. % Ag in the Jasenie-Soviánsko (Luptáková, 1999), locally freibergite was observed with more than 31 wt. % (Pršek unpublished data). Ag-tetrahedrite with 17.98 wt. % Ag occurs together with electrum, polybasite, galena and sphalerite in the Pezinok – Staré mesto (Andráš et al., 1990). Furthermore, freibergite containing up to 26 wt. % of Ag and Ag-tetrahedrite containing up to 5 wt. % was observed together with stephanite and argentite near Margecany village in the Veporic Unit (Baláž, 1992).

Ag-sulphosalts are in the Tatric relatively rare; from the base-metals mineralization Pod Babou (Malé Karpaty Mts.) are mentioned Ag-Pb-Sb sulphosalts by Cambel (1959). Polybasite occurs at the locality Pezinok-Staré mesto (Malé Karpaty Mts.) (Andráš et al., 1990). Complex Ag-Bi-Pb sulphosalts are presented at several localities of siderite mineralization. Lillianite homologues are presented in Bacúch (Pršek & Chovan, 2001) and Bruchatý grúnik, pavonite homologues in Vyšná Boca (Ozdín & Chovan, 1999).

Silver free sulphosalts are rarely present in Čavojs locality and are represented by bournonite only. Association of bournonite with galena is characteristic. On the other side, Bi (Pb, Cu) sulphosalts are typical for sulphide mineralization at the siderite veins; bournonite and other Sb (Pb, Cu) sulphosalts are rare.

Conclusions

We consider mineralization at the Čavojs locality as carbonate-sulphide, which belongs to the siderite type of mineralization.

Chemical composition of siderite is characteristic by low content of Mg, and increased Ca and Mn contents. As, Ni and quartz-carbonate-sulphide assemblages are present, galena prevails over other sulphides.

Occurrence of freibergite, Ag-tetrahedrite and other Ag sulphosalts is characteristic for Čavojs locality. Silver minerals in abundant amounts were not found at any other locality of siderite mineralization in Western Carpathians. Freibergite from Čavojs has more than 5 apfu of Ag and Ag tetrahedrite has approximately 10 wt.% of Ag.

Acknowledgements

We thank J. Krištín for provided unpublished analyses of freibergite. The work was financed from grant project VEGA No. 1/8318/01. We thank Dr. Milan Háber and Doc. Vratislav Hurai for their critical comments, which helped to improve the paper.

References

- Andráš, P., Jeleň, S. & Caňo, F., 1990: Paragenetic relations between gold-quartz ore mineralization and antimonite ores of the Pezinok deposit, Western Slovakia. *Mineralia Slovaca*, 22, 429-435 (in Slovak).
- Baláž, B., 1992: Ag-mineralization in Čierna hora in Margecany area. In: *Ag associations in Czechoslovakia*, *Donovaly*. DT Ústí nad Labem, ČSVTS, 1-6 (in Slovak).
- Cambel, B., 1959: Hydrothermal deposits in the Malé Karpaty Mts., mineralogy and geochemistry of their ores. *Acta geol. geogr. Univ. Comen.* 3, 338. (In Slovak).
- Chovan, M., Háber, M., Jeleň, S. & Rojkovič, I. (eds) 1994: Ore textures in the Western Carpathians. *Slovak Academic Press*, 219p.
- Chovan, M., Majzlan, J., Ragan, M., Šiman, P. & Krištín, J., 1998: Pb-Sb and Bi-Sb-Bi sulfosalts and associated sulphides from Dúbrava antimony deposit, Nízke Tatry Mts. *Acta Geol. UC*, 53, 37-49.
- Chovan, M., Póč, I., Jancsy, P., Majzlan, J. & Krištín, J., 1995: Ore mineralization Sb-Au (As-Pb) at the Magurka deposit, Nízke Tatry Mts. *Mineralia Slovaca*, 27, 397-406 (In Slovak)
- Černyšev, I., Cambel, B., Koděra, M., 1984: Lead isotopes in galenas of the Western Carpathians. *Geol. Zbor. Geol. Carpath.* 35, 3, 307-327.
- Dyda, M., 1994: Geothermobarometric characteristics of some Tatric crystalline basement units (Western Carpathians). *Mitt. Österr. Ges.*, 86, 45-59.
- Grecula, P. (ed.) 1995: Mineral deposits of the Slovak Ore Mountains Volume 1. *Geocomplex*, Bratislava, 834p.
- Halahyová-Andrusovová, G., 1972: Reflectivity of gersdorffite from Dobšiná. *Geol. Zbor. Geol. Carpath.* 23,1, 55-68.
- Holec, G., 1968: Report about literary-historic research of the ore-mining in the Upper Nitra. *MS, Banský výskumný ústav, Prievidza*, 47 (in Slovak).
- Hovorka, D. & Fejdi, P., 1983: Garnets of peraluminous granites of the Suchý and Malá Magura Mts. (the Western Carpathians) - their origin and petrological significance. *Geol. Zbor. Geol. Carpath.*, 34, 1, 103-115.
- Kantor, J. & Rybár, M., 1964: Isotopes of ore - lead from several deposits of West Carpathian crystalline. *Geol. Sbor. Slov. Akad. Vied*, 15, 2, 285-297.
- Kantor, J., 1977: Isotopes of sulphur on the barite deposits of the Western Carpathians. *MS, Geofond*, Bratislava, 72.
- Kráľ, J., Goltzman, Y. & Petrík, I., 1987: Rb-Sr whole rock isochron data of granitic rocks from the Strážovské vrchy Mts.: the preliminary report. *Geol. Zbor. Geol. carpath.*, 38, 171-179.
- Luptáková, J., 1999: Pb, Zn, Cu, Sb hydrothermal mineralization at the locality Jasenie-Soviánsko (Nízke Tatry Mts.). *Unpublished diploma thesis, PriFUK*, Bratislava, 1-74 (in Slovak).
- Luptáková, J., Chovan, M. & Huraiová, M., 2001: The base metal deposit of Jasenie-Soviánsko (Nízke Tatry Mts., Slovakia): A fluid inclusion study. In: *Mineral Deposits at the beginning of the 21st Century*. Piestryňský et al (eds), *Balkema*, Netherlands, 297-298.
- Mahel, M., 1985: Geological building of the Strážovské vrchy Mts. *GÚDŠ Bratislava*, 221 (in Slovak).
- Mikoláš, S., Šlepecký, T., Sandanus, M., Komora, J. & Januš J., 1993: Malá Magura and Suchý Mts, Au -W prognoses source of mineral raw materials. *MS, Geofond*, Bratislava, 1-365 (in Slovak).
- Mikoláš, S., Komora, J., Kandra, K., Sandanus, M., Šlepecký, T., Januš, J., Staňa, Š., Očenáš, D. & Stupák, J., 1995: Čavojs – Gápeľ – Ag, Pb, Zn ores – VP, *MS, Progeo*, Žilina, 114 (in Slovak).
- Mozgova, N. N. & Tsepin, A. I., 1983: Fahlores (Peculiarity of the chemical compositions and properties). *Moscow, Nauka*, 280p. (In Russian).
- Ozdín, D. & Chovan, M., 1999: New mineralogical and paragenetic knowledge about siderite veins in the vicinity of Vyšná Boca, Nízke Tatry Mts. *Slovak Geological Magazine*, 5, 4, 255-271.
- Pršek, J. & Chovan, M., 2001: Hydrothermal Carbonate and Sulphide Mineralization in the Late Paleozoic Phyllites (Bacúch, Nízke Tatry Mts.). *Geolines* 13, 27-34.

- Repčok, I., Ferenčíková, E., Eliáš, K., Rúčka, I., Kovářová, A., Sládková, M. & Wiegerová, V., 1993: Isotope and thermometric study of Pb-Zn mineralization in the surrounding of Čavoj locality. *Mineralia Slovaca*, 25, 362-364 (in Slovak).
- Slávik, J. & (EDS.) 1967: Raw materials of Slovakia. *SVTL*, Bratislava, 510 (in Slovak).
- Šlepecký, T., Sandanus, M. & Krištín, J., 1992: Pb-Zn-Ag mineralization in the Čavoj-Gápeľ in the crystalline of Suchý Mts. *Ag associations in Czechoslovakia, Donovaly*. DT Ústí nad Labem, ČSVTS, 149-157 (in Slovak).
- Varček, C., 1976: Main lines of metalogenetic development of the Spišsko-gemerské rudohorie Mts.. In: *Geológia, metalogenéza a prognózy surovín SGR*. *Zborník referátov*, Košice, 163p.

Zoned clinopyroxenes from Miocene basanite, Banská Štiavnica – Kalvária (Central Slovakia): Indicators of complex magma evolution

VIERA KOLLÁROVÁ¹ and PETER IVAN²

¹Geological Survey of Slovak Republic, Mlynská dolina 1, 814 07 Bratislava, Slovak Republic

²Comenius University, Department of Geochemistry, Mlynská dolina G, 842 15 Bratislava, Slovak Republic

Abstract. The basanite neck Banská Štiavnica - Kalvária (7.29 ± 0.41 Ma) belongs to the oldest alkaline basalt eruptive centres from the inner side of the Western Carpathians. This basanite has porphyric texture with olivine, clinopyroxene and plagioclase phenocrysts. Zonation is the characteristic feature of clinopyroxenes. There are some kinds of the zonation: core (centre) - mantle - rim, concentric, sector and oscillatory zoning. Ti-diopsides and Ti-augites of sandy and dark brown color, which constitute centres, mantles and rims of phenocrysts, come from alkaline basalt magma which was not differentiated to the high degree. The variability of Ti and Al contents suggests polybaric crystallization - inner parts of clinopyroxenes with lower Ti contents formed at higher pressures than rim parts with higher Ti contents. The oscillatory zoning of these pyroxenes can reflect changing conditions in the melt. The core corresponding to Cr-augite was found in one of the samples. This Cr-augite can represent fragments of the upper mantle wall rocks which were caught by ascending basaltic magma. The green cores of type I. (ferrian aluminian diopsides and augites) originated in a melt or they come from the vein fillings in the upper mantle. Their origin from the magma melt could be suggested from the zoning and subhedral shape of some cores. Mg-number and variability of the chemical composition of these cores can reflect more differentiated magmas with a variable degree of differentiation. Their origin as fillings of the upper mantle vein systems could be suggested by the cores with shapes resembling fragments. The higher Al^{VI}/Al^{IV} ratios comparable with those of clinopyroxene mantles suggest crystallization of these cores at relatively high pressure. Strongly resorbed cores of type II. (Fe-rich diopsides and augites) are probably xenocrysts which come from the upper mantle metasomatized by rising melts and fluids. It is also possible that some cores of this type originated in more differentiated magma (e. g. zoned subhedral core). Studied clinopyroxenes show the complexity of processes which accompany alkaline basalt magma evolution and its interaction with the subcontinental mantle.

Key words: alkaline basalts, zoned clinopyroxenes

Introduction

Alkaline basalts are an important source of the information about the upper mantle but also about lower parts of the Earth's crust. These information we can obtain, when we study these rocks, because they originate by partial melting of the upper mantle materials and because of their rapid rise from the asthenospheric depths they are little contaminated or almost not contaminated by the crustal material. They contain xenoliths which represent fragments of wall rock material taken to the surface by the magma.

Pyroxenes, the common minerals in basalts, are the worthy source of information about the evolution of alkaline basalt magma to their ascent up to the surface, about its interaction with mantle, respectively crustal wall rock material and the other magmatic melts. Their wide compositional variability is influenced not only by the composition of the material (magma) which they originated from, but also by P, T conditions of their origin.

Clinopyroxenes in Miocene-Quaternary alkaline basalts from the Western Carpathians were more detaily

studied only in one of two regions of alkaline basalt occurrence, in Novohrad (Nógrád) region, which lies at the boundary between Slovakia and Hungary (Dobosi, 1989; Dobosi and Fodor, 1992; Dobosi and Jenner, 1999). The aim of this work is the similar study in the second area, Central Slovak volcanic field, more exactly at the locality Banská Štiavnica - Kalvária.

Geology

The locality Banská Štiavnica - Kalvária (Fig. 1) is one of the several occurrences of alkaline basalts in the Štiavnické vrchy Mts. area. It represents the lava neck formed by nepheline basanite in the surrounding of amphibole-biotite andesite. This neck represented conduit of probably smaller explosive-effusive volcano which was successively eroded (Konečný et al., 1998).

Radiometric age of basanite 7.29 ± 0.41 Ma (Balogh et al., 1981) corresponds to the Upper Miocene (Pontian) and to the oldest stage of alkaline volcanic activity in the inner side of the Western Carpathians.

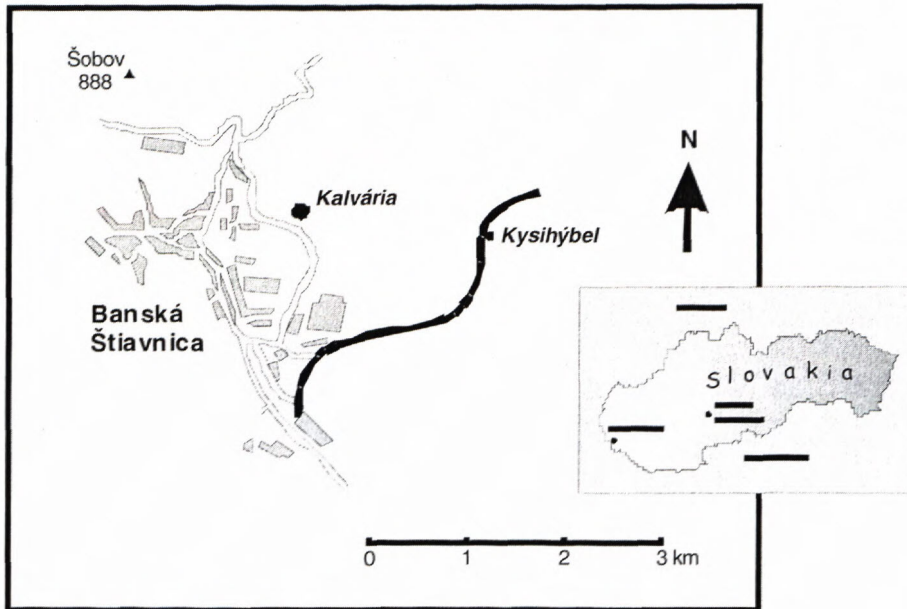


Fig. 1 Two occurrences of alkaline basalt (Kalvária and Kysihýbel) near Banská Štiavnica city

Petrography and mineralogy

The *basanite* from Banská Štiavnica, the locality Kalvária, forms more petrographic types. It has porphyric holocrystalline, more rarely hemicrystalline texture with omnidirectional, ophitic or trachytic groundmass (Fig. 2). Phenocrysts are represented by olivine, clinopyroxene and plagioclase. The matrix consists of these minerals, Ti-magnetite, nepheline, apatite and respectively, of glass (Šímová, 1965).

Olivines are euhedral to anhedral; phenocrysts often have large size (also some mm). They are also present in the groundmass. Starting alteration (e. g. iddingsitization) follows cracks. Olivines contain inclusions of Cr-spinel. They are often zoned, the zonation is visible also optically. Their composition is approximately Fo_{80-88} (central parts) and Fo_{73-77} (rims). According this composition, these olivines are phenocrysts which have crystallized from basalt magma.

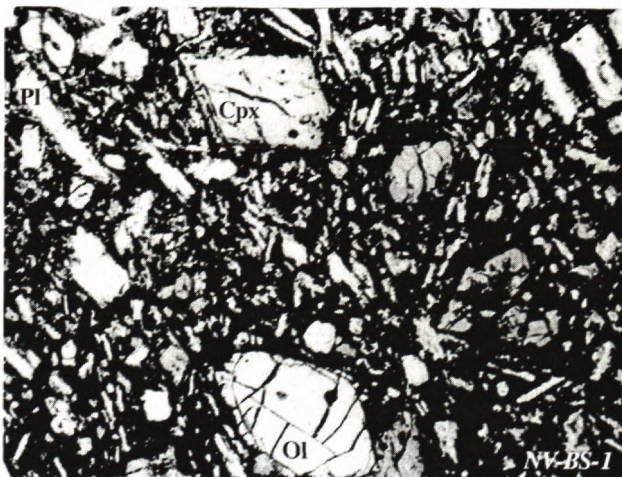


Fig. 2 Alkaline basalt from Banská Štiavnica – Kalvária. Plane-polarized light, magnification 27x. Ol – olivine, Cpx – clinopyroxene, Pl – plagioclase

Clinopyroxenes form euhedral to anhedral phenocrysts and groundmass grains. Phenocrysts are relatively often rounded and embayed. Clinopyroxenes are typically zoned (core, mantle and rim zone, concentric, sector and oscillatory zoning).

Plagioclases form tables and laths, predominantly in the groundmass. They are omnidirectional, ophitic or fluidal. They are characteristically twinned. Phenocrysts are generally non-zoned or weakly zoned with composition An_{74-84} (Balogh et al., 1981). Analyzed plagioclase xenocryst probably of the crustal origin has the inner part of An_{43} composition. It is rimmed by the another plagioclase with An_{69} .

Inner parts of some clinopyroxene crystals are to the various scale replaced by *secondary carbonates* (photo 3, 4, 5, 7). Secondary carbonates with zeolites also fill interstices in the rock.

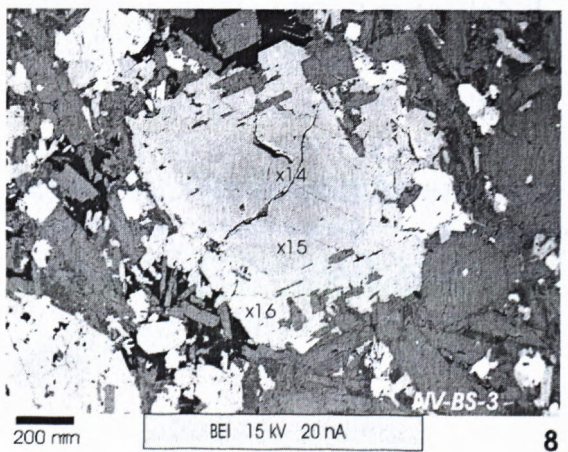
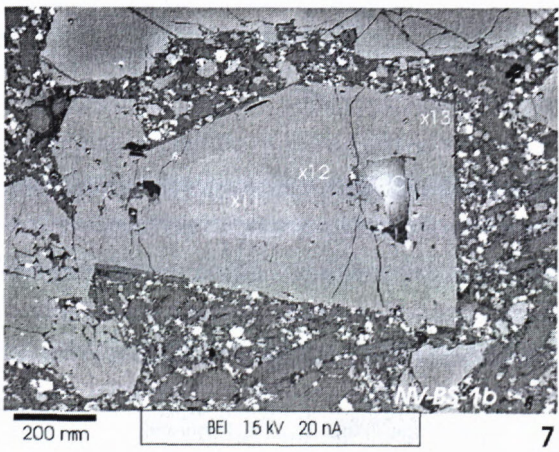
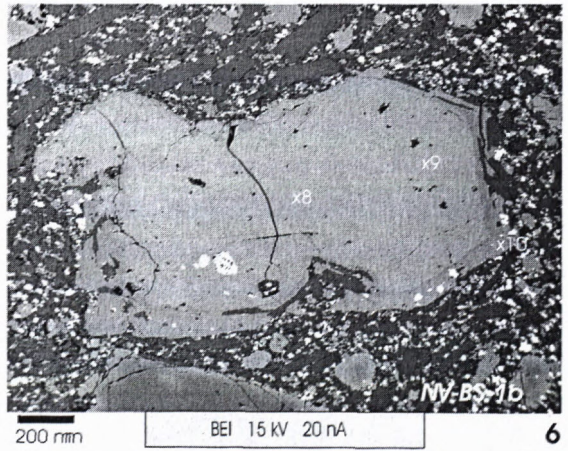
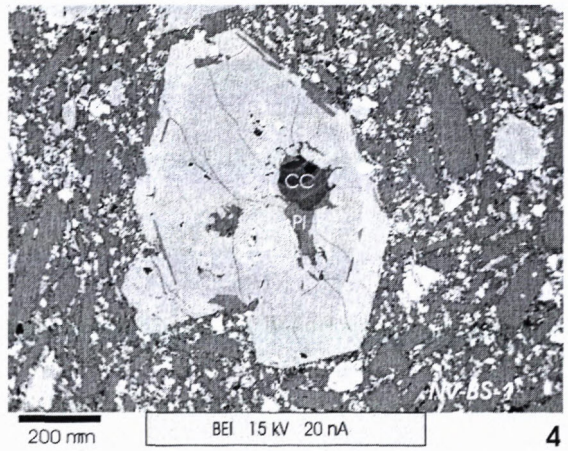
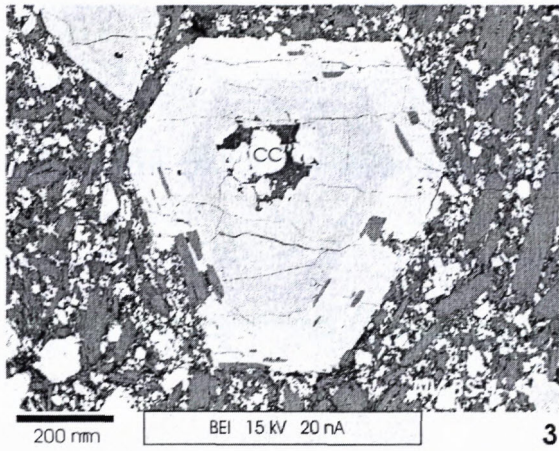
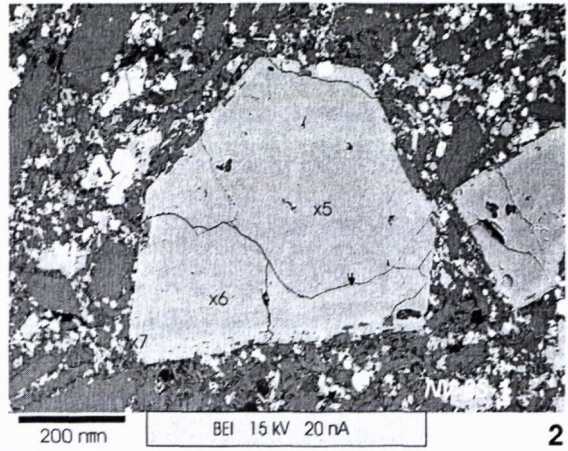
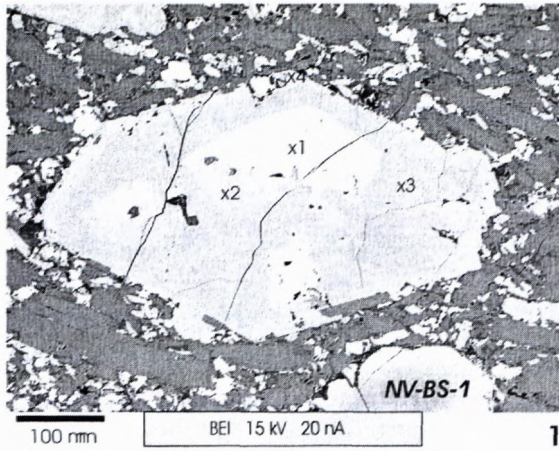
Geochemistry

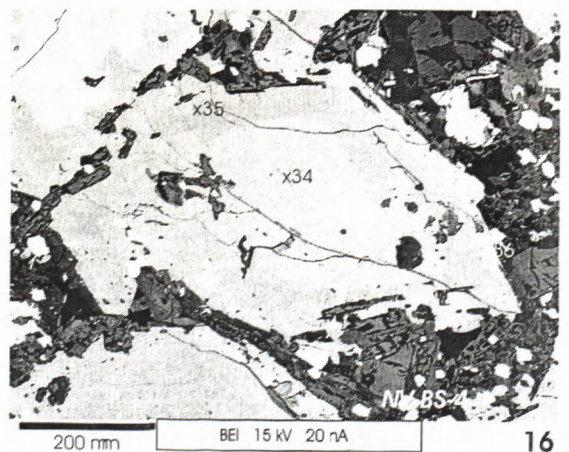
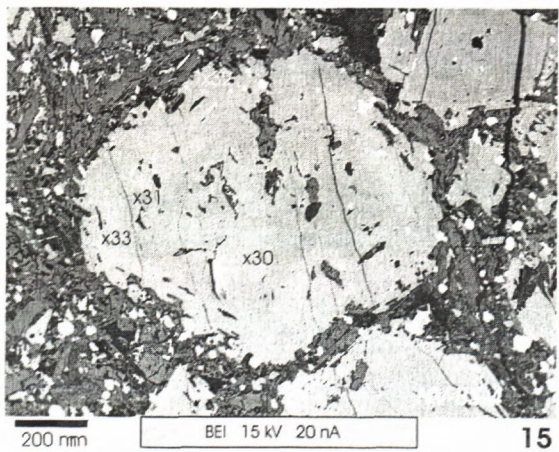
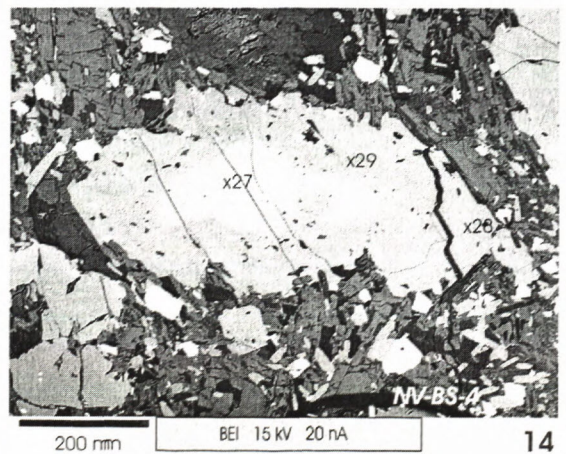
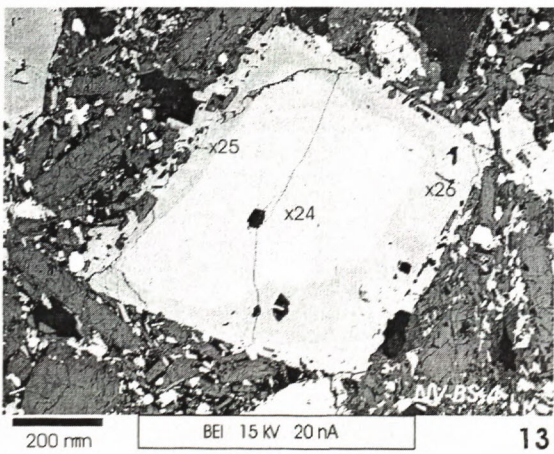
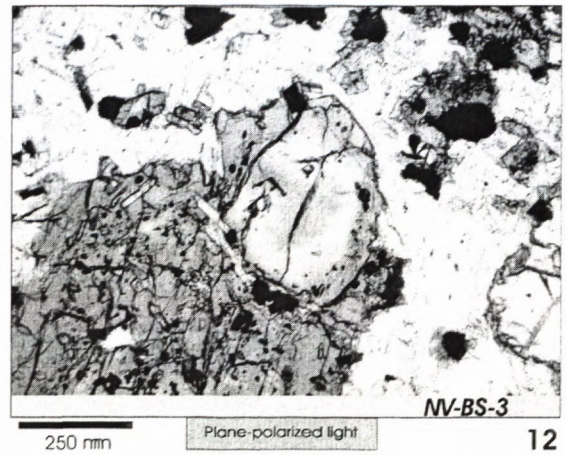
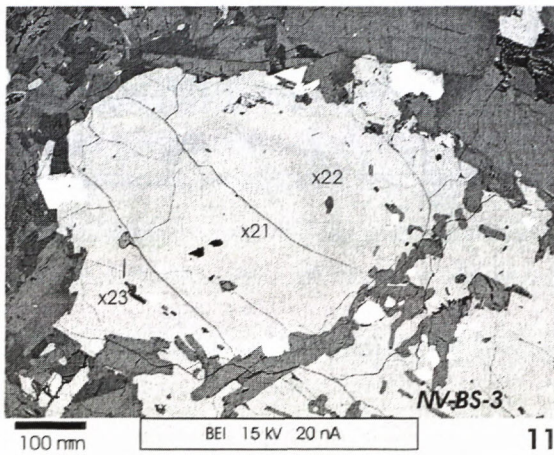
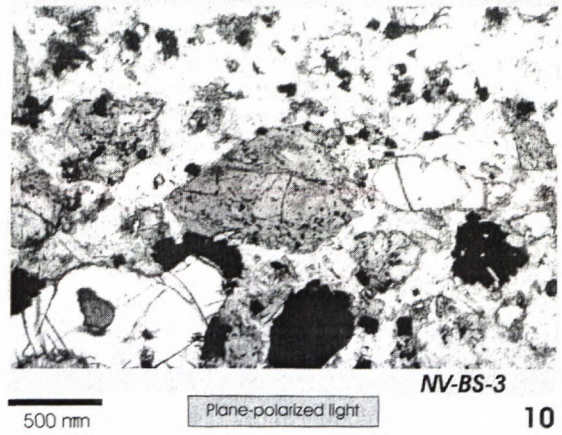
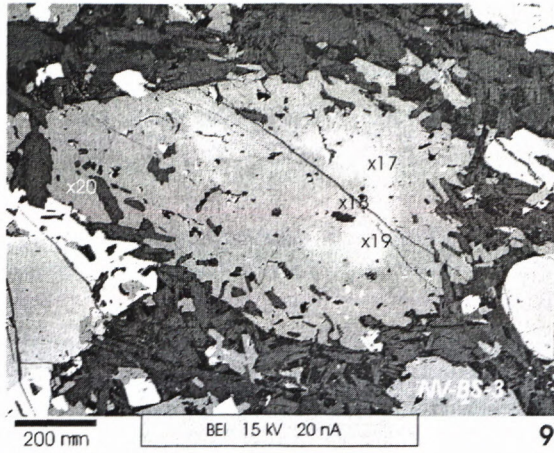
Geochemistry of basanite from Kalvária together with the another alkaline basalts from the Central and Southern Slovakia was described by Miháliková and Šímová (1989), more recently by Ivan and Hovorka (1993). According Ivan and Hovorka (1993) this rock belongs to alkaline withinplate basalts with their characteristics features: LILE and HFSE enrichment and differentiated enrichment LREE/HREE.

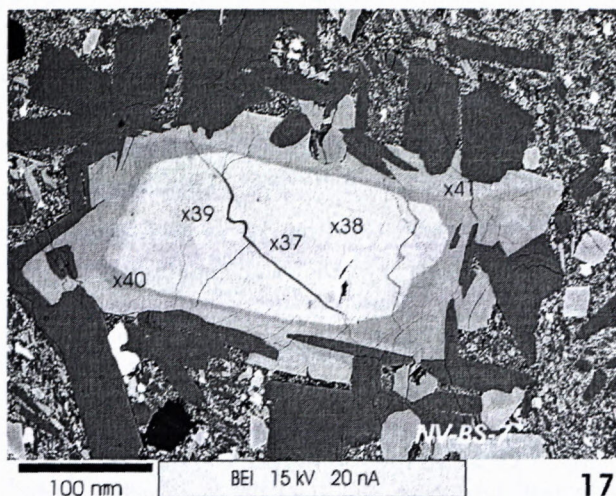
If we compare this basanite with most of the Miocene to Pleistocene Western Carpathian alkaline basalts, this rock as a product of the oldest eruption phase has mildly lowered total abundances of REE and some other incompatible elements such as Th, Zr, Ta.

Analytical techniques

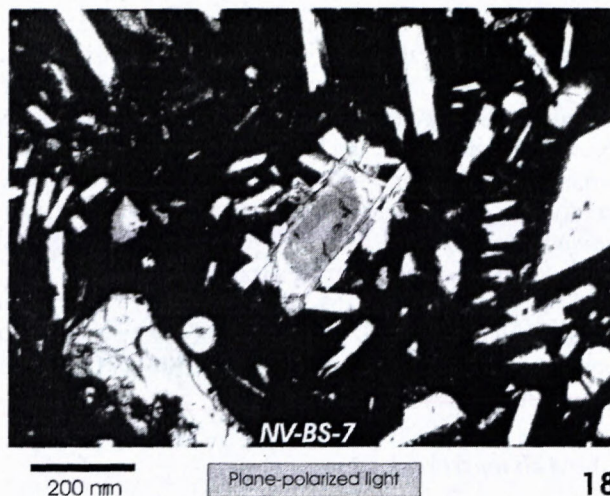
Pyroxenes were analyzed at Cameca SX-100 electron microprobe at Geological Survey of Slovak Republic, Bratislava. An accelerating potential of 15 kV, current 20 nA.



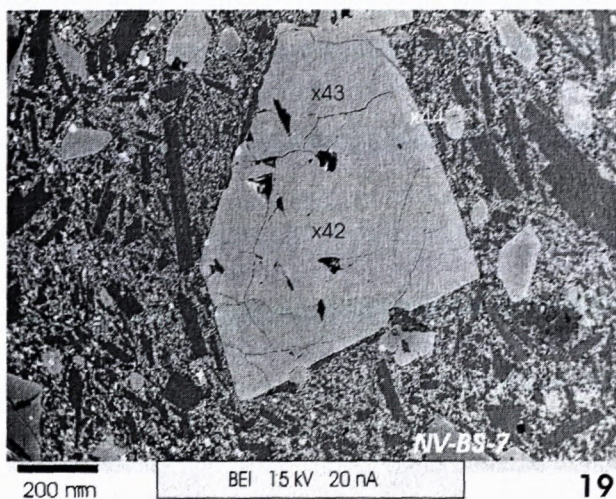




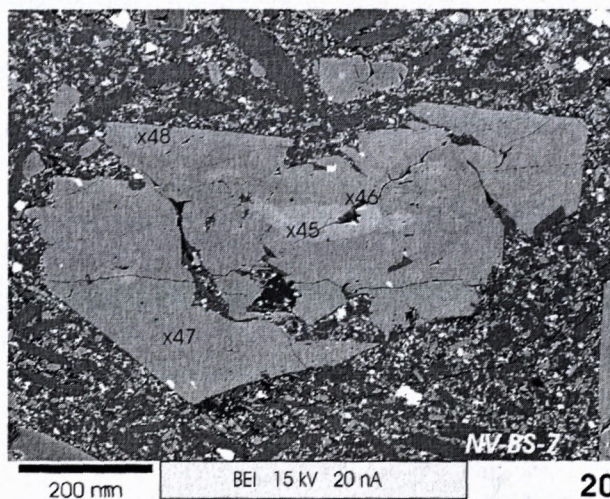
17



18



19



20

Phototables: Zoned clinopyroxenes from alkaline basalt, Banská Štiavnica, Kalvária.
Abbreviations: CC - carbonate, Pl - plagioclase

Standards used for elements: Si, Ca - wollastonite, Al - Al_2O_3 , Ti - TiO_2 , Fe - hematite, Mg - MgO , Mn - Mn, rhodonite, Na - albite, K - orthoclase, Cr - chromite.

Clinopyroxenes are recalculated to 6 oxygens and 4 cations. Fe^{3+} was calculated by charge balance. An analysis was recalculated to 4 cations exactly and Fe^{3+} was calculated as difference between 12 and total charge of cations.

Characteristics of zoned clinopyroxenes from Banská Štiavnica

The basanite from Banská Štiavnica - Kalvária comprises some types of zoned clinopyroxenes which differ in size, optical properties and chemical composition. Individual color hues of pyroxenes described below were observed in optical microscope at plane polarized light.

There are two basic types of the zonation in the studied rocks: continuous and discontinuous. *Continuously zoned* crystal comprises only one type of pyroxene which can have various hues of sandy and brown color. This type of zonation is typical for the most of pyrox-

enes. *Discontinuously zoned* crystal comprises two different types of pyroxenes which also differ in the color (some pyroxenes mentioned above which contain green cores).

Pyroxenes also have concentric, oscillatory, sector and non-regular (individual zones have non-regular shape) zoning.

In the clinopyroxene phenocrysts we can recognize three typical zones: (1) *central core or central part of phenocryst*, (2) *mantle* and (3) *rim*. The rim is narrow or is not present in some cases.

Pyroxenes with various hues of brown and sandy color

The most common types of pyroxenes in studied rocks are those of various hues of brown and sandy color in all parts of a crystal (photo 2, 3, 4). Color hue is determined by the concentration of Ti in an individual part of crystal. The higher is Ti content, the deeper is the color. Sandy color is more typical for the inner parts of clinopyroxenes, deep brown for their rims.

Zoning is a typical feature of these pyroxenes. There are some types of zonation: oscillatory, concentric, sector, non-regular. The optical zonation is of two kinds. *Simply zoned* crystal has inner part of sandy color and deep brown rim of various thickness. Deep brown clinopyroxenes in some samples can be added to this group. More color hues in a single phenocryst are typical for *more complicated zonation*, e. g. pyroxenes with brownish core, complex-zoned pyroxenes (photo 3, 4, 15).

The pyroxenes of this group are relatively often rounded and embayed. Inclusions of Ti-magnetite are concentrated to the rim parts of phenocrysts and to deeper brown pyroxenes.

Green clinopyroxene cores

Some clinopyroxenes in the studied alkaline basalt contain green cores which are rimmed by mantle and rim of sandy and/or deep brown color. We can recognize two types of these green cores:

Type I. represent relatively wide group of pleochroic or weakly pleochroic cores with green - brown pleochroism. These two colors have various hues (photo 1, 5, 7, 11, 12, 13, 16, 17, 18, 20). These cores are mostly anhedral. They have variable optical intensity observed at plane polarized light. There are cores which are not very distinctive from mantling pyroxene to intense cores. The boundary between the core and the mantle can be sharp or more diffuse. They are unzoned or they have non-regular zoning at crossed polars. The shape of some cores resembles fragments. They are often rounded and embayed, what indicates resorption prior to the mantle overgrowth. These cores practically do not contain inclusions. If they do, these inclusions extend also to mantling pyroxene.

Type II. represents non-pleochroic, weakly pleochroic to pleochroic cores of light pale green color (photo 6, 9, 10, 14). These cores are mostly anhedral, rarely subhedral. They are mostly non-zoned at crossed polars. They contain tiny inclusions; in some cases inclusions rim this core what can suggest a resorption. Resorption can be reflected also by rounded and embayed shapes of cores.

Some *clinopyroxenes with composite core* were identified in studied samples - one core is rimmed by the another core, but there are cores of only one type in a single crystal (either the core of type I. - photo 17, or the core of type II. - photo 6). The composite cores are described also by Dobosi and Fodor (1992) in Novohrad region.

Chemical composition of clinopyroxenes

Analyses of studied clinopyroxenes are listed in Tab. 1.

Clinopyroxenes were classified in quadrilateral En-Fs-Wo diagram (the I. M. A. classification, Morimoto et al., 1988, fig. 3). According this diagram almost all studied clinopyroxenes are *diopsides*. But it must be mentioned that these pyroxenes, besides cores of type II., contain

substantial amounts of non-quadrilateral components (mostly Al, less Na, Fe³⁺, Ti) and extensive substitution of these components probably raises values of Wo member (Bédard et al., 1988).

Higher contents of titanium (0,66 - 5,12 % TiO₂) are typical for sandy and deep brown parts of clinopyroxenes. This type of pyroxene is described as *titanaugite* (e. g. Duda and Schmincke, 1985; Dobosi, 1989); in this work they will be named *Ti-augites* and *Ti-diopsides* (according classification). Parts of pyroxenes with more than ≈ 3,7 % TiO₂ can be according I.M.A. classification named as *titanian diopsides*.

One core with relatively high Mg number (Mg# = 0,86) and Cr₂O₃ = 0,91 % can be termed *chromian augite*.

Green cores of type I. correspond on the basis of similar optical properties and chemical composition to *fassaite* and *fassaitic augites* (napr. Duda and Schmincke, 1985; Dobosi, 1989). Dobosi and Fodor (1992) named these clinopyroxenes *ferrous aluminous titaniferous diopsides*. They are characteristically enriched in Al (2,63 - 10,20 % Al₂O₃) and Fe³⁺ so they can be according I.M.A. nomenclature named *ferrian aluminian augites and diopsides*.

Green cores of type II. were described as *salites* and *ferrosalites* (Dobosi, 1989). They probably correspond also to *acmitic augites* in the work of Duda and Schmincke (1985). According I.M.A. nomenclature we can name them *Fe-rich diopsides and augites* (c.f. Dobosi - Fodor, 1992).

We studied the compositional variability of zoned clinopyroxenes from the studied rock at variation diagrams. We compared contents of choosen elements in individual parts of pyroxene phenocrysts, i.e. in the core, mantle and rim. The trends of the compositional change in these parts of phenocrysts were also studied. The results were compared with the data from analogical phenocrysts in alkaline basalts from two regions: Novohrad (Dobosi, 1989; Dobosi and Fodor, 1992) and Eifel (Germany, Duda and Schmincke, 1985). Si, Al, Ti and Na contents and Mg/Fe ratios are the most variable.

Diagram **Si vs. Al** (fig. 4) shows two relatively linear trends. One is formed by the green cores, inner parts and mantles and the second by the rims of pyroxenes. Both of the trends have negative slope - decreasing Si contents at increasing Al contents.

This diagram also informs us about filling of Si deficiency in tetrahedral coordination by Al (Al^{IV}). A deviation from line Si+Al=2 corresponds to the amount of Al in regular octahedral coordination (Al^{VI}). The lower is Si content the higher is this amount. Rims and green cores of type II. have lower Al^{VI} than another parts of clinopyroxenes.

Diagram **Mg/(Mg+Fe²⁺_{sum}; Mg#) vs. Fe³⁺** (Fig. 5) shows variability in Mg and Fe contents in the individual parts of pyroxene phenocrysts. Parts of pyroxenes of sandy and deep brown color are richer in Mg than green cores.

Iron was analyzed as Fe²⁺. Fe³⁺ was calculated by charge balance. The green cores of type I. have the highest Fe³⁺. Ti-augites and Ti-diopsides have a trend of Fe³⁺

Table 1 of zoned clinopyroxenes from alkaline basalt, Banská Štiavnica

NV-BSS	1 1	1 2	1 3	1 4	1 5	1 6	1 7	1b 8	1b 9	1b 10	1b 11	1b 12	1b 13	3 14	3 15	3 16
SiO ₂	47.94	46.08	47.36	44.17	49.54	45.08	43.97	51.44	51.22	42.98	44.03	44.69	48.65	52.33	45.43	43.34
TiO ₂	1.12	2.23	2.13	4.52	1.42	3.14	4.90	0.36	0.38	4.78	2.71	3.16	1.89	0.66	2.78	4.56
Al ₂ O ₃	5.25	8.25	7.28	8.02	6.02	9.30	8.35	1.72	1.68	9.34	10.20	10.53	6.35	3.68	9.65	9.21
FeO	12.48	8.73	6.24	8.24	6.49	6.75	8.28	13.02	12.71	8.16	9.02	6.85	6.12	5.01	5.95	7.36
MnO	0.53	0.35	0.06	0.18	0.13	0.08	0.18	0.76	0.78	0.10	0.15	0.06	0.12	0.10	0.10	0.09
MgO	9.73	12.64	14.01	11.96	14.76	12.66	11.56	10.37	10.68	11.18	10.40	12.43	14.49	17.57	12.85	11.31
CaO	21.89	21.27	22.30	22.43	20.77	22.11	22.42	21.84	22.06	22.37	22.11	21.62	21.75	20.22	22.02	22.86
Na ₂ O	0.98	0.69	0.57	0.57	0.61	0.59	0.70	0.92	0.88	0.67	0.88	0.70	0.51	0.55	0.72	0.71
K ₂ O	0.00	0.00	0.00	0.01	0.00	0.00	0.02	0.00	0.00	0.00	0.00	0.00	0.00	0.00	0.00	0.00
Cr ₂ O ₃	0.01	0.00	0.35	0.00	0.09	0.08	0.00	0.00	0.00	0.00	0.03	0.02	0.21	0.30	0.25	0.06
Sum	99.93	100.24	100.30	100.10	99.83	99.79	100.38	100.43	100.39	99.58	99.53	100.06	100.09	100.42	99.75	99.50
Si	1.836	1.728	1.756	1.669	1.831	1.688	1.658	1.957	1.949	1.633	1.673	1.666	1.799	1.901	1.694	1.644
Al	0.237	0.365	0.318	0.357	0.262	0.410	0.371	0.077	0.075	0.419	0.457	0.463	0.277	0.158	0.424	0.412
Ti	0.032	0.063	0.059	0.128	0.039	0.089	0.139	0.010	0.011	0.137	0.077	0.089	0.053	0.018	0.078	0.130
Fe ²⁺ _{sum}	0.400	0.274	0.194	0.261	0.201	0.211	0.261	0.414	0.405	0.259	0.287	0.214	0.189	0.152	0.186	0.234
Mn	0.017	0.011	0.002	0.006	0.004	0.003	0.006	0.025	0.025	0.003	0.005	0.002	0.004	0.003	0.003	0.003
Mg	0.556	0.707	0.775	0.674	0.813	0.706	0.650	0.588	0.606	0.634	0.589	0.691	0.799	0.951	0.714	0.640
Ca	0.898	0.855	0.886	0.908	0.822	0.887	0.906	0.890	0.899	0.911	0.900	0.864	0.862	0.787	0.880	0.929
Na	0.072	0.050	0.041	0.041	0.044	0.043	0.051	0.068	0.065	0.049	0.065	0.051	0.037	0.039	0.052	0.053
K	0.000	0.000	0.000	0.000	0.000	0.001	0.000	0.000	0.000	0.000	0.000	0.000	0.000	0.000	0.000	0.000
Cr	0.000	0.000	0.000	0.000	0.003	0.002	0.000	0.000	0.000	0.000	0.001	0.001	0.006	0.009	0.008	0.002
Sum cat.	4.048	4.053	4.041	4.044	4.019	4.039	4.043	4.029	4.035	4.045	4.054	4.041	4.026	4.018	4.039	4.047
Fe ³⁺	0.145	0.154	0.123	0.133	0.058	0.115	0.129	0.085	0.104	0.133	0.159	0.117	0.076	0.052	0.114	0.136
Mg#	0.582	0.721	0.800	0.721	0.802	0.770	0.714	0.587	0.599	0.710	0.672	0.764	0.809	0.862	0.793	0.732
WO	48.436	46.569	47.763	49.267	44.771	49.169	49.862	47.040	47.068	50.499	50.676	48.841	46.595	41.640	49.438	51.525
EN	29.989	38.508	41.779	36.571	44.281	39.135	35.773	31.078	31.728	35.144	33.164	39.062	43.189	50.317	40.112	35.496
FS	21.575	14.924	10.458	14.162	10.948	11.696	14.364	21.882	21.204	14.357	16.160	12.097	10.216	8.042	10.449	12.978

NV-BS	3 17	3 18	3 19	3 20	3 21	3 22	3 23	4 24	4 25	4 26	4 27	4 28	4 29	4 30	4 31	4 32
SiO ₂	51.01	49.98	51.02	46.80	44.85	46.99	47.05	45.57	48.52	47.48	51.07	43.22	47.60	45.05	48.18	48.08
TiO ₂	0.17	1.29	0.16	3.71	2.58	2.26	3.43	2.23	1.83	2.17	0.26	3.91	2.09	2.90	1.81	2.50
Al ₂ O ₃	1.07	2.63	1.10	6.45	9.74	7.63	5.79	9.66	6.85	7.77	1.49	10.34	7.34	9.36	6.60	5.22
FeO	17.00	11.69	17.24	7.22	8.76	6.08	7.10	8.21	5.72	6.28	13.54	6.99	6.30	7.95	6.06	5.22
MnO	1.11	0.54	1.29	0.11	0.18	0.10	0.15	0.22	0.10	0.12	0.82	0.15	0.14	0.13	0.12	0.14
MgO	9.25	11.78	9.28	13.02	11.38	13.43	13.04	11.28	14.25	13.76	11.04	11.60	13.54	12.17	12.17	13.54
CaO	19.99	21.90	19.65	22.65	21.52	22.10	22.81	21.85	21.75	21.82	20.21	22.20	21.93	20.98	21.94	22.58
Na ₂ O	0.56	0.48	0.61	0.57	0.93	0.57	0.62	0.86	0.54	0.54	0.65	0.56	0.62	0.77	0.54	0.94
K ₂ O	0.00	0.00	0.00	0.00	0.00	0.00	0.00	0.00	0.00	0.00	0.00	0.00	0.01	0.00	0.00	0.00
Cr ₂ O ₃	0.00	0.03	0.00	0.08	0.00	0.34	0.03	0.33	0.30	0.24	0.00	0.25	0.28	0.00	0.36	0.02
Sum	100.16	100.32	100.35	100.61	99.94	99.50	100.02	100.21	99.86	100.18	99.08	99.22	99.85	99.31	99.78	99.80
Si	1.974	1.894	1.972	1.744	1.690	1.754	1.764	1.708	1.795	1.758	1.965	1.636	1.770	1.699	1.790	1.800
Al	0.049	0.117	0.050	0.283	0.433	0.336	0.256	0.427	0.299	0.339	0.067	0.461	0.322	0.416	0.289	0.231
Ti	0.005	0.037	0.005	0.104	0.073	0.064	0.097	0.063	0.051	0.061	0.008	0.111	0.058	0.082	0.051	0.071
Fe ²⁺ _{sum}	0.550	0.370	0.557	0.225	0.276	0.190	0.223	0.258	0.177	0.195	0.436	0.221	0.196	0.251	0.188	0.212
Mn	0.037	0.017	0.042	0.003	0.006	0.003	0.005	0.007	0.003	0.004	0.027	0.005	0.005	0.004	0.004	0.005
Mg	0.533	0.666	0.535	0.723	0.640	0.748	0.729	0.630	0.786	0.760	0.633	0.655	0.751	0.684	0.785	0.756
Ca	0.829	0.889	0.814	0.904	0.869	0.884	0.916	0.877	0.862	0.866	0.833	0.901	0.874	0.848	0.873	0.906
Na	0.042	0.035	0.046	0.041	0.068	0.041	0.045	0.062	0.039	0.039	0.048	0.041	0.045	0.056	0.039	0.069
K	0.000	0.000	0.000	0.000	0.000	0.000	0.000	0.000	0.000	0.000	0.000	0.000	0.000	0.000	0.000	0.000
Cr	0.000	0.001	0.000	0.002	0.000	0.010	0.001	0.010	0.009	0.007	0.000	0.008	0.008	0.000	0.011	0.001
Sum cat.	4.019	4.026	4.021	4.029	4.055	4.030	4.036	4.042	4.021	4.029	4.017	4.039	4.029	4.040	4.030	4.051
Fe ³⁺	0.054	0.080	0.063	0.088	0.162	0.088	0.101	0.124	0.060	0.083	0.052	0.116	0.087	0.117	0.086	0.144
Mg#	0.492	0.643	0.490	0.763	0.699	0.797	0.766	0.709	0.816	0.796	0.592	0.748	0.793	0.732	0.807	0.781
WO	43.358	46.182	42.707	48.812	48.683	48.518	49.036	49.688	47.233	47.556	43.796	50.703	47.996	47.560	47.291	48.346
EN	27.877	34.597	28.069	39.039	35.854	41.054	39.026	35.694	43.068	41.735	33.281	36.860	41.241	38.362	42.524	40.342
FS	28.766	19.221	29.224	12.149	15.462	10.428	11.938	14.618	9.699	10.708	22.923	12.437	10.763	14.077	10.184	11.313

NV-BS	4 33	4 34	4 35	4 36	7 37	7 38	7 39	7 40	7 41	7 42	7 43	7 44	7 45	7 46	7 47	7 48
SiO ₂	44.76	46.54	49.14	42.83	48.87	46.05	48.45	45.75	41.15	44.54	51.67	48.06	49.11	46.84	44.21	42.59
TiO ₂	3.41	2.03	1.65	4.80	1.04	1.97	1.31	2.70	5.12	3.33	0.69	2.51	1.38	2.42	3.74	4.87
Al ₂ O ₃	8.04	8.46	6.34	10.31	3.93	6.43	4.48	9.00	11.73	10.54	4.10	5.64	4.61	8.39	10.24	10.41
FeO	7.76	7.98	5.53	7.78	13.89	14.55	12.41	6.21	7.87	6.10	4.88	7.07	12.28	6.15	6.99	8.07
MnO	0.12	0.17	0.13	0.16	0.65	0.53	0.56	0.11	0.14	0.14	0.07	0.11	0.37	0.13	0.13	0.10
MgO	12.10	11.98	14.69	11.22	9.16	7.90	9.91	12.83	10.65	12.31	16.84	13.74	10.60	13.29	11.93	11.17
CaO	22.52	21.96	21.96	22.34	22.02	21.69	22.04	22.22	22.64	22.18	20.64	22.74	21.49	22.51	22.69	22.66
Na ₂ O	0.69	0.84	0.46	0.70	0.93	1.14	1.03	0.54	0.56	0.72	0.58	0.44	0.90	0.57	0.50	0.56
K ₂ O	0.00	0.00	0.00	0.00	0.00	0.00	0.00	0.00	0.00	0.00	0.00	0.00	0.01	0.01	0.00	0.00
Cr ₂ O ₃	0.00	0.47	0.42	0.00	0.00	0.00	0.01	0.00	0.16	0.08	0.91	0.00	0.03	0.26	0.35	0.09
Sum	99.40	100.43	100.32	100.17	100.49	100.26	100.20	99.93	100.02	99.94	100.38	100.31	100.78	100.57	100.78	100.52
Si	1.697	1.738	1.808	1.615	1.873	1.781	1.851	1.706	1.560	1.661	1.883	1.790	1.856	1.733	1.647	1.604
Al	0.359	0.372	0.275	0.458	0.178	0.293	0.202	0.396	0.524	0.463	0.176	0.248	0.205	0.366	0.449	0.462
Ti	0.097	0.057	0.046	0.136	0.030	0.057	0.038	0.076	0.146	0.093	0.019	0.070	0.039	0.067	0.105	0.138
Fe ²⁺ _{sum}	0.246	0.249	0.170	0.245	0.445	0.471	0.397	0.194	0.250	0.190	0.149	0.220	0.388	0.190	0.218	0.254
Mn	0.004	0.005	0.004	0.005	0.021	0.017	0.018	0.003	0.005	0.004	0.002	0.003	0.012	0.004	0.004	0.003
Mg	0.684	0.667	0.806	0.631	0.523	0.455	0.564	0.713	0.602	0.685	0.915	0.763	0.597	0.733	0.663	0.627
Ca	0.915	0.879	0.866	0.903	0.904	0.899	0.902	0.888	0.919	0.887	0.806	0.907	0.870	0.892	0.905	0.914
Na	0.051	0.061	0.033	0.051	0.070	0.086	0.076	0.039	0.041	0.052	0.041	0.032	0.066	0.041	0.036	0.041
K	0.000	0.000	0.000	0.000	0.000	0.000	0.000	0.000	0.000	0.000	0.000	0.000	0.000	0.001	0.000	0.000
Cr	0.000	0.014	0.012	0.001	0.000	0.000	0.000	0.017	0.005	0.002	0.026	0.000	0.001	0.008	0.010	0.003
Sum. cat.	4.053	4.042	4.020	4.045	4.044	4.059	4.048	4.032	4.052	4.037	4.017	4.033	4.034	4.035	4.037	4.046
Fe ³⁺	0.155	0.126	0.133	0.133	0.129	0.173	0.142	0.093	0.150	0.115	0.052	0.096	0.103	0.102	0.109	0.136
Mg#	0.735	0.728	0.720	0.720	0.540	0.491	0.587	0.786	0.707	0.783	0.860	0.776	0.606	0.794	0.753	0.712
WO	49.593	48.969	50.759	50.759	48.291	49.260	48.417	49.471	51.892	50.341	43.102	47.989	46.900	49.146	50.672	50.919
EN	37.073	37.159	35.469	35.469	27.938	24.932	30.274	39.721	33.992	38.876	48.930	40.370	32.183	40.386	37.122	34.930
FS	13.333	13.872	13.772	13.772	23.771	25.808	21.310	10.808	14.116	10.783	7.968	11.640	20.916	10.468	12.206	14.150

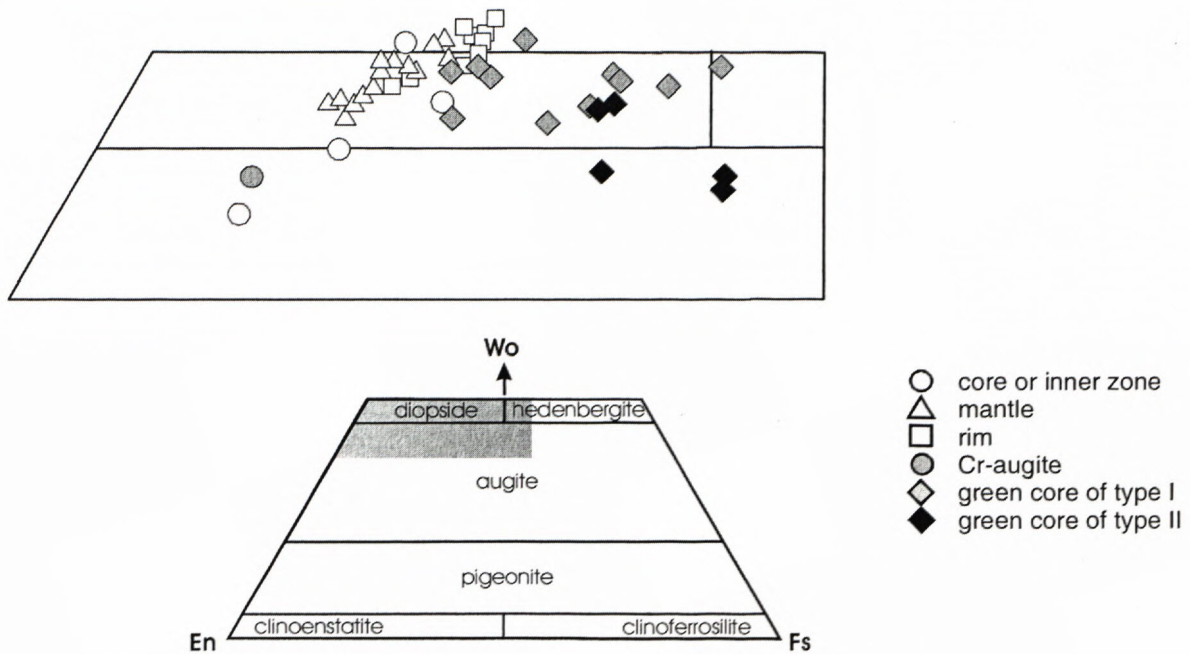


Fig. 3. Clinopyroxene classification. The part of clinopyroxene quadrilateral diagram shows the composition of various parts of clinopyroxenes from Banská Štiavnica.

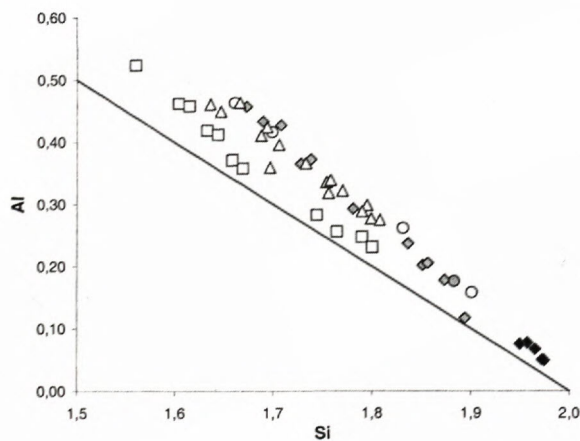


Fig. 4. Si vs. Al variation diagram. Symbols as for Fig. 3.

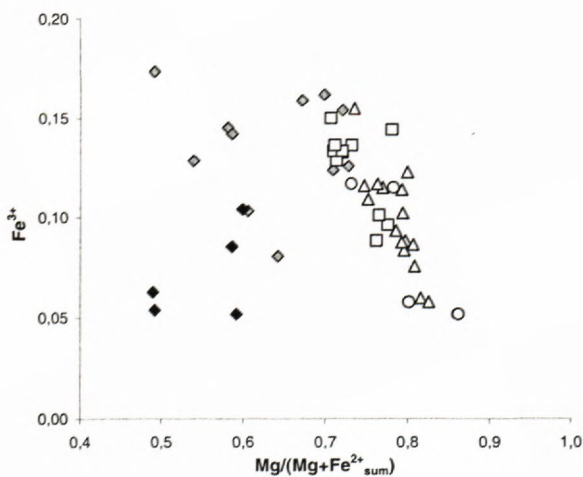


Fig. 5 Mg/(Mg+Fe²⁺_{sum}) vs. Fe³⁺ variation diagram. Symbols as for Fig. 3

enrichment towards the rims which are typically enriched in Ti. Green cores of type II. have lower Fe³⁺ contents than the cores of type I.. Fe³⁺ can be bounded in the molecule of *esseneite* (Fe-Al-tschermakite) $\text{CaFe}^{3+}\text{AlSiO}_6$, respectively *aegirine* $\text{NaFe}^{3+}\text{Si}_2\text{O}_6$.

Relations between Al and Ti contents in the individual parts and types of clinopyroxenes are evident from diagram Al vs. Ti (fig. 6). Ti can be bounded in *Ti-tschermakite* $\text{CaTiAl}_2\text{O}_6$ molecule. Ti:Al ratio in *Ti-tschermakite* has value 1:2. All studied types of clinopyroxenes have this ratio lower than 1:2 (predominance of Al). This fact suggests the presence of the another pyroxene molecules which can bound Al: *esseneite* mentioned above and/or mainly *Ca-tschermakite* CaAlAlSiO_6 , respectively *jadeite* $\text{NaAlSi}_2\text{O}_6$.

Green cores of type II. have the highest Al/Ti ratio but the lowest Al and Ti contents of all studied pyroxenes. Al predominance over Ti is more expressive in the green cores of type I. and in the inner parts of phenocrysts (besides green cores) with Ti/Al ratio 1:4 to 1:8. The rims are richer in Ti (Ti/Al from 1:2 to 1:4).

Similar Al and Ti distribution, although more variable, can be seen in clinopyroxenes from Novohrad and Eifel (Duda and Schmincke, 1985; Dobosi, 1989).

Variation in Al^{IV} and Al^{VI} has connection with clinopyroxene genesis. Diagram Al^{IV} vs. Al^{VI} (Aoki and Kushiro, 1968; fig. 7) separated individual types of pyroxenes. Projection points of pyroxene rims are concentrated in the *field of igneous rocks*. Points of the other parts of phenocrysts are projected to the *field of granulites and inclusions in basalts* with corresponding higher Al^{VI}/Al^{IV} ratio. Green cores of type II. form individual group in this field (low Al^{IV} a Al^{VI}).

Diagram Mg/(Mg+Fe²⁺_{sum}) vs. Ti (fig. 8) demonstrates differences in the Ti contents in the dependance of Mg

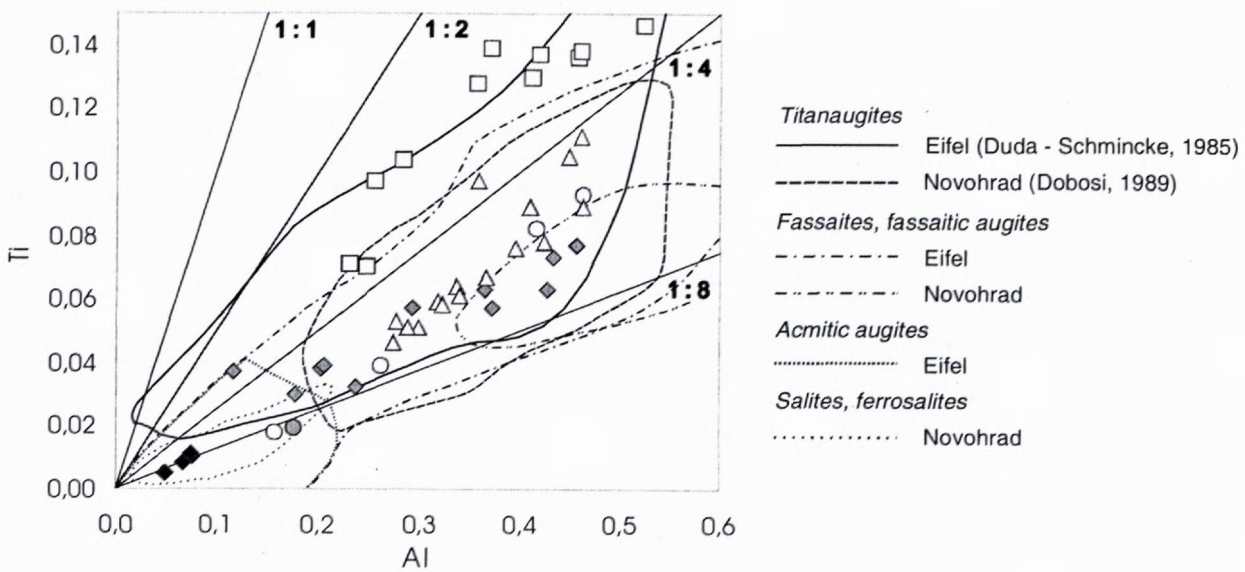


Fig. 6 Al vs. Ti variation diagram. Symbols as for Fig. 3.

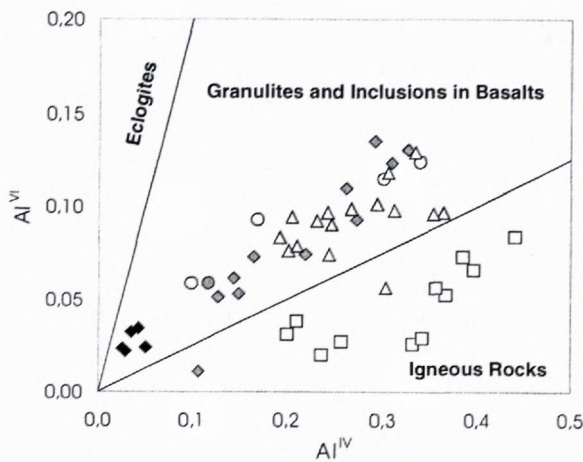


Fig. 7. Al^{IV} vs. Al^{VI} variation diagram. Symbols as for Fig. 3. Fields from Aoki and Kushiro (1968).

umber. Ti-augites and Ti-diopsides show relatively steep increase of Ti content with decrease of Mg number (increase of Fe at the expense of Mg). This phenomenon is typical for clinopyroxene fractionation from mafic alkaline melts (e. g. Tracy and Robinson, 1977). Analogical relations were observed also in the case of titanaugites from Novohrad and Eifel (Dobosi, 1989; Duda and Schmincke, 1985). The diagram also shows that Ti is concentrated predominantly to the rim parts of phenocrysts.

The green cores of type I. form in the diagram two separate groups. The first (close to the trend of Ti-augites and Ti-diopsides) has higher Mg number and Ti contents. It is placed in the field of fassaitic augites from Eifel (Duda and Schmincke, 1985) and titanaugites from Novohrad (Dobosi, 1989). The second group has lower Mg number and Ti contents and it is situated out of fields

formed by fassaites and fassaitic augites from Novohrad and Eifel. The green cores of type II. has low values for both of the components comparable with those of salites and ferrosalites in alkaline basalt from Novohrad region (Dobosi, 1989).

The Na contents demonstrated in $Mg/(Mg+Fe^{2+}_{sum})$ vs. Na (fig. 9) diagram do not show considerable variations among individual parts of clinopyroxenes. But one can see higher Na contents of the green cores of type I. than Na contents of Ti-augites and Ti-diopsides. Na could be bounded in the molecule of aegirine $NaFe^{3+}Si_2O_6$ and jadeite $NaAlSi_2O_6$.

Discussion

The compositional variability of clinopyroxene phenocrysts in alkaline basalts is generally influenced by two factors: (1) the composition of a parental magma (material which individual types of clinopyroxenes have crystallized from and (2) P, T conditions of their crystallization.

Ti-augites and Ti-diopsides

Mantles and cores of these composition are considered to have been formed in the magma (e.g. Duda and Schmincke, 1985). This is reflected by frequent zonality of this parts of the studied clinopyroxenes.

The interpretation of a cause of concentric or oscillatory zoning in a mantle of pyroxenes is still not clear. According Shimizu (1990) it is probably connected with alternation of periods of growing, stagnation and dilution, which can reflect changes in melt bulk composition, temperature, pressure and/or redox state.

The origin from magma can be suggested also for central parts of phenocrysts which have not pronounced shape of core.

Chemical composition of Ti-augites and Ti-diopsides gives us special information about conditions of their origin. The general trend shown in the direction pyroxene mantle - rim is Mg depletion, Ti enrichment and decrease in Al/Ti and Al^{VI}/Al^{IV} ratios (fig. 6, 7, 8). The decrease of Mg# towards pyroxene rims (e. g. fig. 8) can reflect a crystallization of the rim parts from more differentiated melt.

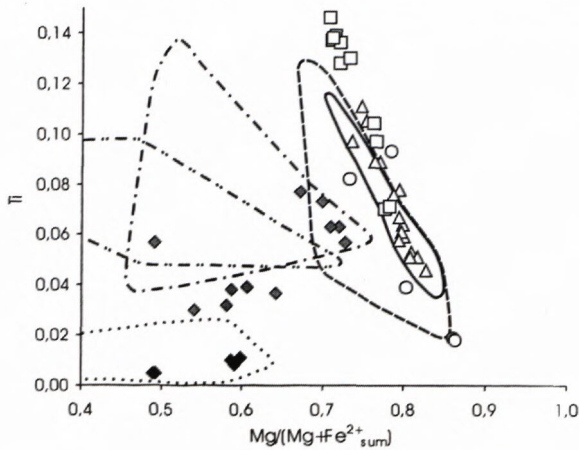


Fig. 8. Mg/(Mg + Fe²⁺_{sum}) vs. Ti variation diagram. Symbols and fields as for Figs. 3 and 6.

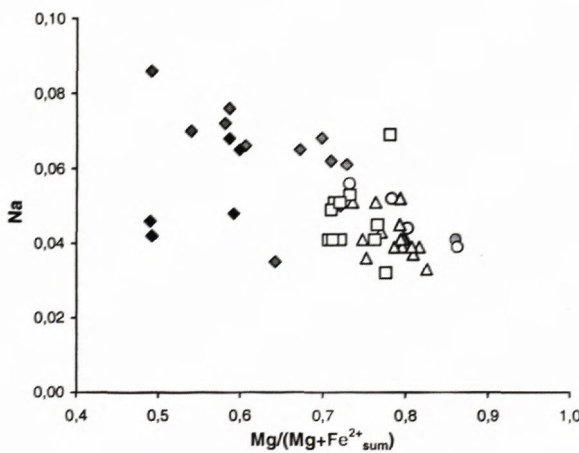


Fig. 9. Mg/(Mg + Fe²⁺_{sum}) vs. Na variation diagram. Symbols as for Fig. 3.

Changes in Ti composition cause color changes. The higher Ti content, usually the deeper brown color of pyroxene. It is considered that Ti contents are sensitive to pressure changes at pyroxene forming. Although the experimental data are to the some extent contradictory (Yagi and Onuma, 1967; Thompson, 1974; Edgar et al., 1980), one can assume that *Ti contents increase with decreasing pressure*. This can be confirmed by the fact that Ti is concentrated to the rim parts of clinopyroxene phenocrysts and groundmass clinopyroxenes, which formed later than inner parts of phenocrysts, at the higher levels of the crust or on the surface (c. f. Duda and Schmincke, 1985; Dobosi and Fodor, 1992; fig. 6 a 8).

Continuous trends in Ti and Fe contents in Ti-augites and Ti-diopsides (especially their mantles and rims) in presented diagrams demonstrate they had the same parental magma which had risen to the surface (c.f. Duda and Schmincke, 1985).

Al contents can similarly suggest the origin of the pyroxene rims at lower pressures than their inner parts. Diagram Al^{IV} vs. Al^{VI} (fig. 7) shows that the rims are projected in the field of low pressure magmatic clinopyroxenes (lower Al^{VI}/Al^{IV} ratio) while the inner parts are projected to the higher pressure field of granulites and inclusions in basalts.

The higher Ti/Al ratios of pyroxene rims (fig. 6) also indicate the origin at lower pressures (c.f. Dobosi and Fodor, 1992).

The calculations of Duda and Schmincke (1985) for titanite phenocryst mantle yielded temperatures of 1050 °C - 1140 °C and pressures 5-10 kbar. Thus, according these authors, this pyroxene zone appears to have crystallized at depths corresponding to the lower crust down to the crust/mantle boundary. Dobosi and Fodor (1992) have mentioned that clinopyroxene rims have formed at low pressure conditions, e. g. crystallization at shallow levels or at the surface after eruption.

A special problem is represented by the brown clinopyroxene cores present in some phenocrysts. Their composition (higher Ti content, lower Mg# and usually also higher Na) suggests crystallisation from more differentiated magma at probably higher pressure than the subsequent crystallisation of the mantling pyroxene. These cores can be connected with crystallization of gabbroic rocks in the uppermost mantle, respectively at the mantle/crust boundary. Xenoliths of this type with pyroxene of analogic composition were found in alkaline basalts (e. g. Colville and Novak, 1991; McGuire and Mukasa, 1997). The mantle of these brown cores which crystallized from less differentiated magma probably indicates entrapment of these cores by the injection of new, more primitive magma batch.

Cr-augite

Cr-augite core was found in the phenocryst in the sample NV-BS-7. It has anhedral shape and it is mantled by Ti-diopside. Wass (1979) and Duda and Schmincke (1985) interpreted cores of Cr-diopside composition as xenocrysts representing fragments of the upper mantle peridotite xenoliths. These xenocrysts served as nucleation sites for subsequent clinopyroxene crystallization (Dobosi, 1989). One can suggest that Cr-augites represent fragments of the upper mantle wall-rocks, which were trapped by rising basalt magma.

Green cores of phenocrysts

The green cores of studied phenocrysts are enriched in Fe and depleted in Mg if we compare them with mantling Ti-augites and Ti-diopsides. The cores of type I. have similar Al and Ti contents as inner parts of Ti-augite and

Ti-diopside composition, while the cores of type II. have the lowest concentrations of these elements from all of studied clinopyroxenes (fig. 6 and 8). The cores of type I. have the highest Na contents and the cores of type II. have the highest contents of Si (fig. 4 and 9).

There were some views at the origin of the green clinopyroxene cores in alkaline basalts:

1. *They are products of high-pressure differentiation trend of alkaline basalt magmas.*

Wilkinson (1975) mentioned that green clinopyroxene megacrysts represent very probably *the final fraction of clinopyroxene megacryst crystallization*. In this sense Wass (1979) presented that Fe-rich clinopyroxenes represent *an extension of the high-pressure Al-augite series clinopyroxene trend*.

2. *They are xenocrysts from more differentiated melt which was subsequently mixed with more primitive basic magma.*

The existence of mantle-derived differentiated melts has been well documented (e. g. Brooks and Printzlau, 1978; Irving and Price, 1981; Dobosi and Fodor, 1992; Bodinier et al., 1996) and also the possibility of mixing between more differentiated and mafic melt in the upper mantle environment (Bédard et al., 1988). But there is also the possibility that differentiated melt could originate by anatectic melting of crustal rocks (Philpotts, 1976) or metasomatized lower-crust rocks (Morogan and Martin, 1985).

Crystallization of Fe-rich clinopyroxenes and subsequent magma mixing could take place in the crust (Thompson, 1977; Barton et al., 1982) or in the upper mantle (Brooks and Printzlau, 1978; Wass et al., 1980).

According to Brooks and Printzlau (1978) green pyroxene cores have formed from *intermediate to salic magmas*. They suggest that more evolved melts, enriched in incompatible elements, probably originate by partial melting of metasomatically enriched mantle.

Duda and Schmincke (1985) suggest xenocrystic origin for fassaitic augites present in the cores of clinopyroxene phenocrysts. They are *xenocrysts which have formed from more differentiated magma*. This magma must have been enriched in Fe and incompatible elements, especially in phosphorus what is documented by inclusions of apatite in the cores. The cores formed in the depth of 15–30 km, possibly at the base of the crust.

Liotard et al. (1988) propose *high-pressure differentiated mugearitic magma with characteristically high REE contents* as a parental melt for acmite rich clinopyroxenes. This magma already had contained phenocrysts and subsequently was mixed with more primitive basaltic magma.

Dobosi and Fodor (1992) assume for the fassaitic cores the origin from *more differentiated magma(s) in the upper mantle magma chamber at high pressures*. This magma chamber was periodically filled with more primitive melts. Because of mixing of more differentiated melt which already had contained green cores with this more primitive magma, the green cores were mantled by the more mafic outer core or by the mantle. If the growing

clinopyroxene was trapped by more batches of more primitive magma, the multiple-zoned crystal has originated (e. g. inner core - outer core - mantle).

Pilet et al. (2002) note that green cores of clinopyroxenes have crystallized from *more evolved melts probably of phonolitic composition* at middle to high pressures in the upper mantle to the middle continental crust.

3. *They are xenocrysts from the upper mantle wall rocks.*

Brooks and Printzlau (1978) do not exclude the opportunity that some green cores could be *xenocrysts derived from the upper mantle wall rocks*. These xenocrysts were caught by basaltic magma which was rising through the upper mantle.

Barton and Bergen (1981) suggest the origin of green clinopyroxenes by *the upper mantle xenolith disaggregation*. These xenoliths reflect a local metasomatism or a crystallization from magmas of unknown composition during an earlier igneous event.

Dobosi and Fodor (1992) suggest that Fe-rich diopside cores come from *the upper mantle wall rocks and they are products of earlier event of partial melting and magma fractionation* than fassaitic augites.

Ivan and Hovorka (1993) presented the opinion that green salitic and/or ferrosalitic cores could have been *the products of the upper mantle peridotite metasomatic enrichment by rising melts and fluids*.

The next view of Ivan and Hovorka (1993) has a special place in this group of views. The fassaitic cores are probably products of metasomatism which is the result of the interaction between basaltic melts migrating through a vein system in the mantle and neighbouring mantle peridotite (Witt and Seck, 1989; McDonough and Frey, 1989; Bodinier, et al., 1990). These cores probably represent *disaggregated vein fillings*.

Shaw and Eyzaguirre (2000) describe clinopyroxene megacryst similar to acmites in the work of Duda and Schmincke (1985) which was found in the rocks from Eifel, Germany. This megacryst was probably derived from *the iron-rich cumulate in the upper mantle*.

The green cores of type I. can be assumed to be *xenocrysts*. It could be confirmed by the sharp optical and chemical boundary (higher Fe/Mg ratio) between the core and the mantle and the resorption (c. f. Duda and Schmincke, 1985).

These cores are mostly of anhedral shape. They are often rounded and embayed, what indicate the resorption prior the mantle growing (a dissolution of these cores in the melt). This resorption could have been due to an incorporation of these cores to hotter, pyroxene undersaturated mafic melt (Bédard et al., 1988).

The green cores of type I. from Banská Štiavnica basaltite have not such optical intensity (intensity of the color) in many cases as have i. e. corresponding green cores from Novohrad region (fassaites and fassaitic augites, Dobosi, 1989). Brooks and Printzlau (1978) note that the intensity of green color is dependent at the content of acmite (aegirine) component $\text{NaFe}^{3+}\text{Si}_2\text{O}_6$. Really, although Fe^{3+} values are comparable for both the regions,

Na contents in the green cores of type I. (0,48 – 1,14 % Na₂O) are lower than those in fassaites from Novohrad region (0,97 – 1,54 % Na₂O).

We can observe relatively wide variability in the composition of the type I. cores at variation diagrams. This variability may be according Duda and Schmincke (1985) explained either as the influence of crystallization kinetics or, more likely, by every core crystallizing in a discrete magma batch of a certain degree of fractionation. Mg# of studied cores is lower than Mg# of pyroxene mantles of Ti-augite and Ti-diopside composition which rim these cores. This can suggest the *growing from the more differentiated melt* (cf. Duda and Schmincke, 1985; Dobosi and Fodor, 1992).

Especially at the diagram Mg# vs. Ti (fig. 8) we can see two groups of cores different in Mg, Fe and Ti contents: the first group with higher Mg# and Ti contents and the second one with lower Mg# and Ti contents. They do not create continuous Fe-differentiation trend as do fassaitic cores in pyroxenes from Novohrad (Dobosi and Fodor, 1992). It is possible that lack of more chemical analyses precludes to create an continuous trend but the existence of two types of more differentiated magmas cannot be also excluded. Especially the cores with subhedral shapes and the complex-zoned core with variable chemical composition could originate from more differentiated melt. The higher Al^{VI}/Al^{IV} ratios (field of granulites and inclusions in basalts, fig. 7), comparable with these ratios in clinopyroxene mantles suggest the crystallization at relatively high pressure.

Trace element investigation in megacrysts (Dobosi and Jenner, 1999) confirmed the origin of type I. green cores from alkaline basalt magma. Observed trace element relations and their correlation with changing Mg# can be explained by fractional crystallization of this magma in the upper mantle with the production of a range of fractionated melts. The results of xenolith study at various localities showed that these melts had crystallized in the uppermost mantle as veins of Al-pyroxene gabbro or pyroxenite (Richter and Carmichael, 1993), which can contain amphibole (Colville and Novak, 1991). Mechanism of the fractionation is not obvious, it is very probably the reaction of rising magma with wall rock mantle peridotites, which enriches magma in Al, Ca and Fe (Varfalvi et al., 1996).

It is possible to assume an alternative possibility of the origin of type I. cores (e. g. some cores have the shape which resembles fragments). Ivan and Hovorka (1993) note that these cores probably come from fillings of the vein system through which basalt magmas migrate in the upper mantle peridotite. The reaction of magma with carbonates cannot be also excluded. These carbonates in peridotites can originate as a result of the mantle metasomatism. Pyroxenes compositionally close to the green cores of type I. originate also at contacts of magma with dolomite carbonates (e. g. Shabynin et al., 1984; Bowman and Essene, 1984). Fragments of these green pyroxenes originate by desintegration of vein fillings by next batches of rising alkaline magma. They were consequently rim-

med by a mantle which have crystallized from basaltic magma.

Green cores of type II. are of two kinds. The first of them is represented by *anhedral, strongly resorbed cores*. On the basis of their optical characteristics and similar chemical composition (Fe, Mg, Al, Ti) with salite, ferrosalite and acmite cores (Duda and Schmincke, 1985; Dobosi, 1989), one can assume that they represent *fragments derived from the upper mantle wall rocks metasomatically enriched by rising melts and fluids* (e. g. Ivan and Hovorka, 1993). *The composite core* represent the second kind of core. It has an inner core with a fragmental shape at one of its edges. This inner core is mantled by zoned outer core of subhedral shape with partial resorption of edges. Compositionally it is not very different from the previous kind of cores although it is richer in Ti, Al and Na. It may originated *in more differentiated magma at higher pressures*. The origin from more differentiated magma can be suggested from core Mg# approximately 0,6. The origin at higher pressures is supported by Al^{VI}/Al^{IV} ratios comparable with green cores of type I. and higher Na contents (Fig. 7 and 9).

Unambiguous origin of green cores of this type is noted also by Duda and Schmincke (1985). They are not sure whether acmitic augites have originated in more evolved magma or they are the fragments of the upper mantle wall rocks. Space relations in the phenocrysts and strong resorption suggest they originated sooner than did fassaitic pyroxenes. Dobosi and Fodor (1992) suggest that these green cores present in the upper mantle wall rocks are products of earlier event of partial melting and magma fractionation than fassaitic augites.

Their low Mg# indicates the crystallization from strongly fractionated magma. But the REE pattern in a clinopyroxene megacryst similar to acmites from Eifel (Shaw and Eyzaguirre, 2000) is contradictory with the magma fractionation. This megacryst was probably derived from iron rich cumulate in the upper mantle.

There is also possibility of the continuous trend from cores of type I. to cores of type II.. This trend can be observed very well at the diagram Mg# vs. Ti (Fig. 8) and it could reflect strong differentiation of magma. There are the cores of both types (type I. and type II.) which may originate in magma. The question, whether such trend exists or both types of cores had different evolution, could be resolved by more analytical data, especially by trace element analyses.

Conclusions

The results of this study of zoned clinopyroxenes in alkaline basalt from Banská Štiavnica, locality Kalvária can be summarized as:

- it can be assumed that their origin and evolution are similar to the genesis of analogical pyroxenes from the other areas (e. g. Novohrad and Eifel).
- Ti-augites and Ti-diopsides come from alkaline basalt magma, which does not reach high degree of differentiation. The variability in Ti and Al contents shows the

polybaric crystallization. The mantles with lower Ti content originated at higher pressures as did rim parts of phenocrysts with higher Ti contents.

– Cr-augites represent the fragments of the upper mantle wall rocks which were caught by rising basalt magma.

– The green cores of type I. originated in the melt or they represent disaggregated vein fillings in the upper mantle. Their magma origin can be assumed from zoning and subhedral shapes of some cores. The Mg# value and variability of chemical composition of these cores suggest more differentiated magmas of variable degree of differentiation. There is also possibility that the cores of type I. can represent disaggregated vein fillings (especially those with fragmental shape). Higher Al^{VI}/Al^{IV} ratios comparable with those of clinopyroxene mantles reflect the crystallization at relatively high pressure.

– Intensively resorbed cores of type II. are probably xenocrysts which originated in the upper mantle influenced by metasomatic processes. It is possible that some cores originated in differentiated magma (e. g. zoned subhedral core).

– There is a possibility of continuous trend from the cores of type I. to the cores of type II..

– Zoned clinopyroxenes in basanite from Banská Štiavnica - Kalvária are indicators of complex processes at alkaline magma evolution and its interaction with subcontinental mantle. They confirm inhomogeneity of this mantle, its probable veining and gradual evolution due to metasomatic processes, interaction of basaltic magma with wall rock peridotites and crystallization of part of basalt magma in the upper mantle or at the crustal-mantle boundary. All these processes took place prior to basalt magma rise to the surface.

Acknowledgements.

References

- Aoki, K. & Kushiro, I., 1968: Some clinopyroxenes from ultramafic inclusions in Dreiser Weiher, Eifel. *Contr. Mineral. Petrology*, 18, p. 326-337.
- Balogh, K., Miháliková, A. & Vass, D., 1981: Radiometric dating of basalts in Southern and Central Slovakia. *Západ. Karpaty, Sér. Geol.*, 7, p. 113-126.
- Barton, M. & Bergen, M. J., 1981: Green clinopyroxenes and associated phases in a potassium-rich lava from the Leucite Hills, Wyoming. *Contr. Mineral. Petrology*, 77, p. 101-114.
- Barton, M., Varenkamp, J. C. & Bergen, M. J., 1982: Complex zoning of clinopyroxenes in the lavas of Vulsini, Latium, Italy: evidence for magma mixing. *J. Volcanol. geotherm. Res.*, 14, p. 361-388.
- Bédard, J. H. J., Francis, D. M. & Ludden, J., 1988: Petrology and pyroxene chemistry of Monteregeian dykes: the origin of concentric zoning and green cores in clinopyroxenes from alkali basalts and lamprophyres. *Can. J. Earth. Sci.*, 25, p. 2041-2058.
- Bodinier, J. L., Vasseur, G., Vernières, J., Dupuy, C. & Fabries, J., 1990: Mechanism of mantle metasomatism: Geochemical evidence from the Lherz orogenic peridotite. *J. Petrology*, 31, p. 597-628.
- Bodinier, J. L., Merlet, C., Bedini, R. M., Simien, F., Remaidi & M., Garrido, C. J., 1996: Distribution of niobium, tantalum, and other incompatible trace elements in the lithospheric mantle; the spinel paradox. *Geochim. cosmochim. Acta*, 60, p. 545-550.
- Bowman, J. R. & Essene, E. J., 1984: Contact skarn formation at Elkhorn, Montana I: p-T component activity conditions of early skarn formation. *Amer. J. Sci.*, 284, 597-650.
- Brooks, C. K. & Printzlau, I., 1978: Magma mixing in mafic alkaline volcanic rocks: the evidence from relict phenocryst phases and other inclusions. *J. Volcanol. geotherm. Res.*, 4, p. 315-331.
- Colville, A. A. & Novak, G. A., 1991: Kaersutite megacrysts and associated crystal inclusions from the Cima volcanic field, San Bernardino County, California. *Lithos*, 27, 107-114.
- Dobosi, G., 1989: Clinopyroxene zoning patterns in the young alkali basalts of Hungary and their petrogenetic significance. *Contr. Mineral. Petrology*, 101, p. 112-121.
- Dobosi, G. & Fodor, R. V., 1992: Magma fractionation, replenishment, and mixing as inferred from green-core clinopyroxenes in Pliocene basanite, southern Slovakia. *Lithos*, 28, p. 133-150.
- Dobosi, G. & Jenner, G. A., 1999: Petrologic implications of trace element variation in clinopyroxene megacrysts from the Nógrád volcanic province, north Hungary: a study by laser ablation microprobe inductively coupled plasma-mass spectrometry. *Lithos*, 46, p. 731-749.
- Duda, A. & Schmincke, H. U., 1985: Polybaric differentiation of alkali basaltic magmas: evidence from greencore clinopyroxenes (Eifel, FRG). *Contr. Mineral. Petrology*, 91, p. 340-353.
- Edgar, A. D., Condlife, E., Barnett, R. L. & Shirran, R. J., 1980: An experimental study of an olivine ugandite magma and mechanisms for the formation of its K-enriched derivatives. *J. Petrology*, 21, p. 475-497.
- Irving, A. J. & Price, R. C., 1981: Geochemistry and evolution of lherzolite-bearing phonolitic lavas from Nigeria, Australia, East Germany and New Zealand. *Geochim. cosmochim. Acta*, 45, p. 1309-1320.
- Ivan, P. & Hovorka, D., 1993: Geochemistry and petrology of the Late cenozoic alkali basalts of the Western Carpathians (Czechoslovakia). *Mineral. Petrology*, 48, p. 3-16.
- Konečný, V., Lexa, J., Halouzka, R., Hók, J., Vozár, J., Dublan, L., Nagy, A., Šimon, L., Havrila, M., Ivanička, J., Hojstričová, V., Miháliková, A., Vozárová, A., Konečný, P., Kováčiková, M., Filo, M., Marcin, D., Klukanová, A., Liščák, P. & Žáková, E., 1998: Geologická mapa Štiavnických vrchov a Pohronského Inovca. 1 : 50 000. Bratislava, Geologická služba Slovenskej republiky. I. diel 248 s., II. diel 473 s.
- Liotard, J. M., Briot, D. & Boivin, P., 1988: Petrological and geochemical relationships between pyroxene megacrysts and associated alkali-basalts from Massif Central (France). *Contr. Mineral. Petrology*, 98, p. 81-90.
- McDonough, W.F. & Frey, F.A., 1989: Rare earth elements in upper mantle rocks. In: Lippin, B. R. & McKay, G. A., eds.: *Geochemistry and mineralogy of rare earth elements*. Mineral. Soc. Amer., pp. 99-145.
- McGuire, A. V. & Mukasa, S. B., 1997: Magmatic modification of the uppermost mantle beneath the Basin and Range to Colorado Plateau Transition Zone; Evidence from xenoliths, Wikieup, Arizona. *Contr. Mineral. Petrology*, 128, 52-65.
- Miháliková, A. & Šímová, M., 1989: Geochemistry and petrology of the Miocene-Pleistocene alkali basalts of the middle and southern Slovakia. (In Slovak). *Západ. Karpaty, Sér. Mineral. Petrogr. Geoch. Lož.*, 12, p. 7-142.
- Morimoto, N. (1988): Nomenclature of pyroxenes. *Mineral. Petrology*, 39, p. 55-76.
- Morogan, V. & Martin, R. F., 1985: Mineralogy and partial melting of fenitized crustal xenoliths in the Oldoinyo Lengai carbonatitic volcano, Tanzania. *Amer. Mineralogist*, 70, p. 1114-1126.
- Pilet, S., Hernandez, J. & Villemant, B. (2002): Evidence for high silicic melt circulation and metasomatic events in the mantle beneath alkaline provinces: the Na-Fe-augitic green-core pyroxenes in the Tertiary alkali basalts of the Cantal massif (French Massif Central). *Mineral. Petrology*, 76, p. 39-62.
- Philpotts, A. R., 1976: Petrography of monts Saint-Bruno and Rougemont. *Ministère des Richesses naturelles du Québec, Publication ES-16*.
- Righter, K. & Carmichael, I. S. E., 1993: Mega-xenocrysts in alkali olivine basalts: Fragments disrupted mantle assemblages. *Amer. Mineralogist*, 78, p. 1230-1245.
- Shabynin, L. I., Pertzov, N. N. & Zotov, I. A., 1984: Problems of formation of ore-bearing skarns at the dolomite contacts (In Russian). Moscow, Nauka, 104 p.

- Shaw, C. S. J. & Eyzaguirre, J., 2000: Origin of megacrysts in the mafic alkaline lavas of the West Eifel volcanic field, Germany. *Lithos*, 50, p. 75-95.
- Shimizu, N., 1990: The oscillatory trace element zoning of augite phenocrysts. *Earth Sci. Rev.-s.*, 29, 27-38.
- Šímová, M. (1965): Petrography and petrochemistry of the final volcanism in the Slovenské stredohorie Mts. (In Slovak). *Acta geol. geogr. Univ. Comen.*, Geol., 9, p. 9-89.
- Thompson, R. N., 1974: Some High-pressure pyroxenes. *Mineral. Mag.*, 39, p. 768-787.
- Thompson, R. N., 1977: Primary basalts and magma genesis. III. Alban Hills, Roman comagmatic province, Central Italy. *Contr. Mineral. Petrology*, 60, p. 91-108.
- Tracy, R. L. & Robinson, N. P., 1977: Zoned titanium augite in alkali olivine basalt from Tahiti and the nature of titanium substitutions in augite. *Amer. Mineralogist*, 62, p. 634-645.
- Varfalvy, V., Hébert, R. & Bédard, J. H., 1996: Interaction between melt and upper mantle peridotites in the North Arm Mountain massif, Bay of Island ophiolite, Newfoundland, Canada: Implications for the genesis of boninitic and related magmas. *Chem. Geol.*, 129, p. 71-9.
- Wass, S. Y., 1979: Multiple origins of clinopyroxenes in alkali basaltic rocks. *Lithos*, 12, p. 115-132.
- Wass, S. Y., Henderson, P., Elliott, C. J., 1980: Chemical heterogeneity and metasomatism in the upper mantle: Evidence from rare earth and other elements in apatite-rich xenoliths in basaltic rocks from eastern Australia. *Phil. Trans. R. Soc. Lond. A*, 297, p. 222-246.
- Wilkinson, J. F. G., 1975: Ultramafic inclusions and high pressure megacrysts from a nephelinite sill, Nandewar Mountains, northeastern New South Wales, and their bearing on the origin of certain ultramafic inclusions in alkaline volcanic rocks. *Contr. Mineral. Petrology*, 51, p. 235-262.
- Witt, G. & Seck, H. A., 1989: Origin of amphibole in recrystallized and porphyroclastic mantle xenoliths from the Rhenish Massif - Implications for the nature of mantle metasomatism. *Earth Planet. Sci. Lett.*, 91, p. 327-340.
- Witt-Eickschen, G. & Kramm, U., 1998: Evidence for the multiple stage evolution of the subcontinental lithospheric mantle beneath the Eifel (Germany) from pyroxenite and composite pyroxenite/peridotite xenoliths. *Contr. Mineral. Petrology*, 131, p. 258-272.
- Witt-Eickschen, G., Seck, H. A. & Reys, Ch., 1993: Multiple enrichment processes and their relationships in the subcrustal lithosphere beneath the Eifel (Germany). *J. Petrology*, 34, p. 1-22.
- Yagi, K. & Onuma, K., 1967: The join $\text{CaMgSi}_2\text{O}_6\text{-CaTiAl}_2\text{SiO}_6$ and its bearing on the titanaugites. *J. Fac. Sci. Hokkaido Univ., Series IV*, 13, p. 117-138.

Biostratigraphy and radiometric dating in the Vienna Basin Neogene (Slovak part)

¹HUDÁČKOVÁ, N., ¹HALÁSOVÁ, E., ²FORDINÁL, K., ¹SABOL, M., ¹JONIAK, P. and ²KRÁL, J.

¹Comenius University, Faculty of Natural Sciences, Depart. of Geol. and Paleont., Mlynská dolina G, 9842 15 Bratislava, Slovakia

²Geological survey of Slovak Republic, Mlynská dolina 1, 81704 Bratislava

The calcareous nannoplankton and foraminifers were studied in the lithostratigraphic formations of the Lower and Middle Miocene sediments of the Vienna Basin (Slovak part) as well the molluscs, ostracodes and vertebrata species.

The most useful tool for precise stratigraphy seems to be nannoplankton and planktonic foraminifers species. The study of the nannoplankton assemblages enables (unlike the traditional stratigraphy based on the benthic foraminiferal assemblages – assemblage Zones and ostracods zonation) to define the correlation time slices regardless of paleoenvironment and substratum. The rapidly reproduced calcareous nannoplankton can show the short-term marine incursions and the marine corridors. The main results of this work are as follows:

NN 2, NN3, NN4, NN5 and NN6 nannoplankton zones have been identified there. On the basis of the mentioned zones a correlation with the Paratethys, Mediterranean and with standard zonation is possible (Tab. 1).

The nannoplankton assemblage proves the transgressive marine Otnangian in the Lužice Fm. (upper part). Based on the nannoplankton association the Badenian sediments of the Vienna Basin (Slovak part) could be divided only into two parts – the lower part (NN5) and the upper part (NN6). NN5/NN6 boundary seems to be the most distinct correlation marker in the whole Central Paratethys and it can be identified in the continuous sections of the Vienna Basin. Nannoplankton preservation and occurrence in the studied area are strongly affected by the tectonic activity and by the deltaic system productions.

From the foraminiferal point of view, in the Lower Miocene were found CPN3 - CPN5 zones, with leading planktonic foraminiferal species.

The sediments of the NN4 contain highly diversified foraminiferal associations with *Bulimina elongata* d'Orbigny, *Bulimina schischkinskaye* Samoylova dominance, a lot of small *Globigerina* and *Cassigerinella*, common *Globigerina otnangensis* Roegl, *Globorotalia bykova* (Aisenstat), *Globigerinoides bispheicus* Todd and *Uvigerina graciliformis* Papp et Turnovsky are rare. The association is ranged to the M4 Zone (BERGGREN et al., 1995) and probably to the CPN5 „*Globigerinoides*

sicanus“ Zone sensu CICHA ET AL (1975) the *Praeorbulina sicana* (de Stefani) was not identified here. The two Zones sensu GRILL (1943) have been identified in the studied material containing nannoplankton of the NN5. The first one was the upper lagenide Zone rich in planktonic forms, containing mainly *Globorotalia* genus (*G. peripheroronda* Blow et Banner, *G. bykova* (Aisenstat), *Paragloborotalia mayeri* (Cushman et Ellisor) and *Globigerinoides quadrilobatus* (d'Orbigny) in the north-western part of the basin. The second Zone - *Spiroplectammia carinata* Zone sensu GRILL (1941) = agglutination Zone characterized by agglutinated species as *Spirorutilus carinatus* (d'Orbigny), *Martinotiella communis* (d'Orbigny), *Textularia pala* Czjzek, *T. mariae* d'Orbigny, *Haplophragmoides vasiceki* Cicha et Zapletalova, *Budashewaella wilsoni* (Smith), poor in planktonic foraminifer types (rare *Globigerina bulloides* d'Orbigny and *G. falconensis* (Blow)) developed mainly in the northeastern part of the studied area. Samples with nannoplankton assemblages of the NN6 Zone contain associations of traditional foraminiferal Zones (*Spiroplectammia carinata* Zone sensu Grill 1941 = agglutinated Zone, *Bolivina dilatata* Zone sensu GRILL (1941), *Bulimina / Bolivina* Zone sensu PAPP ET TURNOVSKY (1953) and *Rotalia* Zone sensu GRILL (1941)). Nannoplankton and foraminiferal study was depleted by study of the molluscs and ostracods, highly used as stratigraphic marker in the Middle Miocene sediments. As new, relatively good tool for the regional stratigraphy seems to be organic walled dinoflagellate species, which allow us to correlate Pannonian sediments in the Central Paratethys area (Tab.1).

Beside the biostratigraphy, the radiometric methods based on the ⁸⁷Sr/⁸⁶Sr ratio in the foraminiferal shales there were used. Measured isotope ratio was transform into numerical age according to Look – up Table (HOWARTH – MCARTHUR, 1997) as is shown on the Tab. 2. Results relatively good corresponds to them by (RÖGL, 1996, STEININGER, 1999).

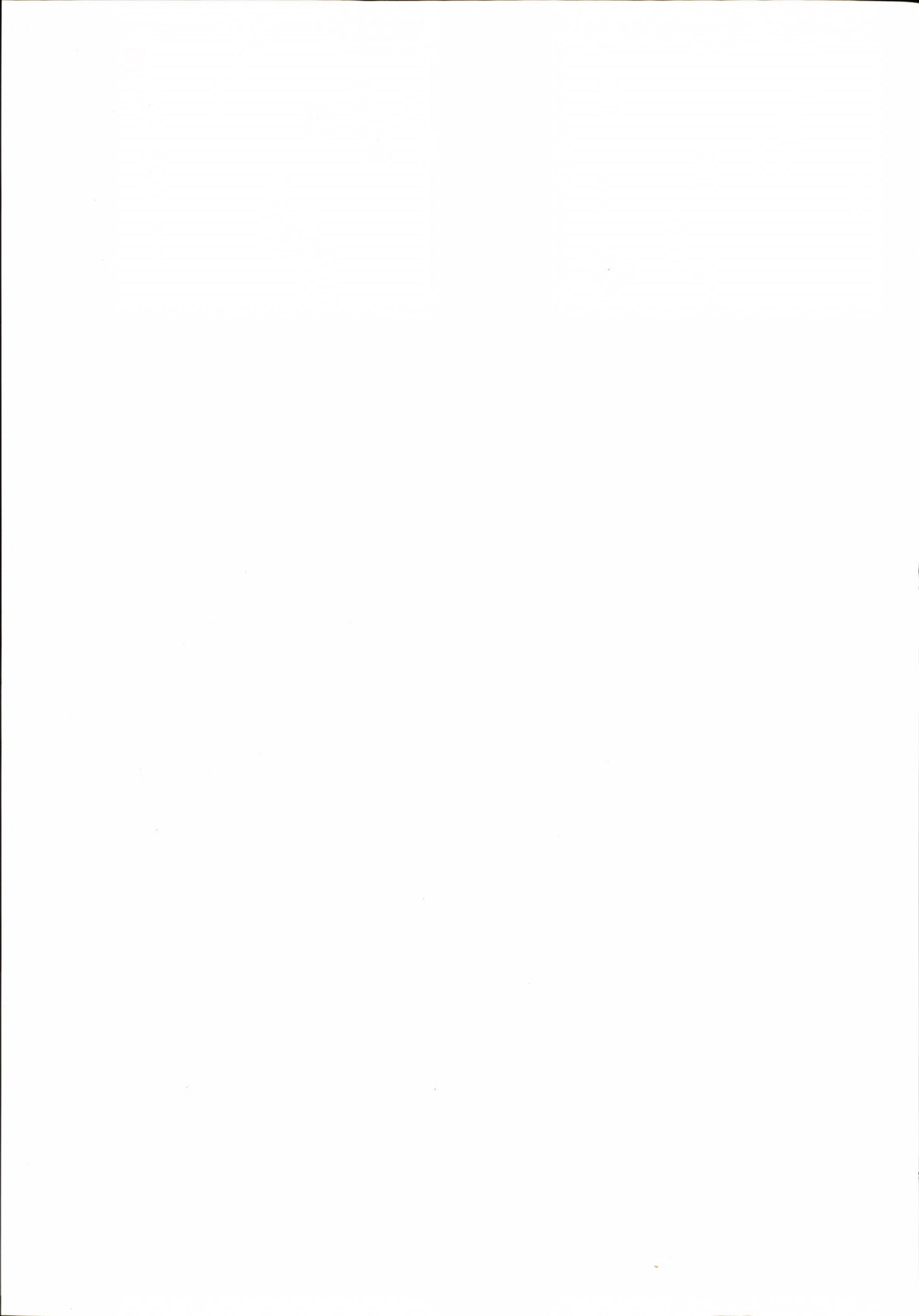
Financial support of this research came from project of Slovak Ministry of Environment VTP 130 and projects of Slovak Scientific Grant Agency VEGA 7087,1/0080/03,2074.

Table 2 Radiometric ages and processed material

Borehole, number	Deep (m)	NN Zones-	Stage	Foraminifera shales – 5mg/sample	Range with deviation	Registered
Cunín 21	930–935	NN3	Otnagian	<i>Pappina breviformis</i> , <i>Amphicoryna otnangiensis</i>	16.9–17.01	16.95
Gbely 100	1100–1105	NN4	Karpatian	<i>Lenticulina melvili</i>	15.9–16.3	16.05
Moravský Ján 3	1251.9–1258	NN4	Early Badenian	<i>Lenticulina echinata</i> (? calcite fill)	14.21–14.52	14.36
Kúty 45	506.4	NN6	Late Badenian	<i>Amphistegina mammila</i>	13.58–13.91	13.73
Devínska Nová Ves	clay pit	NN6	Late Badenian	<i>Pappina neudorfensis</i>	13.39–13.70	13.54
Široké Diely	outcrop		Sarmatian	<i>Elphidium spp.</i>	12.12–12.40	12.25

References

- Berggren, W. A., Kent, D. V., Swisher III., C. C. & Aubry, M.-P. A., 1995: Revised Cenozoic geochronology and chronostratigraphy. In: Berggren, W. A., Kent, D. V. & Hardenbol, J. (eds.): Geochronology, Time scale and Global stratigraphic correlations: a unified temporal framework for a historical geology. Society of Economic Paleontologists and Mineralogists, Special Publication No.54, 129-212.
- Cicha, I., Čtyroká, J., Jiříček, R. & Zapletalová, I., 1975: Principal biozones of the Late Tertiary in Eastern Alps and West Carpathians. In: Cicha, I. (ed.): Biozonal Division of the Upper Tertiary Basins of the Eastern Alps and West Carpathians. I.U.G.S. Proceedings of the VI Congress. Bratislava, 19-34.
- Grill, R., 1941: Stratigraphische Untersuchungen mit Hilfe von Mikrofaunen im Wiener Becken und den benachbarten Molasse-Anteilen, Oel u. Kohle 37, Berlin, 595-602.
- Grill, R., 1943: Über mikropaläontologische Gliederungsmöglichkeiten im Miozän des Wiener Becken, Mitt. Reichsanst., Bodenforsch., 6, Wien, 33-44.
- Martini, E., 1971: Standard Tertiary and Quaternary calcareous nannoplankton zonation. Proc. of the II.Plankt.Conf. Roma 1970, (ed. A. Farinacci), Edizioni Tecnoscienza, Rome, 2, 1971, 739-785.
- Papp, A. & Turnovsky, K., 1953: Die Entwicklung der Uvigerinenim Vindobon (Helvet und Torton) des Wiener Beckens, Jb., Geol. Bundesanst., 96, Wien, 117-143
- R. J. Howarth & J. M. McArthur, 1997: Statistics for strontium isotope stratigraphy: a robust LOWESS fit to the marine strontium isotope curve for the period 0 to 206 Ma, with look-up table for the derivation of numerical age. *Journal of Geology*, 105, 441-456.
- Rögl, F., 1998: Paleogeographic Considerations for Mediterranean and Paratethys Seaways (Oligocene to Miocene). Ann. Naturhist. Mus. Wien, 99A, 279-310.
- Steininger, F. F., 1999. Chronostratigraphy, Geochronology and Biochronology of the Miocene European Land Mammal Mega Zones, (ELMMZ) and the Miocene Mammal Zones, (MN – Zones). In: Rössner G. E. & Heissig K. (Eds.): The Miocene Land Mammals of Europe. Verlag Dr. Friedrich Pfeil, München, Germany.



Depositional Systems of the Northern Vienna Basin

BARÁTH, I.¹, HLAVATÝ, I.², KOVÁČ, M.³ and HUDÁČKOVÁ, N.³

¹Geological survey of Slovak Republic, Mlynská dolina 1, 81704 Bratislava

²Comenius University, Faculty of natural Sciences, Department of Geol. and Paleontol., Mlynská dolina G, 9842 15 Bratislava, Slovakia

³Slovenský plynárenský priemysel, a. s. odštepny závod Výskum a vyhľadavanie nafty a plynu (OZ VVNP),
Votrubova ul. 11/a, 825 05 Bratislava

Key words: Vienna Basin, Neogene, Sedimentology, Depositional systems

Vienna Basin, situated at the Alpine-Carpathian-Pannonian junction is one of the most explored sedimentary basins in Europe, with lots of borehole and seismic data, thus giving a good opportunity to serve as a natural laboratory for various geological studies. The sedimentary pattern of the Miocene fill is presented in lithostratigraphic scheme preferring the interrelation of individual lithotypes of rocks, each of them with conclusive genetic interpretation.

Depositional systems were defined as assemblage of process-related facies (Fisher and McGowen, 1967). The concept of a depositional system helps one to relate laterally adjacent, contemporaneous sedimentary environments and their resulting assemblages of laterally-intergradational and hence contemporaneous sedimentary facies. Thus a sedimentary facies represents a single depositional environment, and a depositional system represents a series of laterally adjacent depositional environments. Sedimentary rocks within a depositional system are related by a dispersal system (Swift and Thorne, 1991) defined as an assemblage of flow-linked depositional environments in a three-dimensional body comprising an amalgamated or averaged recording of countless individual sedimentation events. Marine depositional systems were divided into regressive and transgressive classes, thus reflecting the temporal relative sea-level changes (Swift, Phillips and Thorne, 1991).

The **Eggenburgian depositional systems** of the Northern Vienna Basin are represented mostly by shelf sand ridge depositional systems and show a distinct transgressive pattern. Initial stage of subsidence was manifested by deposition of alluvial variegated clay and sand of the Stráže Fm. in depressions. Transgressive - onshore deposits represent coarse debris aprons and marine conglomerates of Brezová, Chropov and Winterberg types (Baráth and Kováč, 1989). The offshore Eggenburgian Lužice Fm. gradually widened over the coastal sediments (Fig. 1). In the northeastern part of the basin the sedimentation started by upward fining shelf, shoreface, rocky-coast transgressive depositional system, passing upwards/landwards into a barrier-lagoon-estuary system. The southeastern part of the Štefanov depression and the

northeastern part of the Vaďovce depression were marine bays with bay-head deltas, passing upward into estuarine deposits. The brackish environment of deposition in the area of Studienka and Lakšárska Nová Ves (Jiříček, 1983) can indicate a bay-head delta also in the Závod area. At the end of Eggenburgian a relative sea-level fall caused a rapid progradation of the Štefanov regressive deltaic mouth bar depositional system on the south.

During the Early **Ottangian** the backstepping Štefanov deltaic sediments were flooded and covered by basinal Lužice clays (Fig. 1). Barrier-lagoon-estuary transgressive depositional system developed north of Štefanov, reaching a thickness 150 m (Biela, 1978). Similar transgressive system is recorded also in the Dobrá Voda depression, where the bay-head deltaic deposits are covered by dark clays within the Planinka Fm. (Kováč et al., 1991). Northern margin of the Vienna Basin show a dominance of shelf sands transgressive depositional systems, being later cut by regressive erosion. Below the Ottangian/Karpatian boundary a progradation of fluvial-deltaic Bockfliess sandy mouth bars depositional system indicates a new regression. In the Dobrá Voda depression this regression is marked by coarsening upward pattern of the Late Ottangian Planinka Fm. Clastics (Kováč et al., 1991).

The **Karpatian** stage comprises two major transgressive/regressive cycles. The first one starts by well pronounced transgressive depositional system of Týnec shelf sand ridges at the western margin of the basin and by the rapid flooding of Bockfliess deltaic body by open-marine Lakšary Fm. on the south (Fig. 1). The later widespread regression caused the deposition of alluvial Gaensendorf clastics, passing northwards into deltaic Šaštín sands, reaching a thickness of 100-400 m (Jiříček and Seifert, 1990). This north-prograding regressive mouth bar depositional system reached almost the present northern margin of the basin. The second Karpatian cycle started by flooding and capping of the Šaštín sand body by offshore Závod Fm. and by the deposition of deltaic-lagoonal Aderklaa Fm., comparable with the Láb Ostracoda Mb. (Fig. 1). The presented succession is interpreted as a barrier-lagoon-estuary transgressive depositional system. At the end of Karpatian the lagoonal deposition was replaced by the north-prograding gravelly Aderklaa and Jablonica regressive mouth bars (Fig. 6). Large areas of the basin

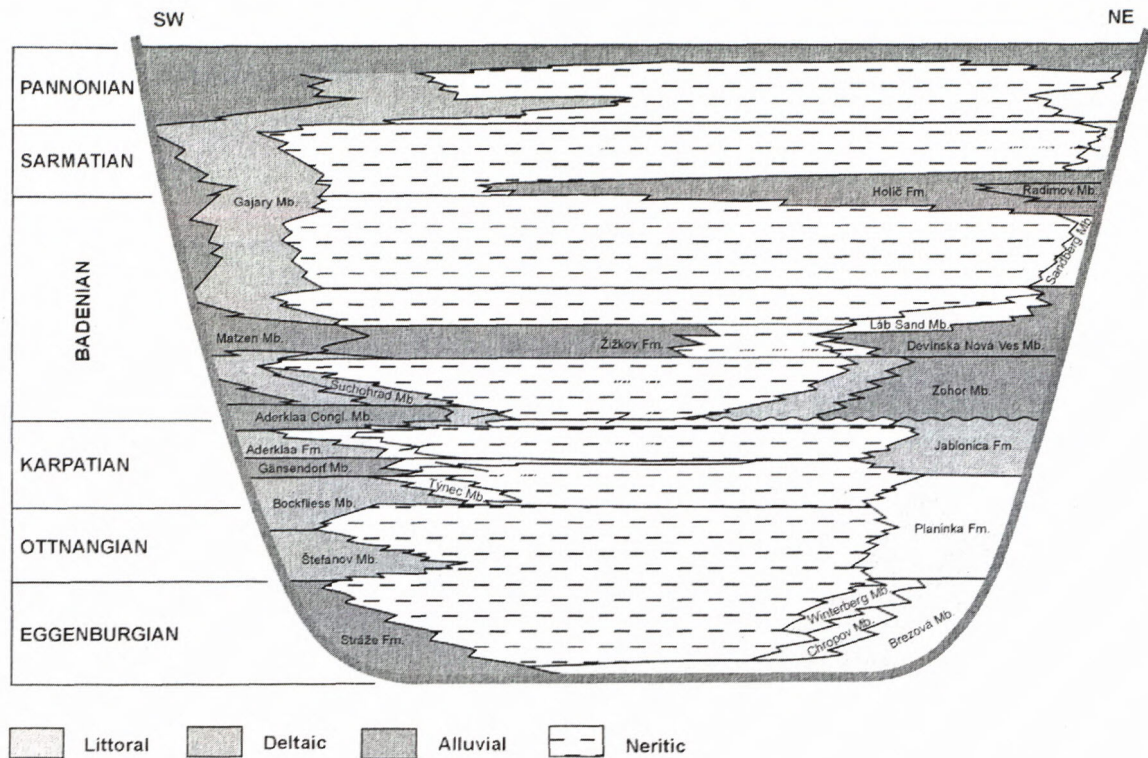


Fig. 1 Chart of the Northern Vienna Basin model of depositional facies, lithostratigraphy, and transgressive/regressive patterns.

have got hypersaline with the deposition of Kúty anhydrite Mb., followed by large-scale erosion in the north-eastern part of the Vienna Basin.

The **Early Badenian** backstepping of the Suchohrad deltaic and Zohor alluvial-deltaic bodies and their gradual transition into shelf sand ridges mirror the new transgression to the southeast (Fig. 1). Similar depositional systems bound the northern margin of the basin, however the transgressive shelf ridges are without deltaic supply, and their clastic material came from the ravined underlying deposits. In this area the shoreface sand is covered by Lanžhot Fm. offshore clays.

At the Early/Middle Badenian boundary a major regression caused the origin of alluvial, deltaic and lagoonal Žížkov Fm., representing the strandplain-shelf and/or prograding mouthbar regressive depositional system. At its base, there occur also littoral Studienka sands, deposited probably in the early-regressive shelf plume system (Fig. 1). Another regressive mouth bar system is represented by Matzen sand in the Gajary and Suchohrad area (Jiříček, 1988, 1990). At the eastern margin of the basin the Láb sand sheet with algal bioherms, capped by offshore Jakubov Fm. clay document a new transgression in the late Middle Badenian time.

The **Late Badenian** sedimentation at both the eastern and northern margins of the basin started by minor regressive progradation of small mouth bars, which were rapidly replaced by transgressive Sandberg shelf sands depositional system with algal biostromes. The Upper Badenian transgression caused a widening of the open-marine Studienka clay Fm. depositional areas northwards (Fig. 1). At the end of Badenian time variegated facies

started to prograde at the northern margin of the basin, thus marking the strandplain-shelf regressive depositional systems. In the same time the prograding Gajary mouth bar regressive depositional system originated on the south. These depositional systems document a new early regressive phase of the basin history.

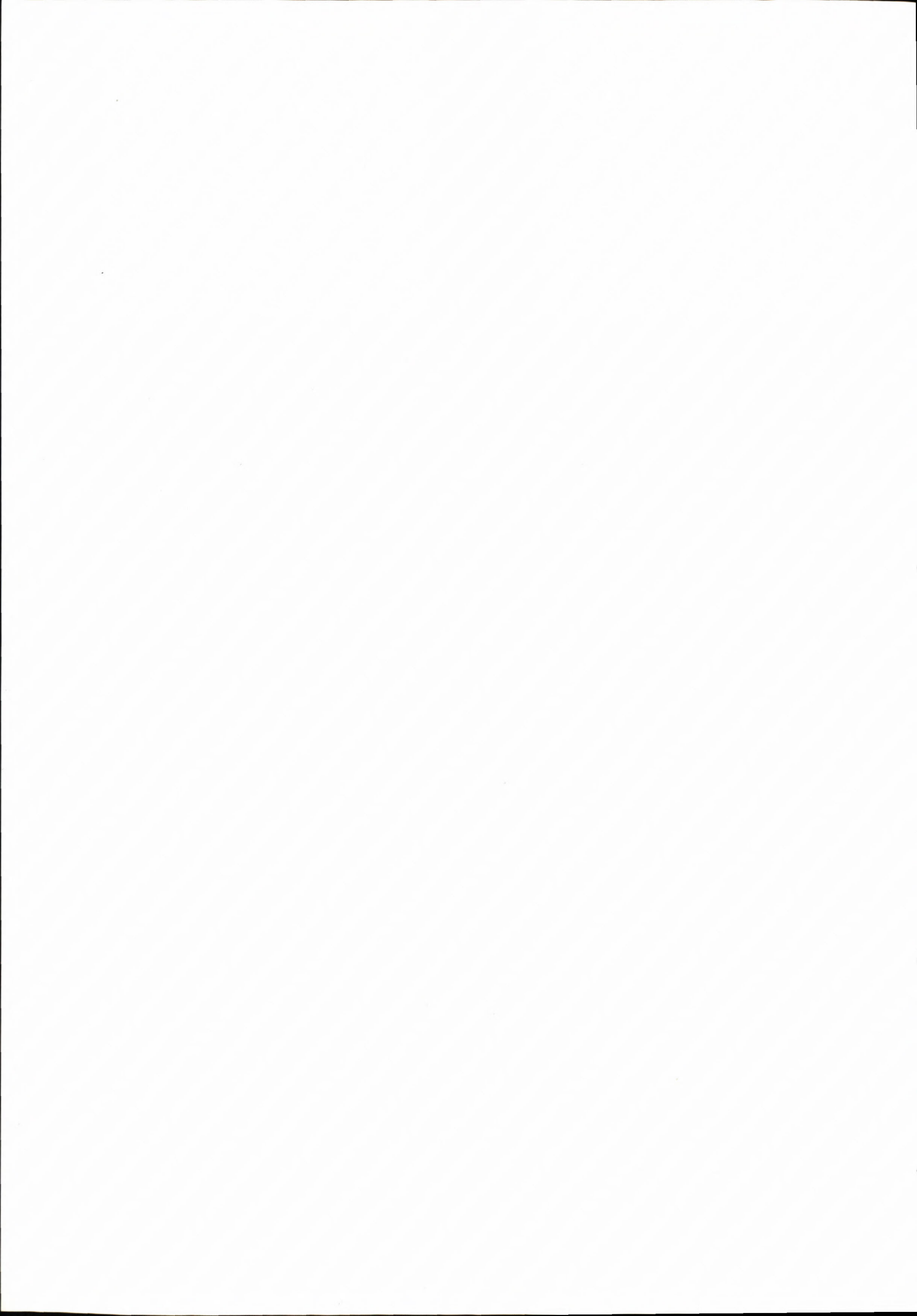
During the early **Sarmatian** time a large-scale regression caused the retreat of brackish sea-shore southwards to the area of Malacky, Láb and Vysoká (Jiříček, 1988). The regressive alluvial plane-strandplain-shelf depositional system is represented by the rapidly prograding Holíč Fm. in the northern part of the basin (Fig. 1). The new Sarmatian transgression is represented by wide flooding of the northern basin margins by brackish-water Skalica Fm., comprising tidal sand bars and bryozoan-serpulid limestones transgressive system (Fig. 1). At the end of Sarmatian the prograding deltaic mouth bars of the paleo-Danube river mirror a regression in the southwestern part of the basin, continuing up to the early Pannonian time (Jiříček, 1985). Similar regressive mouth bar depositional system originated on the north (Elečko and Vass, 2001).

The next **Pannonian** brackish-water transgressive/regressive cycle is represented by the Lower Pannonian Záhorie Fm. (Fig. 1). From the Upper Pannonian time, the sedimentary environments became to be coal-bearing limnic and alluvial in the whole Vienna Basin (Baráth and Kováč, 2000).

Financial support of this research came from project of Slovak Ministry of Environment VTP 130 and projects of Slovak Scientific Grant Agency VEGA 7087,1/0080/03, 2074.

References

- Baráth, I. & Kováč, M., 1989: Sedimentation conditions and source areas of the Eggenburgian clastics in the western part of the Western Carpathians. *Knihovnička Zemního plynu a nafty*, sv. 9. *Miscellanea micropalaentologica IV.*, (Hodonín), pp. 55-86. (in Slovak).
- Baráth, I. & Kováč, M., 2000: Miocene sequence stratigraphic key surfaces and depositional systems tracts in the Western Carpathian basins (Central Paratethys, Slovakia). *Slovak Geol. Mag.* 6, 2-3 (Bratislava), pp. 92-94.
- Biela, A., 1978: Hlboké vrty v zakrytých oblastiach vnútorných Západných Karpát. *Regionálna Geol. Západ. Karpát* 10, Geol. Úst. D. Štúra (Bratislava), 224 p.
- Elečko, M. & Vass, D., 2001: Sarmatian lithostratigraphic units of the Vienna Basin. *Mineralia slov.* 33, 1 (Bratislava), pp. 1-6.
- Fisher, W. L. & McGowen, J. H., 1967: Depositional systems in the Wilcox Group of Texas and their relationship to the occurrence of oil and gas. *Trans., Gulf Coast Ass. Petrol. Geol. Soc.* 17, pp. 105-125.
- Jiříček, R., 1983: Paleogeografie a subsidence neogénu Vídeňské pánve. In: *Závěrečná zpráva úkolu „Vyhledávací průzkum živič ve Vídeňské pánvi“*. MS, Archiv MND Hodonín, pp. 187-226.
- Jiříček, R., 1985: Deltový vývoj spodního panonu v jižní části vídeňské pánve. *Zemní Plyn a Nafta* 30,2, Hodonín, 161-186.
- Jiříček, R., 1988: Stratigraphy, paleogeography and thickness of the Neogene sediments in the Vienna Basin. *Zem. plyn a nafta*, 33,4, (Hodonín), pp. 583-662. (in Czech).
- Jiříček, R., 1990: Fluvial and deltaic systems of Neogene Paratethys. In: *Sedimentologické problémy Západných Karpát. Konferencie-symposiá-semináre*, GUDŠ, Bratislava, pp. 79-88.
- Jiříček, R. & Seifert, P., 1990: Paleogeography of the Neogene in the Vienna Basin and the adjacent part of the foredeep. In: D. Minaříková and H. Lobitzer eds.: *Thirty Years of Geological Cooperation between Austria and Czechoslovakia*. ÚÚG, Praha, pp. 89-104.
- Kováč, M., Baráth, I., Šutovská, K. & Uher, P., 1991: Changes in sedimentary record of the Lower Miocene in the Dobrá Voda Depression. *Mineralia slov.*, 23, pp. 201-213.
- Swift, D. J. P. & Thorne, J. A., 1991: Sedimentation on continental margins, I: a general model for shelf sedimentation.
- Swift, D. J. P., Phillips, S., Thorne, J. A. 1991: Sedimentation on continental margins, IV: lithofacies and depositional systems. In: D. J. P. Swift, G. F. Oertel, R. W. Tillman, J. A. Thorne (eds.): *Shelf Sand and Sandstone Bodies*. *Int. Ass. of Sedimentologists, Spec. Publ.* 14, pp. 89-152.



absence of *Ligerimys*) clearly indicate mammal zone MN5. Furthermore the evolutionary level of *Spermophilinus besanus*, *Palaeosciurus sutteri* and *Glirulus diremptus* point to the early MN5. The magnetostratigraphic data of the sections Teiritzberg and Obergänsersdorf (SCHOLGER, 1998) allow a magnetostratigraphic correlation with the chrons C5Cn2n or C5Cn3n of the latest Karpatian. Since the chron C5Cn2n is correlated with the beginning of the Badenian (BERGGREN et al., 1995), only the earlier normal interval C5Cn3n is plausible which corresponds to an age between 16.5 and 16.7 million years (DAXNER-HÖCK, 1998).

2. The terrestrial vertebrates from Mühlbach and Grund in the Molasse Basin of Lower Austria were deposited in lower Badenian marine sediments, and are mixed with predominating marine fauna. The rodents *Cricetodon meini*, *Democricetodon mutilus*, *Democricetodon* cf. *gracilis*, *Megacricetodon minor*, *Eumyarion* sp., *Spermophilinus besanus* and *Prodryomys satus* indicate MN5. Among them *C. meini* and *M. minor* point to late MN5. The most abundant rodent, *C. meini*, is an immigrant from SW-Asia. In the Middle Miocene (MN5) it migrated from Greece to Central Europe, ultimately reaching Western Europe and becoming extinct at the end of MN5. Its first and last occurrence in the Molasse Basin of Bavaria is below the „Brock“ horizon (i. e. before the Ries event dated at 14.9 million years). In the Alpine Molasse Basin from Austria it was recovered from the upper Grund beds,

which were identified based on the marine fauna to represent the late Lower Lagenidae Zone (RÖGL et al., 2001). According to Rögl et al. (2003) the estimated age is 15.1 million years.

References

- Berggren, W. A., Kent, D. V., Swisher, C. C. & Aubry, M. P. (1995): A revised Cenozoic geochronology and chronostratigraphy.- SEPM (Society of Sedimentary Geology), Special Publication, **54**: 129-212, Tulsa.
- Daxner-Höck, G. (1998): Säugetiere (Mammalia) aus dem Karpat des Korneuburger Beckens. 3. Rodentia und Carnivora.- Beitr. Paläont., **23**: 367-407, Wien.
- Harzhauser, M., Daxner-Höck, G., Boon-Kristkoiz, E., Coric, S., Mandic, O., Miklas-Tempfer, P., Roetzel, R., Rögl, F., Schultz, O., Spezzaferri, S., Ziegler, R. & Zorn, I. (2003): Palaeoecology and biostratigraphy of the section Mühlbach (Gaiendorf Formation, lower Middle Miocene, Lower Badenian, Austria).- Annalen des Naturhistorischen Museums in Wien, **104 A**: Wien (in press).
- Rögl, F., Spezzaferri, S. & Coric, S. (2002): Micropaleontology and biostratigraphy of the Karpatian-Badenian transition (Early-Middle Miocene boundary) in Austria (Central Paratethys).- Cour. Forsch.-Inst. Senckenberg **237**: 47-67, Frankfurt a. M.
- Rögl, F. & Spezzaferri, S. (2003): Paleocology and biostratigraphy of the foraminifera in the Mühlbach section (Gaiendorf Formation, Badenian).- Annalen des Naturhistorischen Museums in Wien, **104 A**: Wien (in press).
- Scholger, R. (1998): Magnetostratigraphic and palaeomagnetic analysis from the Early Miocene (Karpatian) deposits Teiritzberg and Obergänsersdorf (Korneuburg Basin, Lower Austria).- Beitr. Paläont., **23**: 25-26, Wien.

Indicators of terrestrial ecosystems in the Karpatian Korneuburg Basin and the Badenian Grund Beds

P. M. TEMPFER¹ and G. DAXNER-HÖCK²

Natural History Museum Vienna, Burgring 7, A-1014 Wien.

¹petra.tempfer@nhm-wien.ac.at

²gudrun.hoeck@nhm-wien.ac.at

The Lower Austrian localities Obergänserndorf and Teiritzberg (both: Early MN5, Lower Miocene) within the Karpatian Korneuburg Basin are compared with Mühlbach and Grund (both: Late MN5, Middle Miocene) of the Molasse Basin in an ecological point of view and based on the terrestrial fauna elements.

The excavations organized by the Natural History Museum Vienna have taken place from 1987 to 1993 in Obergänserndorf and Teiritzberg. They have been financed by the FWF-Project P-80889GEO. Two books have already been published, the last one just this year (Sovis & Schmid, 1998; Sovis & Schmid, 2002).

Relating to the profiles, in Teiritzberg marine/brackish elements are mixed up with the terrestrial fossils, while in Obergänserndorf marine/brackish layers are alternating with terrestrial/limnic ones. Following the Maximal Number of Individuals, rodents are most frequent. Insectivora, Reptilia, Amphibia, Artiodactyla and, concerning Teiritzberg, also the tooth of a bear as a member of the Carnivora are present. Among the rodents, the diversity of glirids as well as the predominance of eomyids as not burrowing animals point to a high groundwater-level. A large flying squirrel is present which needs a stepped wood for flying. Relating to the Insectivora, the water shrew as a member of the Insectivora is typical for a damp environment. The living relatives of the Alligator *Diplocynodon* inhabit fluvial systems along rivers these days. Amphibians which permanently need water closeby for reproduction and often also for hibernation are represented by a. o. *Rana* and *Pelobates*. Summarizing, the terrestrial faunas of Obergänserndorf and Teiritzberg indicate swampy environments along rivers and brackish marshes (Harzhauser et al., 2002).

In Mühlbach and Grund, the excavations have taken place in 1996 and from 1998 to 1999. They have been organized by the the Institute of Paleontology of the Vienna University as well as the Natural History Museum Vienna. Investigations on vertebrates are financed by the FWF-Project P-15724. Part of the material originates from the collecting of Mag. A. Kroh. Papers have already been published (Roetzel, 1999) and two second contributions to these localities are in progress (Boon, E., Coric, S., Daxner-Höck, G., Göhlich, U., Harzhauser, M., Huttunen, K., Miklas-Tempfer, P. M., Roetzel, R., Rögl, F., Schultz, O., Spezzaferri, S., Ziegler, R. & I. Zorn in progress; Pervesler in progress).

In both localities, terrestrial elements are mixed up with marine ones. In Grund, the relatively diverse vertebrate fauna – including fish, amphibians, reptiles, birds, large and small mammals – is represented by only few specimens. Contrary to that, the terrestrial vertebrate groups of Mühlbach consist of small specimens only and single teeth or bone fragments are preserved. Not only large mammals but also adjoined elements are missing. Therefore, the major part of the fossils originates most probably from bird pellets. Among the rodents, burrowing cricetids and gophers predominate which points to the existence of dry woodland and a low groundwater-level. The Erinaceidae as member of the Insectivora are most frequent and typical for woodlands near waters. Amphibians are nearly missing which indicates dry conditions confirmed by the reptile genera *Testudo*, *Ophisaurus* and *Lacerta*. As single exceptions, a terrapin, a water snake and an ide as a freshwater fish need some small freshwater habitats closeby but in general, locally more dry than humid conditions are indicated.

These special and controverse ecological situations can also be explained by the location of the fossil sites. The Karpatian Korneuburg Basin as a side Basin of the Vienna Basin and limited by the Waschbergzone in the West and the Flyschzone in the East offered an Estuary with swampy environments as living space for the terrestrial fauna there (Harzhauser et al., 2002). The locality Mühlbach of the Badenian Grund Beds is situated within the Molasse Basin. Very probably, the coast there was steep leading to a dry hinterland with some small water habitats closeby.

References

- Boon, E., Coric, S., Daxner-Höck, G., Göhlich, U., Harzhauser, M., Huttunen, K., Miklas-Tempfer, P. M., Roetzel, R., Rögl, F., Schultz, O., Spezzaferri, S., Ziegler, R. & I. Zorn (in progress): Ann. Naturhist. Mus. Wien, **104**.
- Harzhauser, M., Böhme, M., Mandic, O. & Ch.-Ch. Hofmann (2002): The Karpatian (Late Burdigalian) of the Korneuburg Basin - A Palaeoecological and Biostratigraphical Syntheses. In: Sovis, W. & B. Schmid (eds.): Das Karpat des Korneuburger Beckens / Teil 2. Beitr. Paläont., **27**: 441 - 457. - Wien.
- Pervesler, P. (in progress): (ed.): Geologica Carpathica.
- Roetzel, R. (1999): (ed.): Arbeitstagung 1999 Retz - Hollabrunn. Beiträge Arbeitstagung Geol. Bundesanst. **1999** Retz - Hollabrunn. - 363 pp. - Wien.
- Sovis, W. & B. Schmid (1998): (eds.): Das Karpat des Korneuburger Beckens / Teil 1. Beitr. Paläont., **23**: 413 pp. - Wien.
- Sovis, W. & B. Schmid (2002): (eds.): Das Karpat des Korneuburger Beckens / Teil 2. Beitr. Paläont., **27**: 467 pp. - Wien.

Stratigraphy of the Grund Fm., based on the Foraminifera

¹IVAN CÍCHA and ²PETR LÍZAL

¹Czech Geological Survey, Klárov 3, 118 21 Prague

²Technical University of Brno, Faculty of Civil Engineering, Údolní 53, 602 00 Brno

New research above all in the Alpine – Carpathian foredeep brought results that correct our opinions of the border lower Miocene in view the global subdivision – Burdigalian s. l. and middle Miocene from the point of view of global analysis – Burdigalian s. l. and middle Miocene (Langhian and Karpatian and lower Badenian). According to the prevailing opinion, the sedimentation was interrupted between the Karpatian and the lower Badenian in Paratethys and basal clastics of Badenian were deposited approximately in one period, divided from underlying Karpatian.

Detailed analysis of foraminifera of Karpatian and lower Badenian proved the sequence developed in the Alpine Carpathian foredeep from the point of view of fauna and lithology corresponds with sequence from Karpatian to lower Badenian. Signs of shallowing in the sedimentation area have been proved in the dividing line of Karpatian and Badenian in many places. This is characterised by alternation of sands, clays and rare gravels. In the Alpine Carpathian foredeep, typical association of the upper Karpatian are accompanied by numerous representatives of genus *Globorotalia* s. l., which appear in the underlying beds of the zone *Globigerinoides bisphericus*. It was only in the overlying beds of this zone where the first representatives of genus *Praeorbulina* were proved, that are accompanied by typical *Uvigerinas* of Karpatian in the oldest Badenian. This community of the oldest Badenian cannot be considered to be lower Lagenidae zone, particularly with *Lenticulina echinata*, *Planularia* div. sp. This development was studied in details in the region of Grund on sheets 1: 50 000 Hollabrunn and Hadres, e. g. between Wullersdorf and Buchberg – Mailberg. By mapping boreholes thicker basal clastics were not proved. They are known from the area of Novosedly, Brno etc., the sequence between typical *Uvigerina* Karpatian (Laaer Formation) and typical Lagenidae Badenian was classified as Grund Formation. The name Grund beds has been generally used since mid 19th century. In 1957, R. Weinhandl used the name Grund layers on sheet Hadres for the uppermost Helvetian (now Karpatian) and the oldest Tortonian (now lower Badenian).

Rögl et al (1998) in Cícha et al. (1998) compare from the point of view of stratigraphy the Grund Formation with lower Lagenidae zone of lower Badenian Roetzel et al (1999) – geological map Hollabrunn 1: 50 000 do not

exclude the Grund Formation to belong to the upper Karpatian before the oncome of *Praeorbulina*. It is necessary to point out that Rögl et al. (1998) consider genus *Uvigerina macrocarinata* and e. g. *Vaginulina legumen* to be typical representatives of Lagenidae zone in this area. In another paper, Roetzel et al. (1999) consider typical locality Grund to be lower Badenian in age on the basis of appearance of small mammal *Megacricetodon*. In this area, Austrian and Italian geologists (Spezzafieri et al. – unpublished) later found 3 small specimens of the genus *Praeorbulina* in association with microfauna of the Laaer Formation.

Stráník, Brzobohatý (2002) are considering the transgression of the Grund Formation to progress from south-east to north-east. The presence of these layers is quite probable in Ostrava region. In the Carpathian foredeep in Moravia, e. g. in the region of Hnanice, in boreholes HJ – 3 Žatěany, HJ – 5 Žaběice, HJ – 2 Otmarov, HJ – 105 Dvorská, HJ – 4 Syrovice, HJ – 103 Opatovice, HJ – 101 Ěrnovice, in the surrounding of Brno, a group of layers can be found, which from faunistic and lithological point of view corresponds to Formation from Karpatian to lower Badenian. Similar development can be supposed in northern part of the foredeep in Austria, too.

The arrangement of layers of lower Badenian is still a problem. This is the case of clastics Formation of the region of Brno, gravels from Troskotovice, Novosedly, Drnholec and clastics in central part of Carpathian foredeep, e. g. in boreholes near Radslavice, Brodek u Pøerova, Vlkoš.

In the Alpine-Carpathian foredeep, younger foraminifera fauna of lower Badenian can be found – *Lenticulina echinata*, *Planularia auris*, *Planularia antillea ostraviensis*, *Planularia dentata*, *Palmula jonesi*, *Lingulina costata* etc. The above mentioned fauna is plentiful in so called „Tegel“ in the surrounding of Brno, the Neogene of the Boskovice furrow (southern part), Boraè, central Moravia etc. These communities are from younger beds as the Grund Formation. The relationship of these *Planularia* etc. developments to Neogene of Appenine peninsula, it is to Langhian and Serravallian. In the Appenine peninsula between type locality of Langhian and Serravallian (Rögl – private information), there exists Hiatus in the period of 1 mio years and border stratotype between Langhian and Serravallian has not been determined yet.



Distributional patterns and shifts of early Middle Miocene Gastropod Faunas in the Central Paratethys

MATHIAS HARZHAUSER

Museum of Natural History, Vienna; mathias.harzhauser@nhm-wien.ac.at

Early Badenian gastropod assemblages of the Central Paratethys are best documented by the Austrian faunas of Styria and Lower Austria and by the Hungarian fauna of Varpalota. The Austrian faunas are known to science for more than 150 years and were usually termed as the „Grund Fauna“. Due to an inadequate definition of the now historical stage „Helvetian“, the separation of the advanced „Grund Fauna“ from the slightly older Early Miocene Karpatian one remained doubtful throughout most of the 20th century. However, during the last years the Middle Miocene status of the fauna was accepted by most workers based on the increased biostratigraphic data. Recently the dating was confirmed by magnetostratigraphy, mammals and planktonic foraminifera. These data document a gap between the Karpatian gastropod fauna of the Korneuburg Basin and the Badenian section Grund of approximately 1.5 ma.

Both faunas may be considered as typical migrational faunas, since both faunas coincide with a marked transgressive event from the Mediterranean area into the Central Paratethys.

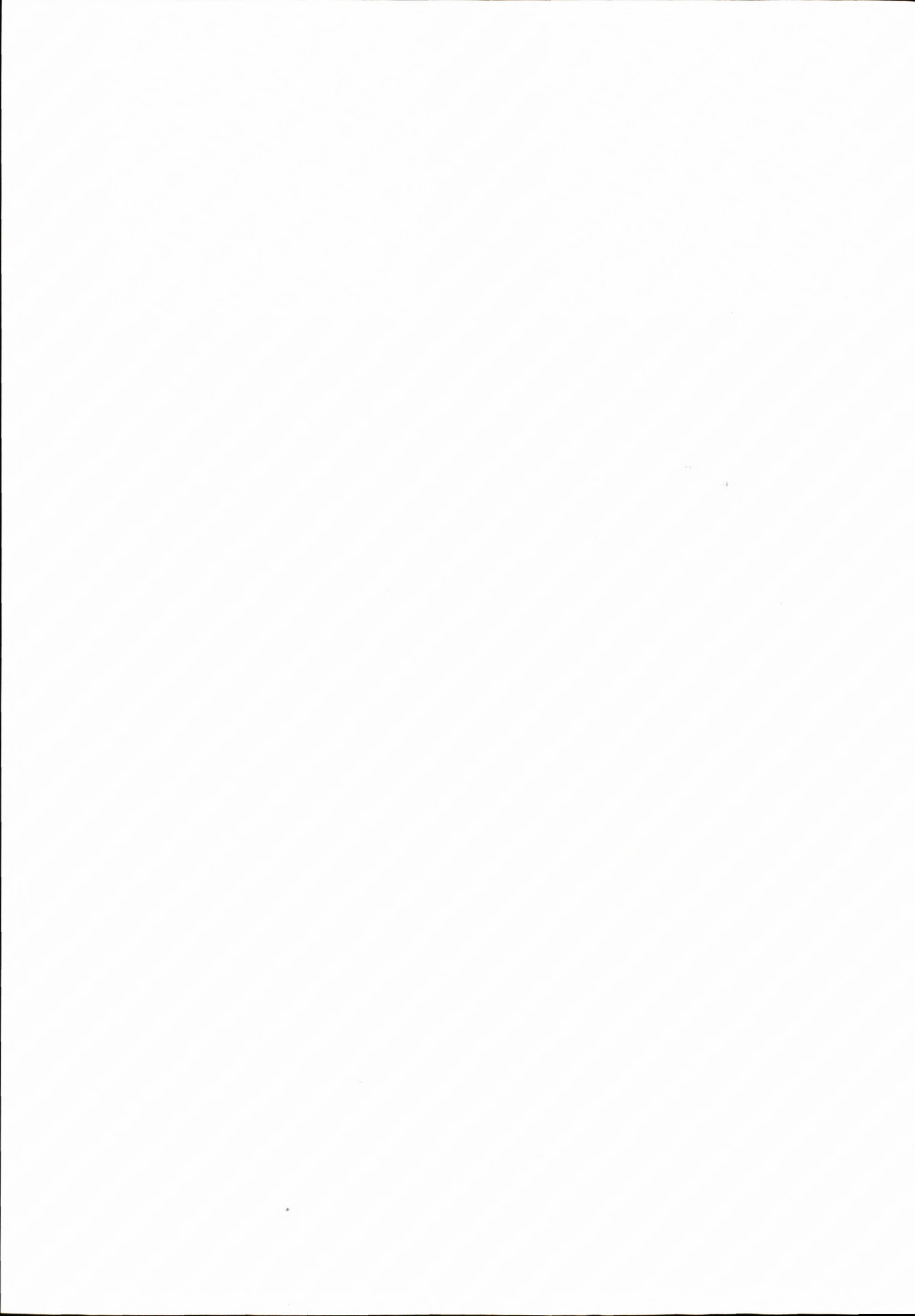
One of the main differences between the late Early Miocene Karpatian gastropod faunas of the Western Paratethys and those of early Middle Miocene Badenian faunas is a sudden increase in diversity. About 150 gastropod species of the Karpatian are opposed by more than 300 species of the Early Badenian. This „bloom“ can be observed within most gastropod families but is most conspicuous within the cypraeids, turrids, cancellariids, nassariids, or muricids. However, the modern character of the fauna is not only based on the evolution of new Paratethyan taxa (e.g. within nassariids) but is probably only a result of immigration from the adjacent Mediterranean. Nonetheless, the Karpatian fauna was also characterised by a high number of immigrations, resulting in more than 70% of „Mediterranean“ species within the Central Paratethyan Korneuburg Basin (Austria).

Despite the documented open seaways and the fair possibilities for migration, several Early Miocene Mediterranean species did not enter the Central Paratethys before the Badenian. Among these species *Rimella (Dientomochilus) decussata* (DEFR.), „*Pseudonina*“ *reysi* COSSM. & PEYR., *Fasciolaria (Pleuroploca) tarbelliana* (GRAT.), or *Morum (Oniscidia) cythara* (BROCCHI) are typical. Mediterranean origin is also likely for taxa such as *Malea (Cadium) denticulata* (DESH.) and *Pereiraea gervaisi* (VÉZIAN). Obviously, the ecological conditions

allowing the northward migration of these species were established not before the Early Badenian. Similarly, the strombid *Tibia dentata* (GRAT.) is unknown from the Karpatian of the Paratethys but forms extraordinary large populations in the Mediterranean at that time (Mut Basin in Turkey, Qom Basin in Central Iran). Nevertheless, the same species starts to form equivalent populations within the Styrian Basin in the Early Badenian, witnessing a distinct extension of its optimum-zone into the southern Central Paratethys. Comparable northward restrictions in their Middle Miocene distribution area can be documented for the stromboids *Pereiraea gervaisi* (VÉZIAN) and *Strombus schroeckingeri* (HOERN.) which both are restricted to the southern basins of the Central Paratethys.

Within the Paratethys the Early Badenian gastropod fauna is also highly indicative in respect to biostratigraphy. Several species, such as *Trigonostoma crenatum* (HÖRN.), *Rimella (Dientomochilus) decussata* (DEFR.), *Pereiraea gervaisi* (VÉZIAN), *Strombus (Euprotomus?) schroeckingeri* HÖRNES, *Malea (Cadium) denticulata* (DESH.), and *Cassidaria cingulifera* HOERN. & AUING. seem to be restricted to this rather short time slice. Furthermore, the surprising bloom of many Early Miocene (Karpatian, Burdigalian) relics characterises the fauna. Thus, the Central Paratethys acted as Early Badenian sanctuary for several Early Miocene species, which are otherwise highly characteristic for the Karpatian assemblages of the Paratethys. These „old fashioned“ survivors such as *Tympanotonos papaveraceus* (BAST.), *Turritella gradata* MENKE, *Protoma cathedralis* BAST., *Euthriofusus burdigalensis* (DEFR.), *Ocenebra (Ocinebrina) crassilabiata* (HILBER), and *Perrona louisae* (HÖRN. & AUING.) have a last but strong acme in the „Grund Fauna“ but fade abruptly without reaching the Middle Badenian. Some of these relics are not „Kümmerforms“ indicating a near extinction but display rather a peak concerning numbers of individuals as well as size. But even within persistent species such as *Volema (Melongena) cornuta* (AGASSIZ), *Genota ramosa elisae* HÖRN. & AUING., *Tibia dentata* GRAT., *Gyrineum (Aspa) marginatum* (MARTINI), *Mitra scrobiculata* (BROCC.), *Tudicla rusticula* (BAST.) and the *Nassarius dujardini-edlaueri-schoenni* group a similar „bloom“ can be observed in the Early Badenian.

Generally, the thermophilic character of these assemblages – indicated among others by a maximum diversity of strombids throughout the history of the Paratethys – agrees well with an Early Langhian climatic optimum.



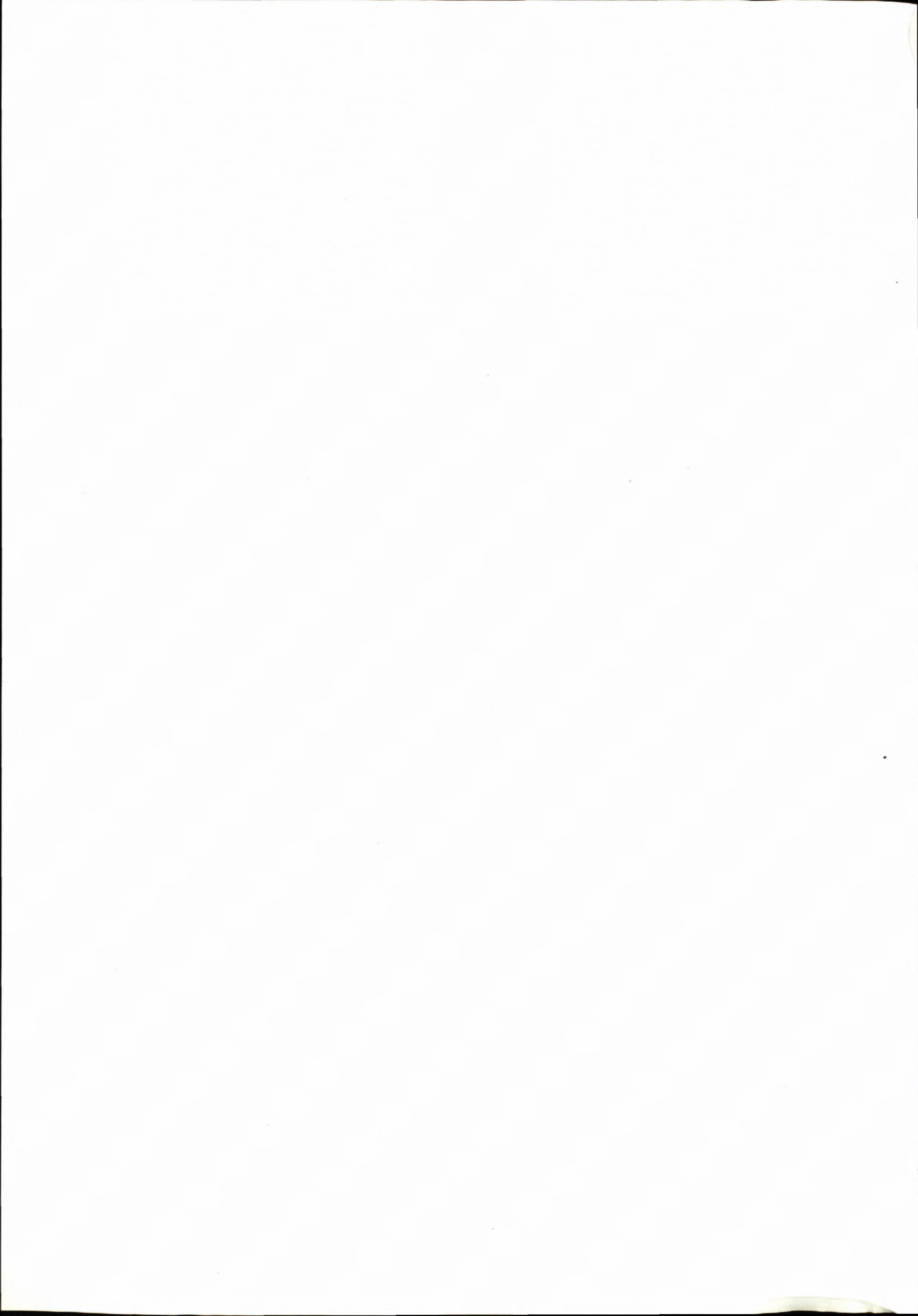
A simple method of depth estimation based on presence/absence data using benthic foraminifera

JOHANN HOHENEGGER

Institut für Paläontologie, Universität Wien

A two-step procedure for estimating paleogradients is presented. The first step requires ranges of variates corresponding to the fundamental (general) distributions at the gradient. These distributions are independent of local variations. Using species as variates and samples as objects, fundamental ecological niches along the environmental gradient represent these general distributions. The second step involves a transfer equation. It is based on the arithmetic mean of location parameters of these distributions that are weighted by their dispersion parameters. This procedure gives weight to variates with smaller dispersions, which yield more information about the location at the gradient than variates with wide dispersion. The method proposed here does not require information about

frequencies; solely the presence of variates is sufficient. Objective criteria are used to eliminate variates like species, which do not overlap in living individuals along a gradient but are mixed in samples of empty tests. This is important in estimating paleogradients because mixing of non-overlapping variates is a common effect due to taphonomic processes like transport, bioturbation, or sediment reworking. The new method is successfully applied for depth estimation using shallow-living benthic foraminifera and empty test from the NW Pacific, living smaller benthic foraminifera from the shelf and continental slope of Senegal, and benthic foraminifera with low planktic forms from the Upper Karpatian below the Styrian unconformity.



Palaeoecological evaluation of the Karpatian sediments in the southern part of the Carpathian Foredeep using trend analysis

PAVLA PETROVÁ

Czech Geological Survey, Leitnerova 22, 658 69 Brno, Czech Republic

Key words: Carpathian Foredeep, Karpatian, Foraminifera, Palaeoecology, Biostratigraphy

The objectives of the abstract include characteristics of foraminifers in Karpatian sediments in the southern part of the Carpathian Foredeep, Moravia, the trend analysis of the assemblages and application of statistical methods to reconstruct the palaeoecological evolution of the depositional area. In the resulting model the palaeogeographical and biostratigraphic aspects are also addressed.

Majority of the foraminiferal assemblages characterized by abundance of uvigerinas and pappinas (*U. graciliformis* Papp & Turn., *P. breviformis* (Papp & Turn. etc.) belong to the „lower part“ of the Laa Formation (Rögl, 1969). Nevertheless, few assemblages with *Globigerinoides bisphericus* Todd have been recorded and compared with the „upper part“ of the Laa Formation. Sediments of the Grund Formation with abundant *Globigerinoides bisphericus* Todd lying unconformable on sediments of the Laa Formation (Rögl et al., 2002) were not recorded in the area under study.

Generally, the palaeoecological conditions were not equal in the Karpatian deposits in Moravia. The juxtaposed assemblages are often different. Alternation of the depleted foraminiferal assemblages with the richness as well as alternation of assemblages with dominance of planktonic genera and benthic ones indicate unbalanced environment. This phenomenon has been already observed by Nehyba & Petrová (2000).

Based on study of foraminiferal microfauna and correlation of the boreholes, the following model is proposed for development of Karpatian basin. Two transgressions within Karpatian sediments has been recognized.

1. The transgression of Karpatian sea reached the southern part of the Carpathian Foredeep from Mediterranean. During the first period of the transgression covered the area of nowadays Mikulov, Pohořelice and Nový Přerov villages and documents the maximum thickness of Karpatian sediments. Later, during the Savian orogeny, these strata were overthrust by the nappes of the Carpathian Flysh Belt. Microfaunistic assemblages indicate anoxic conditions at beginning of the transgression. Locally, foraminiferal microfauna with *Siphonodosaria* div. sp. and *Valvulineria complanata*

d'Orb. was recorded. Horizons with agglutinated foraminifers (NP-1, NP-2, Břez-2 boreholes) characterized by genera *Bathysiphon*, *Haplophragmoides* and *Cribrostomoides*, were recognized in the wide environs of Mikulov and Laa an der Thaya towns. Their presence reflects the cold deeper water conditions from lower littoral to upper bathyal.

2. Next transgression proceeded in direction of the western part of the Carpathian Foredeep and overlaps the sediments of the Eggenburgian-Ottngian (?) age alike in the eastern part. In the lowermost part of these sediments, anoxic conditions appear. Later, euryoxybiont taxa such as *Bolivina* div. sp., *Bulimina* div. sp., *Praeglobobulimina* div. sp., *Uvigerina* div. sp. predominate and document the improvement of the palaeoenvironmental conditions, stability of the oxygen supply and subsidence of the basin.

In the overlying deposits, number of reduced horizons decreases, horizons with euryoxybiont foraminifers (in the Nos-3, HV-304, HV-306 boreholes) alternate those with high number of planktonic specimens. The sudden alternations of depleted horizons that characterize reduced environment with the euryoxybiont ones with locally shallow-water fauna can be explained by upwellings accompanied by oscillation of sea level, probably with restricted water circulation. This explanation is further evidenced by lithological analyses.

Depleted microfauna is observed in the majority of boreholes in the Upper Karpatian and reflects an aggravation of the living conditions. In the uppermost part of borehole profiles the shallow-water assemblages were observed with exception of HV-301, HV-305 and Zn-12 boreholes. Palaeogeographically, the conditions of sedimentation in the Karpatian in the southern part of the Carpathian Foredeep can be compared with conditions of anoxic silled basins with positive water balance and so-called estuarine type water circulation.

The synsedimentary tectonic deformations are documented within the terminal shallow-water sedimentation and especially in its overlying strata that were deposited W of the front of the Žďánice Unit. Based on foraminiferal study, two blocks can be delimited in the studied area and in cross-sections. The western block is limited by the normal fault that is closing in the Karpatian. The increasing of thickness of Karpatian sediments may result

from the overthrust fault tectonics in the eastern block. According to seismic profile interpretations the overthrust fault tectonics has character of sinistral faults (Čížek, personal comm.). The changing thickness of Karpatian sediments in the western block where the final shallow-water sediments are missing (HV-301, HV-305, Zn-12) is due to the post-Badenian erosion.

Tectonic movements were formerly interpreted on the seismic profiles (Adámek, personal comm.). The present study of foraminiferal assemblages provides a model that further documents existence of the tectonic deformations.

References

- Nehyba, S. & Petrová, P. (2000): Karpatian sandy deposits in the southern part of the The Carpathian Foredeep in Moravia. *Věst. ČGÚ*, 75, 1, 53-66. Praha.
- Rögl, F. (1969): Die miozäne Foraminiferenfauna von Laa an der Thaya in der Molassezone von Niederösterreich. *Mitt. Geol. Gessel.*, 61, 63-123. Wien.
- Rögl, F., Spezzaferri, S. & Coric, S. (2002): Micropaleontology and biostratigraphy of the Karpatian-Badenian transition (Early-Middle Miocene boundary) in Austria (Central Paratethys). *Cour. Forsch.-Inst. Senckenberg*, 237, 47-67. Frankfurt a. M.

The palaeoenvironment of an early Middle Miocene Paratethys sequence in NE Austria with special emphasis on paleoecology of mollusks and foraminifera

OLEG MANDIC¹, MATHIAS HARZHAUSER², SILVIA SPEZZAFERRI¹ and MARTIN ZUSCHIN¹

¹ Institute of Paleontology, University of Vienna, Althanstrasse 14, 1090 Wien, Austria.

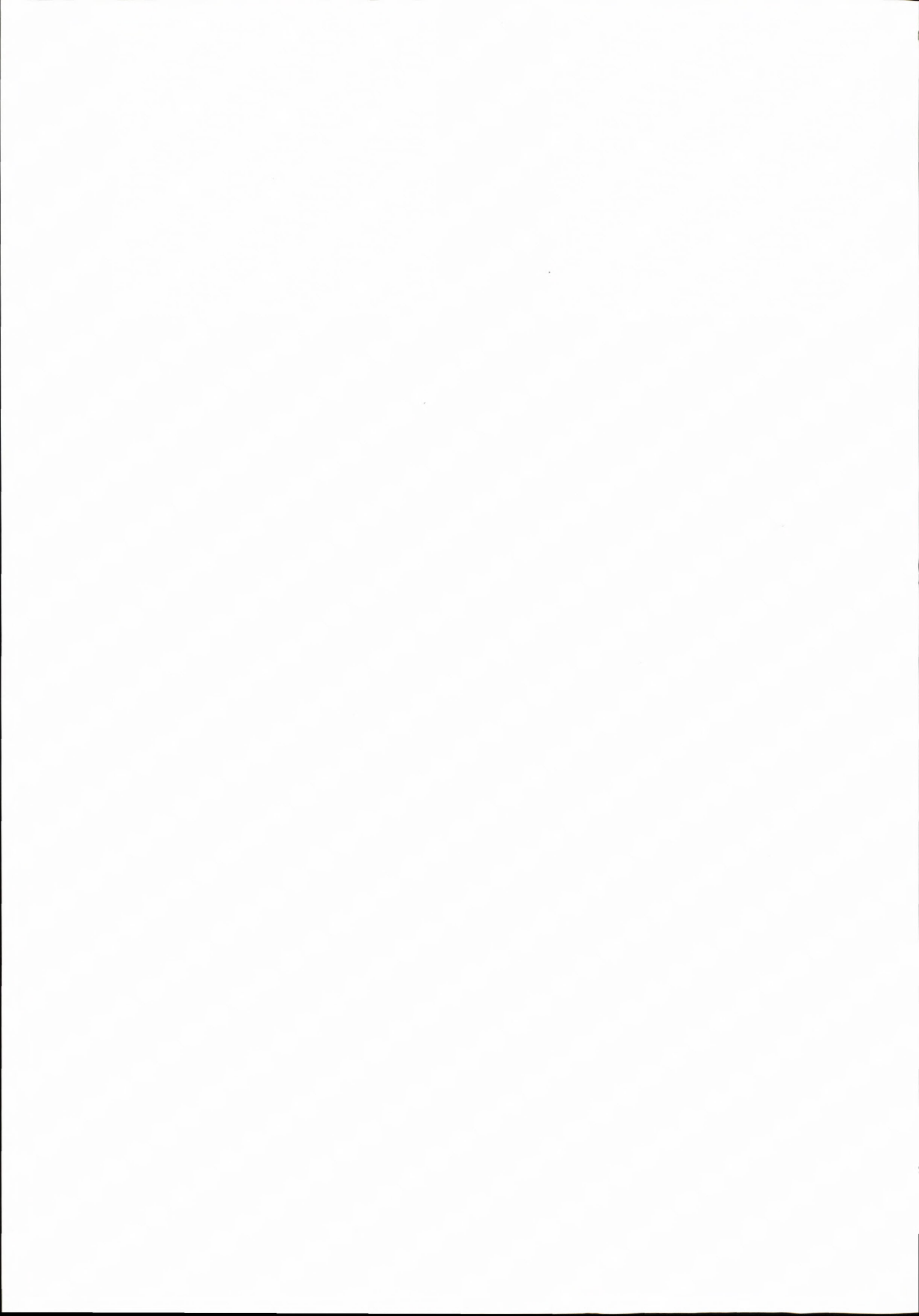
² Museum of Natural History, Burgring 7, BOX 417, A-1014 Wien, Austria.

In a multidisciplinary approach including data on paleoecology of foraminifera, mollusks, balanids and coralline algae, as well as on taphonomy, sedimentology, sequence stratigraphy and regional geology, the environmental reconstruction for the Niederleis Basin (a satellite depression of the Vienna Basin and important fossiliferous site of the Central Paratethys region) is provided. The data came from two sections in proximal (section Buschberg) and distal (section Bahnhof) position relative to the northwesterly exposed basement chain (Leiser Berge). The accomplished analysis confirmed the presumed bathymetric and paleogeographic differences. The study represents a partial results of Austrian Scientific Foundation (FWF) projects „Temporal and spatial changes of microfossil associations and ichnofacies in the Austrian marine Miocene” (P 13743 - BIO) and „Evolution Versus Migration: Changes in Austrian Marine Miocene Molluscan Paleocommunities” (P 13745 - BIO).

The data on foraminifera suggest that the sediments from the section Buschberg were deposited in water depth not exceeding 100 m and that a possible displacement episode occurred at the base of the studied sequence. The composition and taphonomy of shell beds within that partial section indicates proximal storm deposition within the inner shelf area. The masses of balanids implies the presence of abundant littoral hard substrata. Relatively deep water-sediments at only 200 m distance from the paleo-

shore indicate the presence of a drowned paleocliff, that may correspond to the northwestern tectonic margin of the Niederleis basin.

The sediments from the section Bahnhof were deposited in deeper water. A paleodepth from 100 to 500 m for the Bahnhof-section is indicated by foraminifera. Water depth increased from the bottom to the top of the section. Suboxic conditions prevailed at its base, more oxic condition prevailed upward. A massive displacement episode occurred in the middle part of the section and involved sediment from a shallower environment. Displaced benthic foraminifera and mollusks suggest water depth not exceeding 30 m. Whereas the fossil record from autochthonous layers implies deepening upward, the mixed fossil assemblage from tempestites implies shallowing of the supply center, respective gradual installation of extended onshore to lagoonal habitats within the basin's marginal area. Thus a synsedimentary tectonic sagging respective the subsidence of the basin as a result of synchronous extensional tectonics is inferred. This interpretation can be underpinned with the regional geologic situation. Moreover it stays in accordance with the inferred biostratigraphic position of studied series within the late Lower Lagenidae Zone corresponding with the regional maximal flooding surface respective with the following high stand system tract of the Vienna Basin.



Lower Miocene of the Hustopeče Gate

ZDENĚK STRÁNÍK

Czech Geological Survey, Leitnerova 22, 658 69 Brno, Czech Republic

Hustopeče Gate in South Moravia represents a young morphologic depression probably of the Early Quaternary age. This depression originated on the Lower Miocene deposits superimposed on the Ždánice unit.

The Lowermost strata of Miocene deposits are represented by Šakvice Marl characterized by grey, white weathering unstratified marls with the concretions of dolomitic limestones. According to the micropaleontological studies (Cicha & Pícha, 1964, Molčíková in Stráník a kol., 1982) the marls provided Foraminifera assemblages with rich bathysiphons and genera *Cyclamina*, *Bolivina*, *Bulimina*, *Globigerina* that indicate deeper neritic environment. Nannofossils are represented by species *Discoaster druggi*, zone NN2 and *Sphenolithus belemnos*, zone NN3. Both Foraminifera and Nannofossils indicate the Eggenburgian age. Šakvice Marl does not manifest any distinct discontinuity with the underlying Ždánice-Hustopeče Formation.

The upper part of the Šakvice Marl is characterized by a layer (horizon) of slightly calcareous clays with scales of fish. The thickness of Šakvice Marl reaches up to 300 m.

The Pavlovice Formation overlying the Šakvice Marl is characterized by green-grey and brown clays with some intercalations of pelosiderites and volcanoclastics. According to Nehyba (pers. com.) these volcanoclastics correspond to the upper horizon of volcanoclastics (horizon 2) of the SW part of the Carpathian Foredeep (Nehyba, 2000). Limonite and jarosite are frequently present as products of weathering. The Pavlovice Formation was deposited in the anoxic shallow neritic environment with decreased salinity and unfavourable living conditions.

The overlying diatomite sequence (up to 20 meters in thickness) is formed in its lower part by massive diatomite clays followed by laminated diatomites in the upper part of the sequence. The massive diatomites contain freshwater and brackish diatoms represented by genera *Melosira* and *Coscinodiscus*. The laminated diatomites provided pelagic diatoms of the deeper neritic environment of open sea. The total thickness of the Pavlovice Formation attains 175 m.

The Laa Formation represents the youngest strata of the Lower Miocene fill in the Hustopeče Gate. It overlies the diatomites and consists predominantly of grey stratified calcareous clays with seldom laminae and inter-

calations of sand and sandstone. Based on micropaleontological investigation these strata were described by Pokorný (1961). They contain relatively rich marine foraminiferal assemblages corresponding to zones No. I and No. II of the Karpatian Stage (sensu Cicha and Zapletalová, 1974). Čtyroký (1963) determined from these strata the macrofauna species *Macoma* cf. *elliptica* HOERN. and *Lucina* sp. A lumachelle-layer with representative of genera *Lucina* in the vicinity of Zaječí were found. The same macrofauna is known from the Karpatian strata of the Carpathian Foredeep (locality Zbýšov near Slavkov) and in the Váh Valley, western Slovakia.

Lower Miocene deposits in the Hustopeče Gate form the brachysyncline disturbed by faults. During the Styrian orogeny these deposits were folded and thrust together with the older strata of the Ždánice unit over the sediments of the Pouzdřany unit and Lower Miocene fill of the Carpathian Foredeep. The identical NE-SW directions of the b-axes of folds of the Ždánice-Hustopeče Formation and the overlying Pavlovice Formation support the opinion that the Styrian orogenic movements completely overprinted the phenomenon of previous Savian orogeny. These observations are in agreement with the structural studies by Fodor (1995) and Nemček et al. (1998). According to these authors, the stress-field in the Carpathian Flysch did not change in the period from the Late Oligocene up to Miocene.

The Lower Miocene deposits indicate the marine connection between the Carpathian Foredeep and the Intracarpinian basins across the Flysch belt in the southern Moravia. Their conformable position on the underlying Ždánice-Hustopeče Formation and deep-sea foraminiferal assemblages support the assumption that the realm of Ždánice and Pouzdřany units represented the depocentrum of the Paratethys in the Early Miocene.

Reference

- Cicha, I. and Pícha, F. (1964): Contribution to the stratigraphical and lithological development of the southeastern part of the Ždánice unit. Sbor. geol. Věd, G. 4, 137-158, Praha, (German and Russian res.).
- Cicha, I. and Zapletalová, I. (1974): Probleme of the stratigraphy of the Miocene in the middle part of the Carpathian Foredeep. Zem. Plyn Nafta, 19, 453-460, Hodonín, (in Czech).
- Čtyroký, P. (1963): Note of the micropaleontological and mapping investigations of the Ždánice unit. Zpr. geol. Výzk. v R. 1962, 216-217, Praha, (in Czech).

- Fodor, L. (1995): From transpression to transtension: Oligocene-Miocene structural evolution of the Vienna Basin and the East Alpine - West Carpathian junction. *Tectonophysics*, 242 (1995), 151-182.
- Nehyba, S. (2000): The cyclicity of the Lower Miocene deposits of the SW part of the Carpathian Foredeep as the depositional response to the sediment supply and sea-level changes. *Geol. Carpatica*, 51, 1, 7-17, Bratislava.
- Nemčok, M., Houghton, J. J. and Coward, M. P. (1998): Strain partitioning along the western margin of the Carpathians. *Tectonophysics*, 292 (1998), 119-143.
- Pokorný, V. (1961): Contribution to the microstratigraphical division of the „Hustopeče Marls“ in the vicinity of Trkmanec and Zaječí (Ždánice unit, southern Moravia). *Čas. Min. Geol.*, 6, 3, 305-315, Praha, (English res.).
- Stráník, Z. (1983): Outer Carpathians in the South Moravia. In Samuel, O. & Gašpariková, V. eds.: 18th European Colloquy on Micropaleontology (excursion guide). *Konference, Symposia, Semináře, Geol. Úst. D. Štúra*, 167-175, Bratislava.
- Stráník, Z. et al. (1982): Note explicative to the geological map 1:25 000, 34-213 Hustopeče. – MS, Czech geol. Survey, Praha.

Middle Miocene nanofossils in the Carpathian Foredeep, Czech Republic (state-of-the-art)

LILIAN ŠVÁBENICKÁ

Czech Geological Survey, Klárov 131/3, P. O. Box 85, CZ-118 21 Praha, Czech Republic; svab@cgu.cz

Two different nanoplankton horizons were recognized in the Middle Miocene (Lower Badenian) deposits of the Carpathian Foredeep in the territory of the Czech Republic (southern and central Moravia, approximately in quadrangle of towns Znojmo – Mikulov – Přerov – Olomouc). Horizons were described by Švábenická (2002a, b) and their precise stratigraphic correlation is recently under discussion. Material was obtained during mapping and other geological works and was taken from the same samples as used for the foraminiferal study. No continuous section crossing the Karpatian-Badenian and the overlying Lower Badenian strata has been available yet.

I. Horizon with *Helicosphaera waltrans*

Nanofossil assemblages are characterized by presence of *H. waltrans* and by only occasional occurrence of *Sphenolithus heteromorphus*. They are represented by high number of helicoliths complemented by small placoliths of family Prinsiaaceae (*Reticulofenestra pseudoumbilicus*, *R. haqii* etc.). Horizon should be subdivided into two parts:

1. co-existence of rare *H. waltrans* and *H. ampliaperata*, helicoliths and reticulofenestrids prevail,

2. *H. waltrans* relatively common; rare appearance of specimens of genera *Discoaster*, *Umbilicosphaera*, *Pontosphaera* and *Calcidiscus*. Species *H. ampliaperata* is already absent.

Horizon was observed in clays and siliciclastic sediments of the Grund Formation and in the basal Lower Badenian deposits where planktonic foraminifers *Globigerinoides bisphericus*, *Praeorbulina* ex gr. *glomerosa* and *Orbulina suturalis* appear (Cicha, 2001). Sediments yield generally poorly preserved nanofossils of low species diversity. Reworked coccoliths from the Upper Cretaceous and Paleogene strata prevail, Miocene specimens form only 10-20% of taphocoenoses.

Character of nanofossil assemblage, especially the predominance of helicoliths indicates the shallow epicontinental sea (sensu Báldi-Beke, 1980, Nagymarosy, 1985).

II. Horizon with *Sphenolithus heteromorphus*

Nanofossil assemblages are characterized by high species diversity and show following attributes:

- presence of *Sphenolithus heteromorphus*,
- absence of *Helicosphaera waltrans*,
- genus *Helicosphaera* is represented by common *H. carteri*. Species *H. walbersdorfensis* if present has been observed in higher numbers
- high number of small placoliths of family Prinsiaaceae including species *Reticulofenestra minuta*, *R. haqii* and *R. pseudoumbilicus* (forms <5µm and >5µm).

Assemblages are mostly complemented by species *Pontosphaera multipora*, *Umbilicosphaera rotula*, *Calcidiscus premacintyreii*, *C. macintyreii*, *C. leptoporus*, *Discoaster exilis*, *D. variabilis*, large forms of *Coccolithus miopelagicus* (>10µm in size), *Rhabdosphaera* ssp. (sensu Young 1998) including *R. sicca* etc.

In some deposits (probably going with the upper part of horizon), elliptical varieties of *Coronocyclus nitescens* appear, along with 5-rayed symmetrical discoasters and enigmatic specimens of genus ?*Catinaster*. The last mentioned specimens could be explained also as a central part of *Discoaster musicus*, nevertheless, this species has not been observed in studied material.

Calcareous nanofossils form a significant component in sediment and specimens are moderately well preserved. Compare to underlying deposits and horizon with *H. waltrans* respectively, taphocoenoses are characterized by increasing number of Miocene specimens forming about 50-70%. Reworked coccoliths are mostly of the Upper Cretaceous and Middle Eocene age. According to Cicha (2001), horizon was observed in the Lower Badenian basal and marginal siliciclastic sediments and clays („tegel“). They are characterized by the occurrence of benthonic species *Vaginulina legumen* and Lanzendorf microfauna (Čtyrká and Švábenická, 2000).

Influx of Miocene nanoflora and character of assemblage indicate the deepening of depositional area and open-sea conditions and reflect the transgression.

Paleoenvironmental notes:

High number of helicoliths indicates a shallow epicontinental sea and the occasional occurrence of other coccoliths probably a beginning of transgression.

The change in quality and quantity of nannofossil assemblages, that is enrichment in discoasters and coccoliths gives evidence for the open-sea conditions and reflects transgression in the Lower Badenian. This change probably coincides with the last occurrence (absence) of *Helicosphaera waltrans*.

References

- Báldi-Beke, M., 1980: The nannoplankton of the Oligocene-Miocene sediments underlying the Börzsöny Mts. (Northern Hungary) and sites. *Földt. Közl., Bull. Hung. Geol. Soc.* 110, 159-179 (in Hungarian with English abstract).
- Cicha, I., 2001: Outline of the stratigraphy of the Middle Miocene in the Alpine-Carpathian foredeep (Lower Austria, Moravia). *Scr. Fac. Sci. Nat. Univ. Masaryk. Brun., Geol.* 30, 2000, 23-26.
- Čtyroká, J. & Švábenická, L., 2000: Biostratigraphic evaluation of Badenian deposits on the Olomouc map-sheet (Foraminifers and Calcareous Nannofossils). *Zpr. Geol. Výzk. v roce 1999*, 17-20 (in Czech with English abstract).
- Nagymarosy, A., 1985: The correlation of the Badenian in Hungary based on nannofloras. *Ann. Univ. Sci. Budapest, Geol.* 25, 33-86.
- Švábenická, L., 2002a: Calcareous nannofossils of the Upper Karpatian and Lower Badenian deposits in the Carpathian Foredeep, Moravia, Czech Republic. *Geol. Carpathica* 53, 3, 197-210.
- Švábenická, L., 2002b: Calcareous nannofossils of the Middle Miocene deposits in the Carpathian Foredeep, Czech Republic. *Geol. Carpathica* 53, spec. issue, 71-72.

Around the Early/Middle Miocene (Karpatian/Badenian) Boundary in the Austrian Neogene Basins. A Story of Gaps.

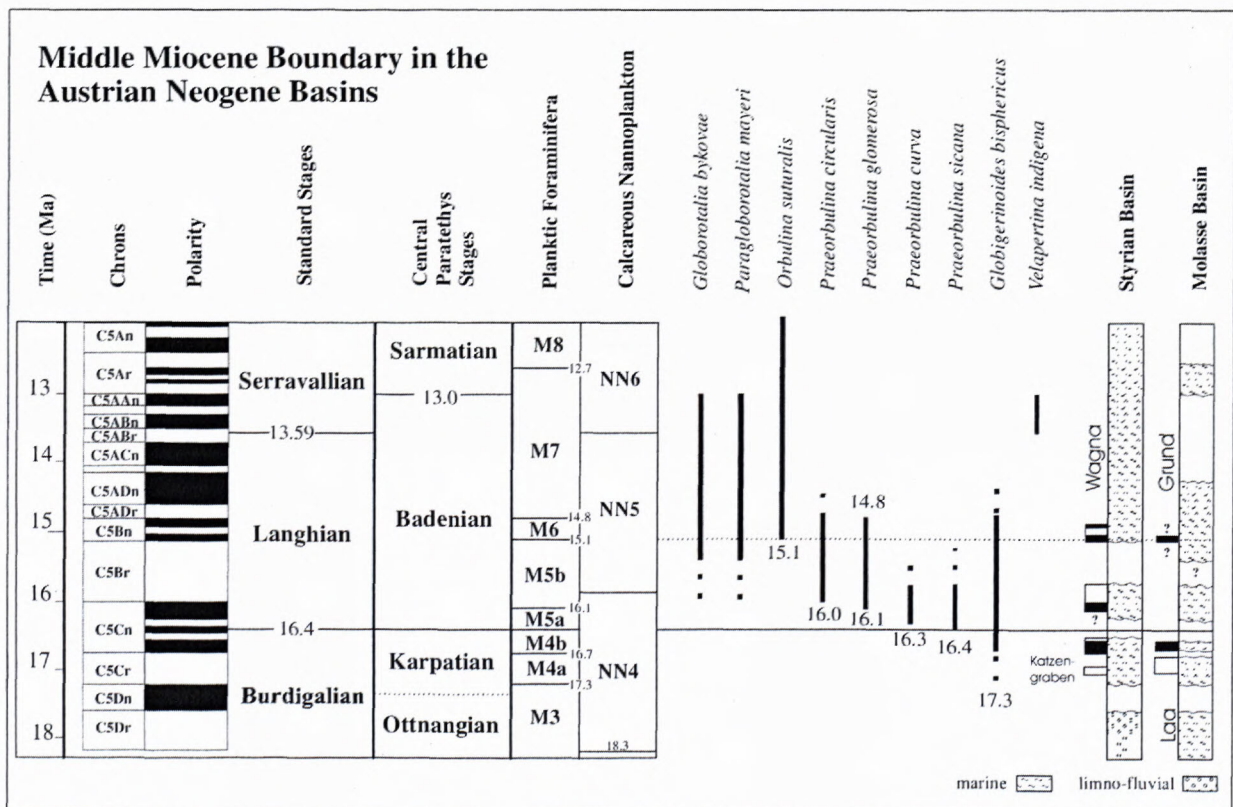
STJEPAN CORIC, JOHANN HOHENEGGER, PETER PERVESLER, REINHARD ROETZEL, FRED RÖGL,
ROBERT SCHOLGER, SILVIA SPEZZAFERRI and KARL STINGL

FWF Project P 13743-BIO
FWF Project P 13738-TEC

Investigations of sedimentary sequences around the Karpatian - Badenian boundary were carried out on sections in the Austrian part of the Alpine-Carpathian Fore-deep (Molasse Basin), the southern Vienna Basin, and predominantly the Styrian Basin. Results are based on calcareous nannoplankton, planktonic foraminifera, and palaeomagnetic measurements. No continuous sedimentation between the Karpatian and Badenian has been recorded. In response to the Styrian tectonic phase the Lower Badenian similarly shows a series of gaps.

In the Wagna section (Styrian Basin) the Karpatian is represented by calcareous shales and interbedded dolomitic -sideritic limestone beds from an upper bathyal environment. Stratigraphic results show NN 4, *Globige-*

rinoides bisphericus, and for the most part normal magnetization, with a short reversal at the top. The Lower Badenian sediments follow with a slight angular unconformity, with silts and fine sands of littoral environment, and a clay pebble layer at the base; dated as NN 4, with very scarce *Praeorbulina sicana*, and no paleomagnetic signal. Higher up, the fine sands are rich in biogeneous detritus, and have a small coral patch reef intercalated; stratigraphy is still NN 4 and a zone of normal and reversed magnetization. Discordantly follow knobby calcareous sandstones (very rich mollusc fauna in casts) and fine sands; these are dated as NN 5 and fall in a normal chron. Apparently there exists a long gap, spanning most of chron C5Br, with a duration of about 600 000 yrs. The



upper part of the sequence belongs to the „Leithakalk“, coralline limestones and marls lying on fine sands of the arenitic sequence, probably with a short gap. Stratigraphically, the „Leithakalk“ belongs to NN 5, yielding *Po. glomerosa* s.l. and in the uppermost part also *Orbulina suturalis*. The lower part of the limestones still lies in a normal chron, followed by a short reversal, and again a normal magnetization on top.

In the southern Vienna Basin a drill site for mineral water was studied. The Badenian transgressed on Mesozoic dolomites with a non-fossiliferous breccia. For the first time NN 4 is recorded here. The lowermost soft sediments are brown marls, with a rich assemblage of *Helicosphaera ampliaperta*, and blue-grey silty marls („Badener Tegel“) which belong to NN 5. In both sediments the *Po. glomerosa* group occurs, and in the blue-grey marl also *O. suturalis* (Lower Lagenidae Zone).

Karpatian sediments were studied in the Molasse Basin north of the Danube (Alpine-Carpathian Foredeep) at Laa an der Thaya, brickyard and drill site. The blue-grey calcareous shales of the Laa Formation belong to NN 4 and are reversed magnetized. Discordantly follow green-

ish clays and yellowish brown fine sands, which are normally magnetized. The normal chron is correlated with the Karpatian of the Korneuburg Basin, and dated as C5Cn.2n.

The Grund Formation was studied at the type locality, where the layered fine sands and silts are deeply cut by mollusc bearing channels. Nannoplankton with *Helicosphaera waltrans* gives a zonation of NN 5, which is supported by the rare occurrence of *Po. glomerosa circularis*. The extent of the Grund Fm. is verified in the OMV drill site Roggendorf-1, where clastics and gravels transgress at a drill depth of 360 m on the Laa Fm. The clastic sequence is dated as NN 4, whereas the higher part with finer sediments belongs to NN 5. Only the topmost part contains a rich benthic and planktonic foraminiferal fauna with *Po. glomerosa circularis* and *O. suturalis*. Additionally the Badenian transgression was dated in prospecting drill sites in the Krems embayment, where the basal conglomerates are equally dated as NN 4, together with *Po. glomerosa*. Palaeomagnetic measurements in the Grund type locality show a normal polarisation, and are correlated with chron C5Bn.2n.

The molluscan composition of the tempestitic shell beds of the Grund Formation (Lower Badenian, Middle Miocene) in Lower Austria

MARTIN ZUSCHIN^A, MATHIAS HARZHAUSER^B and OLEG MANDIC^A

^AInstitute of Palaeontology, University of Vienna, Althanstraße 14, A-1090, Vienna, Austria,

^BMuseum of Natural History Vienna, Burgring 7, A-1014, Vienna, Austria

Artificial outcrops in the Grund Formation identified its typical shell beds as distinctly allochthonous tempestites, which are inappropriate to reconstruct paleocommunities and their ecological parameters. Quantitative bulk samples from five of these shell beds are very similar to each other with regard to the faunal composition of their most abundant taxa. We identified 129 morphospecies from more than 4200 individuals. Only thirteen of them can be considered to be abundant, because they contribute at least 1% to the total abundance present in the five samples. In contrast to the faunal composition of

the most abundant taxa, species richness and the frequency distribution (and their descriptive parameters) of shell sizes differ strongly between the five shell beds. A regression analysis identifies the diversity (measured as species richness) of the shell beds as functions of shell sorting: Badly sorted shell beds have higher species richness than well sorted shell beds. The species richness present in Grund is therefore taphonomically controlled, because the sorting of the allochthonous shell beds is ruled by their transport history.



Paleogeography and sequence stratigraphy of the Northern Vienna Basin

¹HLAVATÝ, I., ¹ŠÁLY, B., ²KOVÁĚ, M. and ³HUDÁČKOVÁ, N.

¹Slovenský plynárenský priemysel, a. s. odštepny závod Výskum a vyhľadavanie nafty a plynu (OZ VVNP),
Votrubova ul. 11/a, 825 05 Bratislava

²Comenius University, Faculty of natural Sciences, Depart. of Geol. and Paleontol., Mlynská dolina G,
98 42 15 Bratislava, Slovakia

Key words: Vienna Basin, Neogene, Sequence stratigraphy

Paleogeography and sequence stratigraphy of the Vienna Basin, similarly as other Western Carpathian Neogene basins, was heavily overprinted by tectonics during the Carpathian orogen collision with the European platform and evolution of the Pannonian back arc basin.

Southward migration of the Early Miocene depocenters, followed by deepening in the northern part during the Middle Miocene is a common feature of basin paleogeography. These facts are in good agreement with tectonics controlling basin evolution:

a) the Eggenburgian–Ottangian transpressional tectonics led to piggy-back basin development on the top of the thrust nappes of the Flysch zone belonging to the Western Carpathian accretionary wedge, as well as development of the wrench fault furrow type basins in front of the paleoalpine consolidated part of the orogen,

b) during the Karpatian and the Early Badenian transpressional tectonics controlled formation of the pull-apart basin depocenters,

c) whole crustal extension led to graben and horst structure evolution in the Middle – Late Miocene.

Sedimentary gap (hiatus) and erosion at the Early / Middle and Middle / Upper Miocene boundary can be recognized not only on the basin margins but often also in the basin fill. As good correlation levels in the Vienna Basin, similarly as in all Western Carpathian basins can be used:

- Eggenburgian transgression (NN 2) ca 20.5 My
- Karpatian transgression (NN4, *Uvigerina graciliformis*) ca 17.5 My
- Early Badenian transgression (NN5, *Orbilina suturalis*) ca 15.1 My
- Late Badenian transgression (NN6, *Velapertina* sp.) ca 13.8 My
- Early Sarmatian transgression ca 13.0 My
- Early Pannonian transgression ca 11.0 My

The Vienna Basin depositional pattern shows at least ten 3rd order sequence stratigraphy cycles (different in the individual depocenters). The global sea level changes are accelerated or overprinted by regional tectonics and sedi-

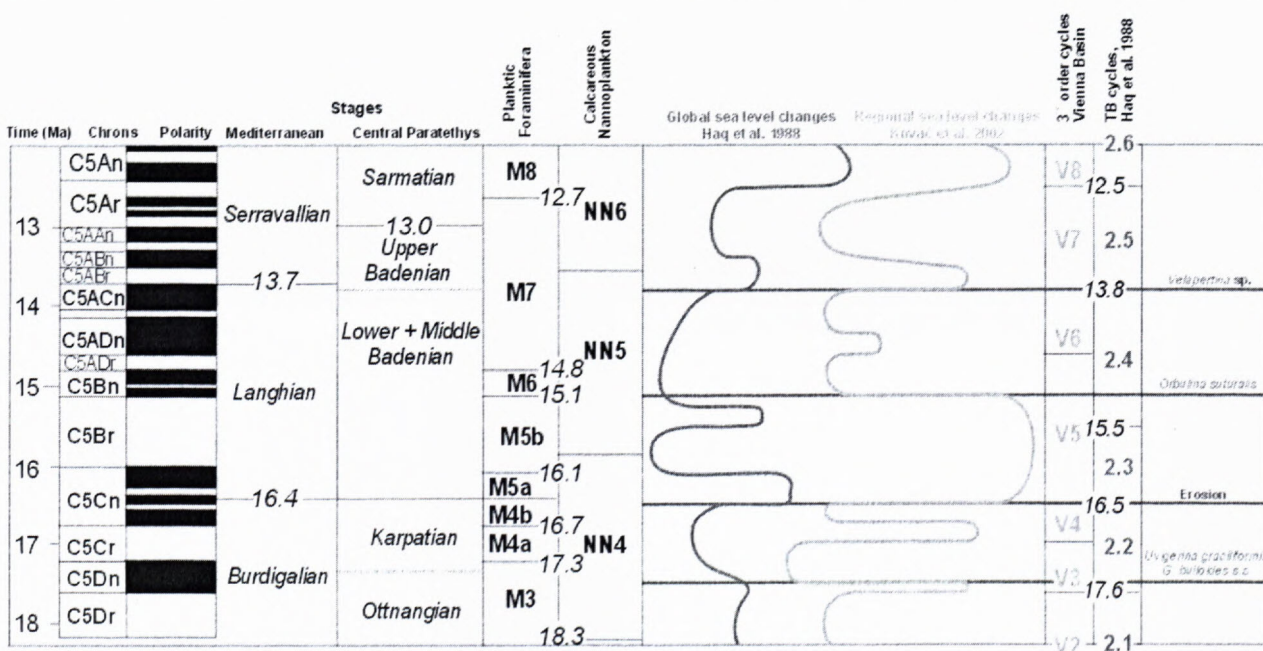


Fig.1. Sea level changes and correlation levels in the Northern Vienna Basin

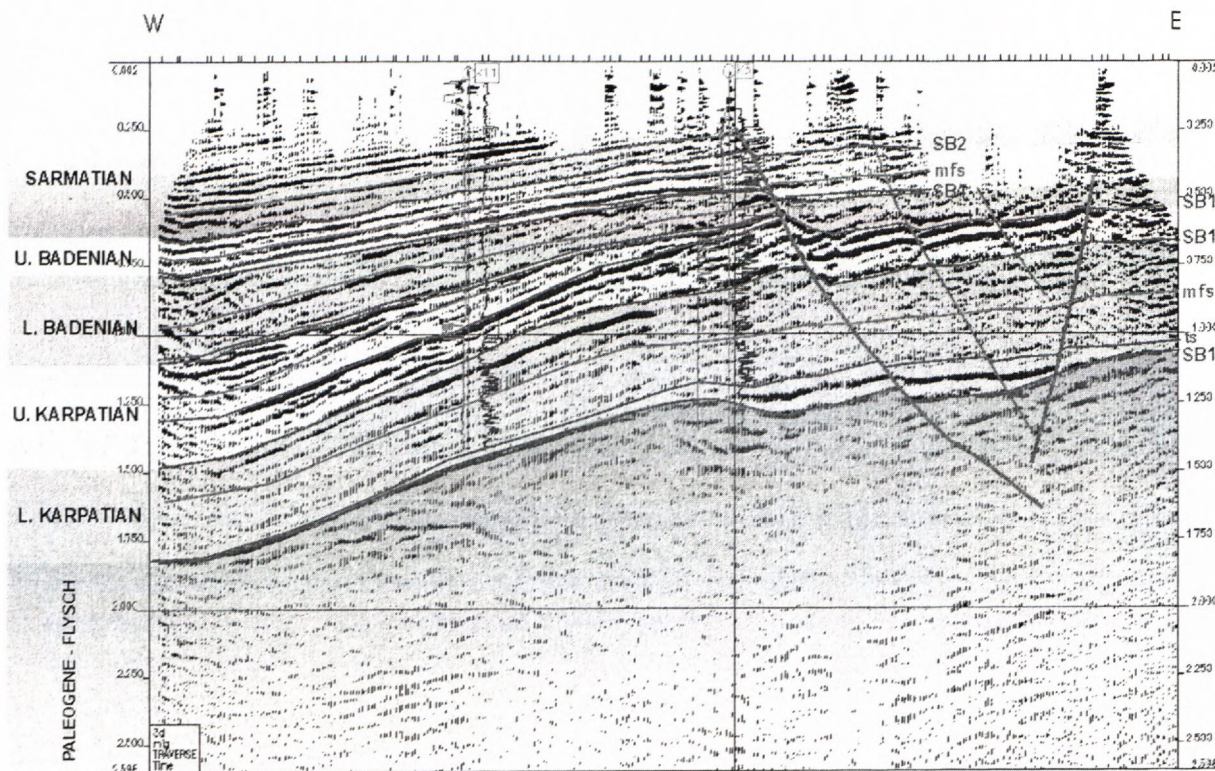


Fig.2 Seismic section from the northeastern part of the Vienna Basin with sequence stratigraphic interpretation

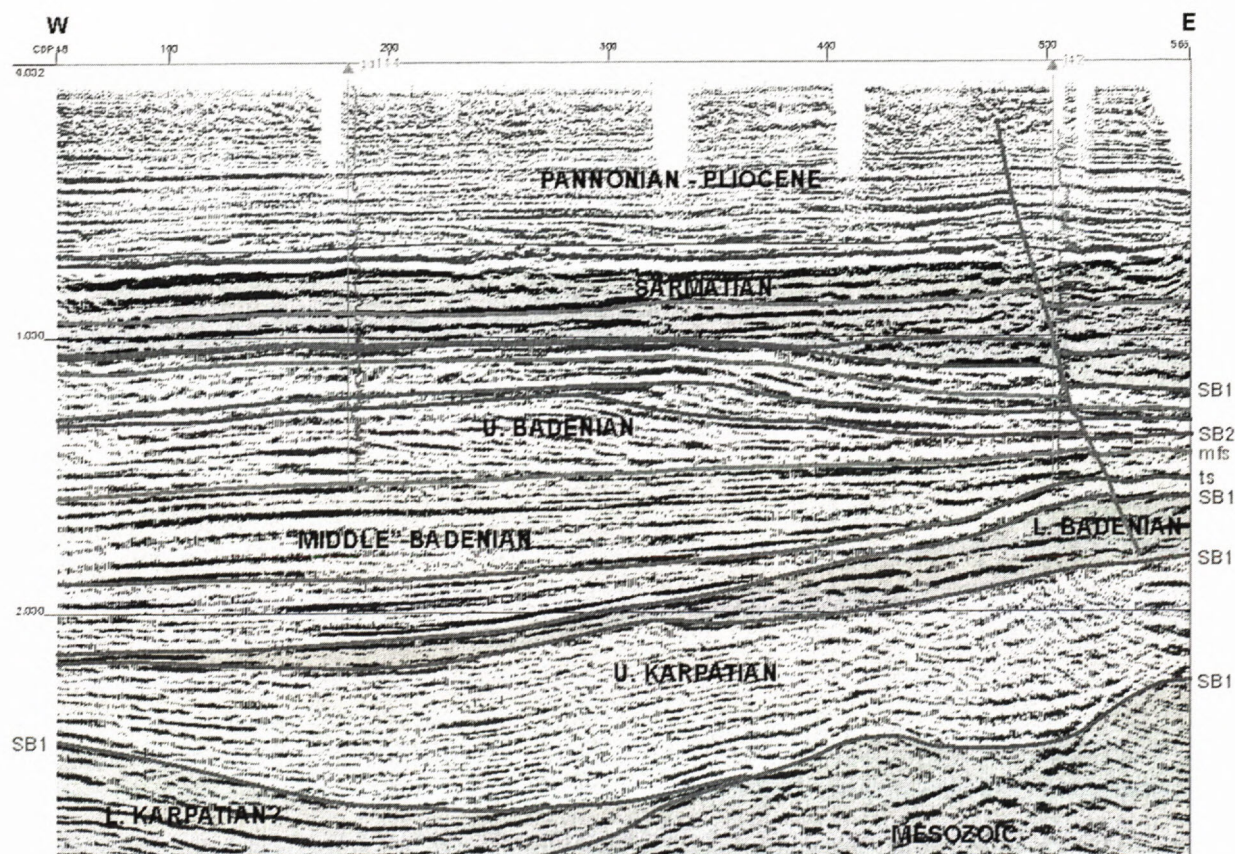


Fig. 3 Seismic section from the central part of the Vienna Basin with sequence stratigraphic interpretation

ment input (Fig. 1). The Miocene basin fill sequence stratigraphy 3rd order cycles were observed by geophysical and geological methods (seismic lines, logs, borehole cores, micropaleontology – paleoecology) in stratigraphical position: the Eggenburgian, Ottnangian, Early Karpatian, Late Karpatian, Early Badenian, „Middle Badenian“, Late Badenian – Sarmatian, Sarmatian and in the Pannonian.

Many seismic sections and borehole data (logs & cores) were analyzed to create sequence stratigraphic model of the Neogene sedimentary fill of the Vienna Basin. The erosional boundaries, truncations on seismic profiles, and also angular unconformities documenting depositional movement can be observed as a result of tectonic

activity (Fig. 2). There are good examples of prograding clinoform bodies in the upper Badenian highstand systems tract (HST) sediments, parallel reflections of transgressive systems tract (TST) sediments with onlaps as well as downlap surface marking the maximum flooding surface (mfs) shown on Fig. 3.

Borehole data (logs & cores) were used for detailed analysis of lithology, sedimentology and paleoecology. There were identified general fining upward transgressive trends on log curves with mfs on the top, coarsening upward trends in prograding HST and LST sedimentary bodies and isolated blocky patterns documenting erosive channel fill.

Neogene of the Vienna Basin and Alpine - Carpathian Foredeep

KOVÁČ, M., HOHENEGGER, J., PERVESLER, P. and HUDÁČKOVÁ, N.

The workshop "Neogene of the Vienna Basin and Alpine - Carpathian Foredeep" in Bratislava devoted to tectonics, biostratigraphy, paleogeography, paleoecology, eustatic and climatic changes during the Miocene was organized by the Department of Geology and Paleontology, Comenius University, Bratislava together with the Institute of Palaeontology and the Institute of Geology, University of Vienna, and the Institute of Geophysics, University of Leoben during November 22 – 23, 2002.

All contributions result from programs of the Austrian Science Fund FWF (Projects P 13743-BIO, P 13745-BIO, P 13740-GEO, P-15724-GEO and P 13738-TEC), the Slovak Grant Agency VEGA (1122, 1/7087/20, 2/7215/20, 2/7068/2, 2/2074/2, 2/2074/22, 1/0080/03), KEGA 3/0108/02, the Czech Republik Grant Agency GAČR Nrs.: GACR 205/01/0085 and activities within the

international research programs of the RCMNS, ESF - EEDEN and V4.

The workshop attended 32 participants from Austria, the Czech Republic, and Slovakia. Problems in paleontology, sedimentology and tectonics of the Alpine-Carpathian junction were discussed in a fruitful scientific atmosphere. Possibilities for cooperation on scientific topics concerning stratigraphy and paleoecology were outlined, especially the exchange of knowledge as well as personal contacts. The definition of the Early / Middle Miocene boundary (Karpatian / Early Badenian) - studies are well progressed in Austria - was the most important task. At the end of the workshop all participants estimated that the main goals - to perform scientific activities and to give a base for common research in the participating countries - were fulfilled.

Heavy Minerals in Alluvial Sediments of the Boca River (Nízke Tatry Mts., Slovakia)

ALEXANDER SMIRNOV* and MARTIN CHOVAN**

Department of Mineralogy and Petrology, Faculty of Natural Sciences, Comenius University, Mlynská dolina,
84215 Bratislava, Slovakia

**To whom correspondence should be addressed; Martin Chovan, phone: +421 (0)2 60296298, email: chovan@fns.uniba.sk

* Present address: Department of Geosciences, State University of New York, Stony
Brook, NY 11794-2100, USA

Abstract. Mineralogical studies of pan-samples from the Boca River revealed a wide variety of heavy minerals. Anatase, apatite, arsenopyrite, barite, carbonates, cinnabar, epidote, garnets, gold, chlorites, ilmenite, magnetite, micas, monazite, quartz, pyrite, rutile, scheelite, titanite, xenotime, zircon as well as anthropogenic material were identified. With the exception of cinnabar and scheelite, provenance of all minerals can be assigned to one or more rock complexes and/or ore mineralizations present in the drainage area of the Boca River and its tributaries. Alluvial gold reaches considerable concentrations and was actively exploited in the past.

Keywords. heavy minerals, gold, alluvium, provenance, Nížná Boca

Introduction

The idea of studying heavy minerals in the Boca River alluvial sediments was originally spurred by our investigations of ore mineralizations in the area of the Nížná and Vyšná Boca Villages (Smirnov, 2000). The objective of this study is to: a) characterize heavy minerals in alluvial sediments in a qualitative and quantitative manner; b) attempt to resolve the provenance of heavy minerals; c) map the area with preserved man-made features of alluvial gold exploitation.

Area Description

The Boca River is located in the Bocianska dolina Valley (Fig. 1), south of Liptovský Hrádok. The valley stretches in a general N-S direction with an approximate length of 17 km. The Boca River originates on the northern slopes of the Ďumbierske Nízke Tatry Mountains, 400 m northeast of the Kumštové saddle. The longitudinal profile and stream gradient for each kilometer of the Boca River is shown in Fig. 2 and Fig. 3, respectively. The Boca River has a stream gradient of 260 m/km (14.6°) at its headwaters with a gradual decrease to 6 m/km (0.3°) towards the mouth. The slope of the river [°] was calculated as $\tan^{-1}(\Delta y/x)$, where Δy is the altitude difference per 1 km of river (x).

The Boca River's headwaters cut through rocks of the Tatric crystalline basement. Its middle and lower courses cut through the Late Paleozoic and Triassic rocks of the Hronicum tectonic unit (Fig. 1).

In the headwater area, the Tatric crystalline massif is represented mainly by biotite to two-mica paragneisses and by granitite rocks of two types: the Ďumbier and the Králička (Biely et al., 1992). Other types of metamorphic rocks, such as garnet-biotite gneisses, orthogneisses or metaquartzites, are present to a lesser extent. The Ďumbier-type granitoid is represented by biotite tonalities to granodiorites (metaaluminous I-type granitoid) (Petrík et al., 1993). Cambel et al., (1990) calculated a crystallization temperature of 670–700 °C and age of $\sim 368 \pm 22$ Ma. The Králička-type granitoid is less abundant and was classified by Petrík et al., (1993) as peraluminous S-type granitoid with a crystallization temperature of 670 – 690 °C and age of 365 ± 17 Ma.

The Variscan Tatric basement is enveloped by Mesozoic sequences. Preserved remains of the sedimentary cover are made up of Lower Triassic quartzites and sandstones. The central part of the studied area is built of a megastructural, Alpine-formed, Hronicum unit, which consists of several nappes. Late Paleozoic volcano-sedimentary sequences (Upper Carboniferous - Permian in age) are represented by conglomerates, sandstones, siltstones, shales, tholeiite basalts and andesites, tuffites and tuffaceous sandstones. Basal complexes of the Hronic nappe are referred to as the Ipolitica Group and consist of the Nížná Boca and Malužiná Formations. Triassic sequences are represented by sandstones and quartzites (Scythian), shales and sandstones (Carnian), gray and white dolomites (Amnesia-Norian), hauptdolomites (Carnian-Norian) and Dachstein limestones (Norian) (Vozárová & Vozár, 1988; Biely & Bezák, 1997).

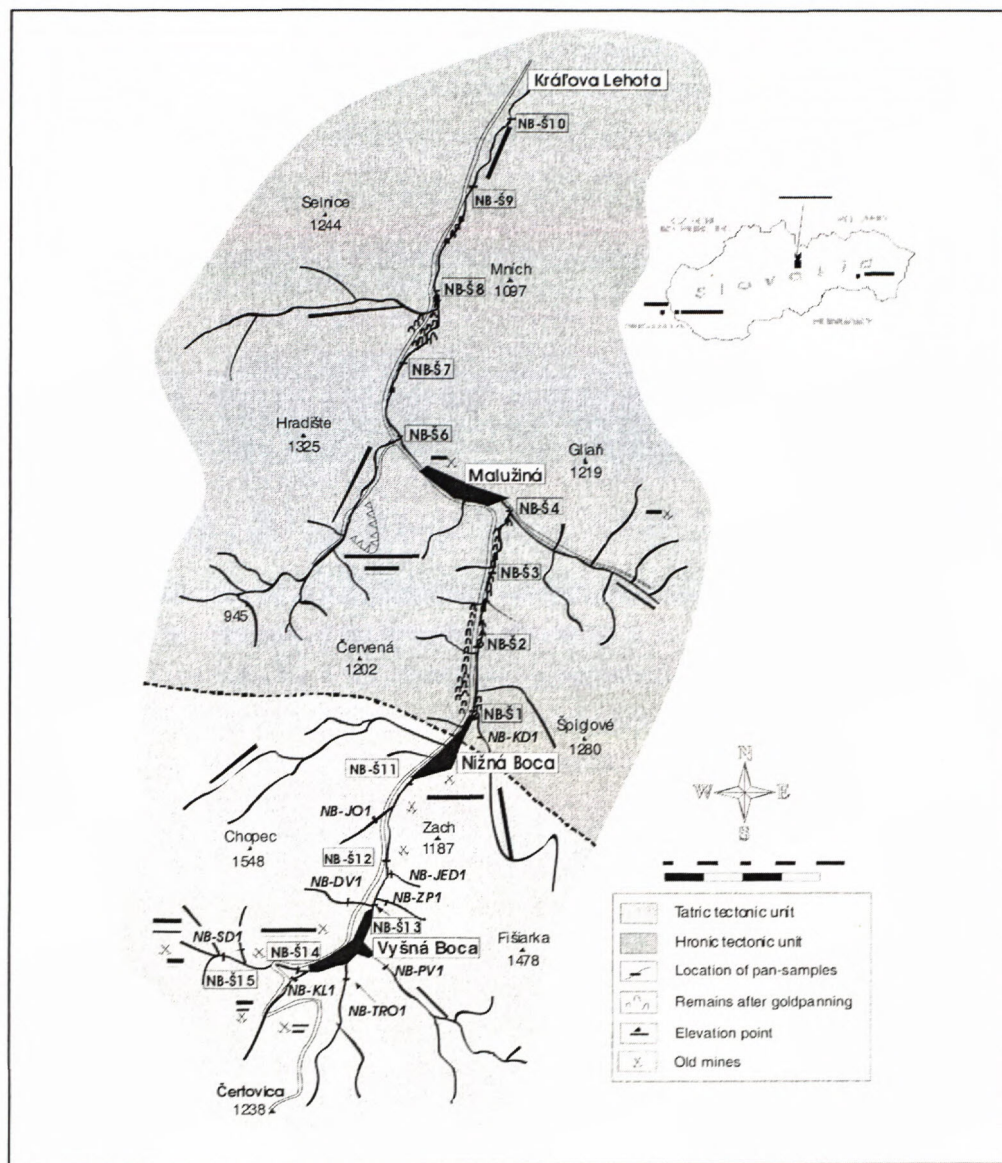


Fig. 1. Map of the Boca River drainage system.

The dominant types of ore mineralization in the area are the hydrothermal quartz – carbonate veins with Sb-Au mineralization, located in the Variscan Tatric basement, south of the Nižná Boca Village. Gold, and later stibnite, were the main objects of exploitation in the 16th century at the Zach locality (Fig. 1) where the terrain morphology is significantly affected by numerous remains after mining. Less intense gold exploitation took place at the Chopec mining field, west of the Vyšná Boca Village. The most abundant minerals of this mineralization are pyrite, arsenopyrite, chalcopyrite, gold, stibnite and Pb-Sb sulfosalts (Smirnov, 2000). The gold is weathered out of its host rock and becomes part of alluvial sediments and was exploited as early as the 13th century.

Siderite veins west and south of the Vyšná Boca Village (Stará Boca – Čertovica) were exploited in the 18th and 19th centuries. These veins stretch several kilometers to the north (localities Zach, Chopec) and occur together with Sb-Au mineralization in the rocks of the Tatric Basement. The dominant minerals of siderite minerali-

zation are: siderite, barite, quartz, pyrite, tetrahedrite and chalcopyrite. Cu(Bi,Pb) sulfosalts are scarce (Ozdín & Chovan, 1999).

Base metal mineralization is located in carbonate sediments of the Hronic Nappe (Olovienka) north of the Malužiná Village. It comprises carbonate veinlets with galena and sphalerite.

Barite veins were exploited at the Doštianka Deposit, east of the Malužiná Village. Virtually monomineral barite veins are hosted by volcano-sedimentary rocks of the Hronic Nappe. Occurrences of barite and quartz-carbonate veins of lesser significance can be found in basalts of the Hronic Nappe at the Svidovo Quarry, west of the Malužiná Village.

Methods and Material Studied

To map the remains after gold panning, reconnaissance trips on both banks of the Boca River were conducted and the results were plotted into topographic maps

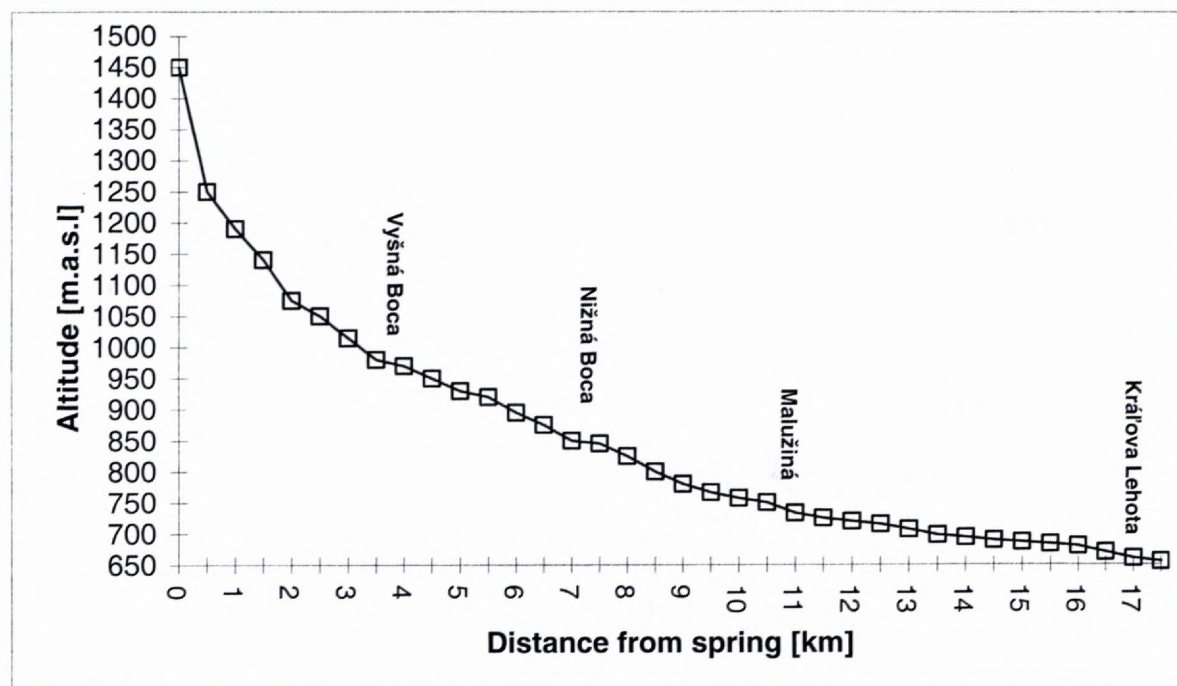


Fig. 2. Longitudinal profile of the Boca River.

of 1:10000 scale [36-22-12 (Nižná a Vyšná Boca), 36-22-07 (Malužiná), 36-22-17 (Čertovica) and 36-22-02 (Kráľova Lehota)].

Alluvial sediments of the Boca River were sampled for heavy minerals in the summer seasons of 1998 and 1999. Samples NB-Š1 to NB-Š15 were taken in approximately 1 km steps between the Starobocianska dolina Valley and the Kráľova Lehota Village. Tributaries of the Boca River that drain the rocks of the crystalline Tatic basement were sampled within 0.5 to 1 km distance from the confluence (to avoid contamination of the tributary sample with possible flash flood or storm sediments from the Boca River). These samples include: Kráľovská dolina (NB-KD1); Joachymstahlská dolina (NB-JO1); Jedlinská (NB-JED1); Za Pavčovým (NB-ZP1); Dievčia voda (NB-DV1); Podvrch (NB-PV1); Trojička (NB-TRO1); Kliesňová dolina (NB-KL1) and Sklepská dolina (NB-SD1).

The sampling depth varied between 40–80 cm and was generally limited by local bedrock and alluvium character. Preceding the standard panning procedure (Hvožd'ara, 1980, Matula & Hvožd'ara, 1985), the sample was sieved on a 2–3 mm mesh sieve to achieve a total of ~15 kg of alluvium material.

In the laboratory, each sample was closely studied for fluorescent minerals using an ultraviolet lamp (wavelength 254–366 nm) and the observations were compared with those compiled by Warren (1962) and Gleason (1972). After the permanently magnetic fraction was removed, the sample underwent a process of heavy liquid separation in tribromomethane (CHBr_3 , density at $20^\circ\text{C} = 2.894 \text{ g/cm}^3$). The resulting heavy fraction was electromagnetically separated (separator fi. Cook) into paramagnetic and diamagnetic fractions. Both para- and diamag-

netic fractions were subsequently sieved into three size fractions (>0.5 mm; 0.5–0.2 mm; <0.2 mm). Only the 0.5–0.2 mm and <0.2 mm size fractions (in both para- and diamagnetic fractions) were optically studied using a binocular magnifying glass. Observations were compared to data summarized by Rost (1956). Each sample was quarted and the quantity of minerals was expressed as percents of a 200 grain count except for cinnabar, scheelite and gold (expressed in number of grains). Thus, each sample yielded data for four fractions (para- 0.5–0.2 mm; dia- 0.5–0.2 mm; para- <0.2 mm; dia- <0.2 mm) (Hvožd'ara, 1980).

SEM and BSE imaging techniques, as well as electron microprobe (WDS) analyses, were performed using JEOL JXA 840A microprobe analyzer (CLEOM, Comenius University). Analytic conditions for WDS analysis of gold were: 20 kV, 15 nA, ZAF and Phi-Rho-Z corrections, standards: Hg – HgS, pure metals Au, Ag, Cu, Sb, Bi, Te and Fe.

Results

Morphologically distinct, knoll-shaped remains after gold panning from past exploitation (Bergfest, 1952) (Fig. 4) were observed along the total 10 km distance between the Nižná Boca and Kráľova Lehota Villages (Fig. 1), with the highest concentration of knolls at the confluence of the Boca River and the Michalovský potok Brook. This is in good agreement with the morphology of the river valley (Figs. 2, 3). Decreasing stream gradient directly influences (lowers) stream velocity and overall energetics of the stream - allowing the stream to deposit its load (Abbot, 1999). In this area, alluvial sediments with sufficient gold content were subjected to intensive exploitation

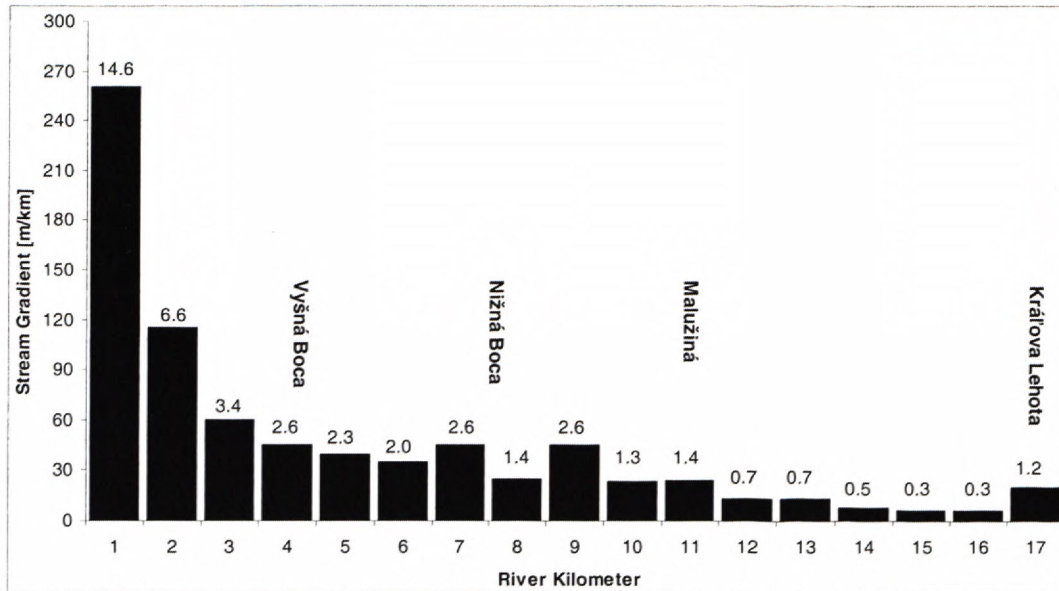


Fig. 3. Stream gradient values of the Boca River.

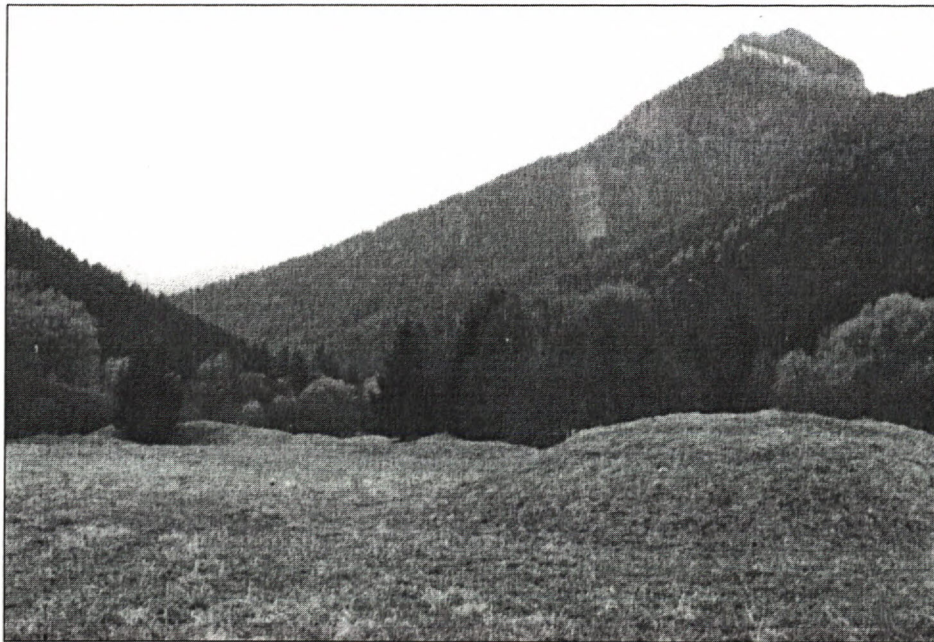


Fig. 4. Remains after gold panning located at the confluence of the Boca River and the Michalovský potok Brook.

by means of gold panning. The size of the knolls varies, but their height rarely exceeds 3 m and volume of few cubic meters

On the left bank of the Boca River, near the confluence with Kráľovská dolina Brook, numerous gold panning remains are visible on the ancient river terrace. They spread a distance of ~ 1 km towards the Malužiná Village.

Anatase

Anatase occurs rarely in the diamagnetic fraction. Only a few well-preserved euhedral crystals with tetragonal-dipyramidal habitus and striated faces were observed. Grain color varies from indigo-blue to dark blue

with sub-metallic luster. Possible source rocks of anatase are igneous and/or metamorphic Tatric complexes (Biely & Bezák (eds.), 1997) and to a lesser extent sedimentary and/or volcano-sedimentary suites of the Hronicum unit (Vozárová & Vozár, 1988).

Anthropogenic Material

Admixtures of various anthropogenic materials are present in all samples, predominantly in the paramagnetic and permanently magnetic fraction. It's typically of black color, with varying shape and sub-metallic to metallic luster. Anthropogenic material is presumably introduced from municipal waste and/or road maintenance.

Apatite

Apatite is very abundant and occurs in the diamagnetic fraction of all samples. Euhedral crystals occur in two forms: short stubby and long slender. The latter usually forms prisms with simple pyramidal termination. Fragments of crystals are also frequently present, mostly of irregular shape. A considerable amount of grains exhibit rounding and scratched faces. Cleavage is poor. Bigger grains contain various inhomogeneities. Apatite is usually colorless, but white, bluish and grayish colors were also observed. Color variations are caused by admixtures of various chemical elements (Mange & Mauer, 1992). A maximum apatite content of 79% was found in sample NB-Š3 (the Boca River) (Fig. 5). The sample from the Sklepská dolina Valley (NB-SD1) contained 57% of apatite.

Potential source rocks of apatite are crystalline rocks of the Tatric unit in the headwater area (Biely & Bezák (eds.), 1997), and to a lesser extent Paleozoic sequences of the Hronic unit (Vozárová & Vozár, 1988).

Arsenopyrite

There is a scarce occurrence of arsenopyrite in the diamagnetic fraction. Arsenopyrite from the Boca River forms euhedral crystals of prismatic habitus sometimes with characteristic striation. It possesses typical tin-white to steel-gray color and high metallic luster. Arsenopyrite was found in hydrothermal siderite and Sb-Au mineralizations (Ozdín & Chovan, 2000; Smirnov, 2000).

Barite

Barite is abundant in the diamagnetic fraction of all samples (Fig. 5).

The most habitus is irregular or rectangular (tabular). The latter is caused by excellent {001} cleavage. Barite grains have milky-white, yellowish-white, grayish-white or brownish-white color and vitreous (glassy) luster. Color variations can be caused by thin Fe-oxyhydroxides coatings. Fe-oxyhydroxides fill tiny cracks in barite grains as well. Frequently, barite is overgrown with quartz, pyrite and/or Fe-oxyhydroxides.

Barite content in samples from the Boca River varies from 2 to 93% (Fig. 5). Rost (1956) stressed that because of the excellent cleavage, barite is incapable of transport for very long distances. The barite content of the samples steadily increases, suggesting barite sources along the entire Boca River. Potential barite sources in the headwaters are siderite and, to a lesser extent, also Sb-Au mineralizations (Ozdín & Chovan, 2000; Smirnov, 2000). In the middle and lower course, the possible sources are numerous barite veins occurring in the Hronic unit (Ferenc & Rojkovič, 2001; Friedl, 1987; Turan, 1962).

Carbonates (undistinguished)

Carbonates are in both dia- and paramagnetic fractions. In the diamagnetic fraction, carbonate grains are usually irregularly angular, rectangular cleavage frag-

ments or tabular. Euhedral rhombohedra were scarcely present. Perfect cleavage was observed in a majority of grains. Color varies from colorless to white, light-grayish and light-brownish to white with vitreous luster. Fe-oxyhydroxides coatings were rarely observed. The content of carbonates in the diamagnetic fraction does not exceed 3%. Because of their presence in this fraction, these carbonates are probably of calcite or dolomite composition.

In the paramagnetic fraction, the carbonate content does not exceed 5%. The grains are usually variously rounded rhombohedral crystals and fragments with grayish to yellow-brown color and glassy luster. The surface of the grains is frequently covered with thin Fe-oxyhydroxide coating owing to the higher Fe content of the carbonate.

The perfect cleavage and low hardness results in low resistance to river transport (Rost, 1956) and explains the low content of carbonates in the Boca River. The dominant sources of carbonates are the Mesozoic sequences in the middle and lower course of the Boca River. Ore mineralizations: siderite (Ozdín & Chovan, 2000); barite (Friedl, 1987; Turan, 1962); Sb-Au (Smirnov, 2000) can be considered a minor source of carbonates in the alluvium.

Chlorite group (undistinguished)

Minerals from the chlorite group are frequently present. The chlorite content in samples varies greatly, presumably due to the Fe content and/or separation methods (tribromomethane quality, electric current setting during electromagnetic separation).

Chlorites usually form thin flaky plates of round, oval or irregular shape; sometimes with curled margins. Pseudo-hexagonal euhedral crystals are scarce. Chlorites have excellent cleavage and their platy crystals are elastic. Typically greenish to gray- and brown-green in color with pearly luster. The samples usually contain up to 2% and 12% in dia- and paramagnetic fraction, respectively. Sources of chlorites can be some or all of the following: a) hydrothermally altered wall rocks of ore mineralizations (Ozdín & Chovan, 2000); b) primary minerals and/or weathering products of primary minerals in both Hronic and Tatric Units (Biely & Bezák (eds.) (1997), Friedl (1987), Vozárová & Vozár (1988); c) post-volcanic mineralization in the basaltic rocks of the Hronic Unit (Friedl, 1987).

Cinnabar

Usually forms irregular, variously rounded grains with no visible cleavage. It typically has typical cherry-red, brownish-red or light-red color with a highly glassy luster.

Cinnabar is a regular admixture in the diamagnetic fraction of samples, occurring in the Boca River in quantities varying from 3 to 35 grains. It is also present in samples from the Boca River's tributaries (X grains per sample) with the exception of the Kráľovská dolina Valley.

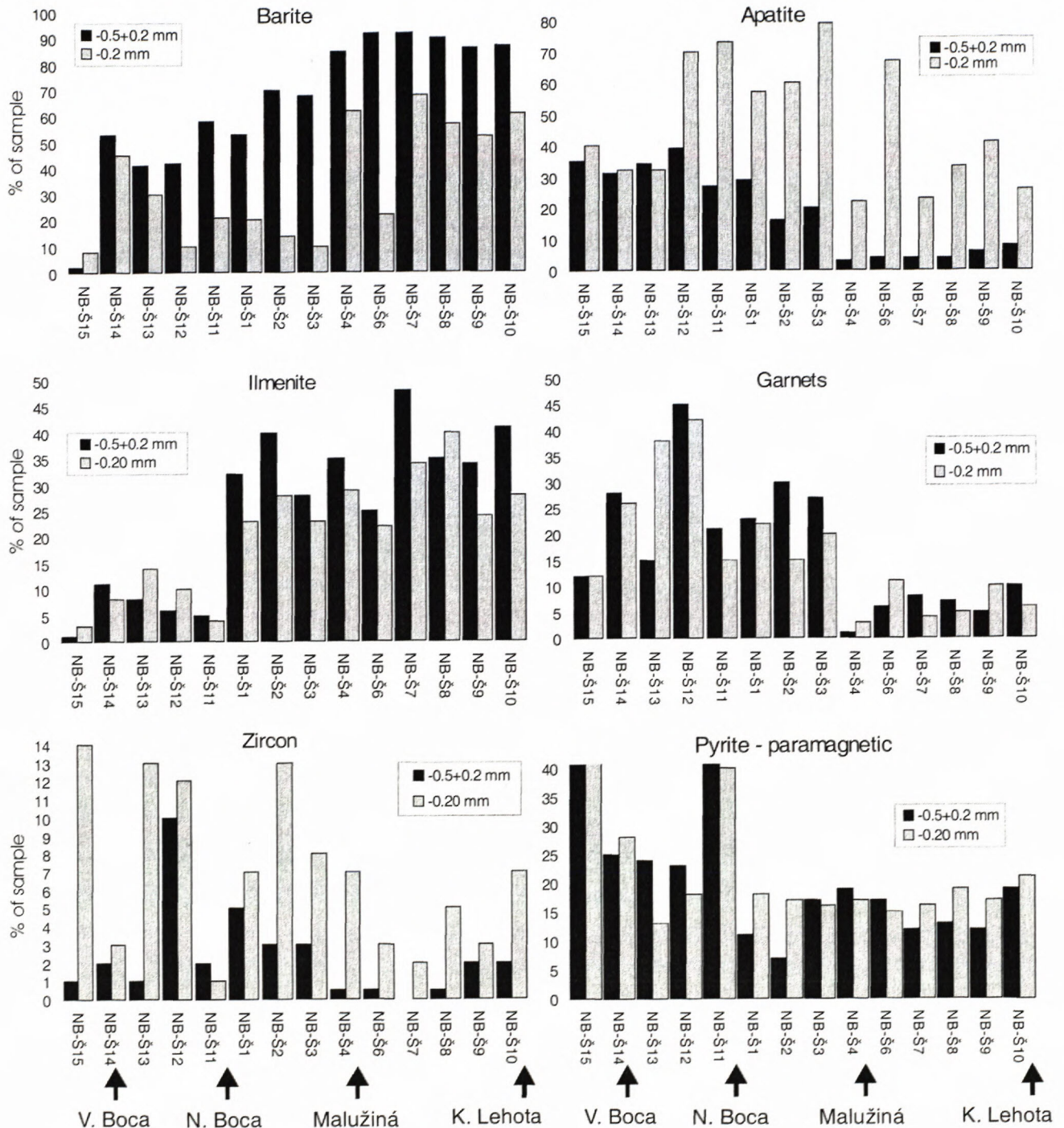


Fig. 5. Contents of selected minerals in pan-samples from the Boca River sediments (-0.5+0.2; -0.2 mm fractions).

Epidote group (undistinguished)

Minerals of this group (zoisite, epidote, pumpellyite) are usually colorless or of greenish to brownish color. They can occur in paramagnetic fraction as short stumpy prisms, needle-shaped crystals, tabular and platy fragments, but mostly as variously rounded and irregular fragments. Epidote content in the Boca River gradually increases towards its mouth, which implies an increasing abundance of its source rocks.

In the Boca River's upper course, the dominant sources are the rocks of the Tatric crystalline; while in the middle and lower course, epidote is an important constituent of post-volcanic mineralizations in basaltic rocks of the Hronic Unit (Friedl, 1987).

Garnet group (undistinguished)

Abundant in the paramagnetic fraction, usually occurs as isometric sub-rounded to rounded grains and irregular

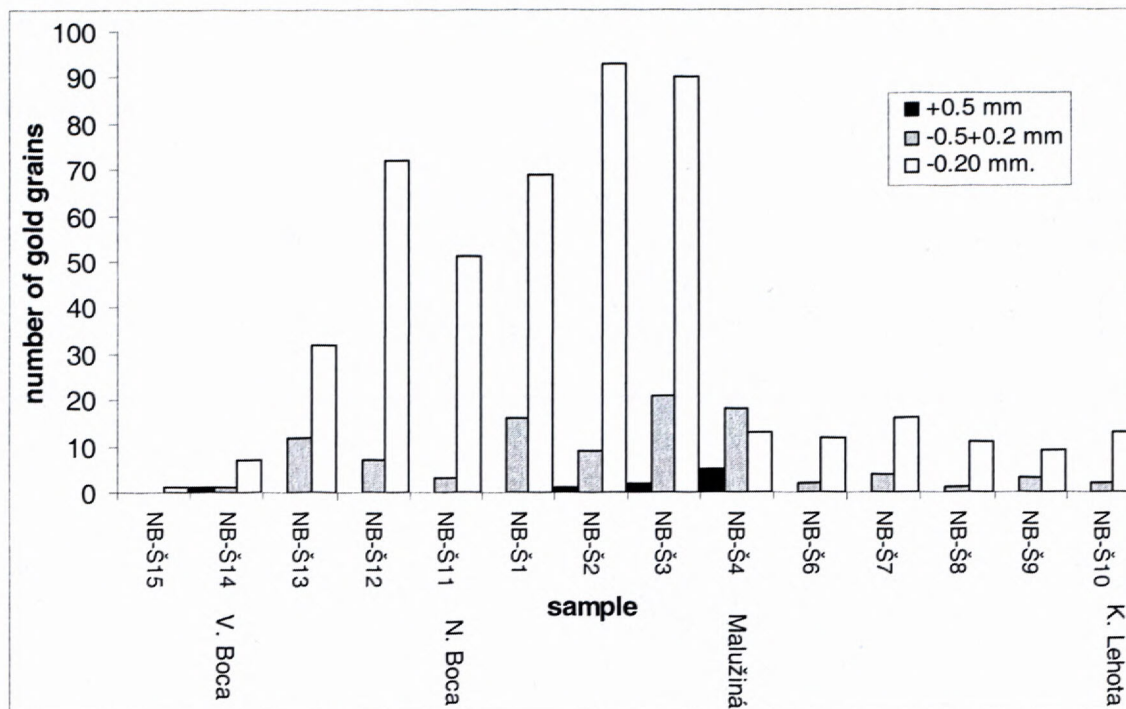


Fig. 6. Gold content in pan-samples from the Boca River sediments as a function of transport length.

sharp fragments with a typical glassy luster. Crystal faces are often scratched. Euhedral crystals are rare. Color varies from pink and red to brownish-red and yellowish-brown. Garnet content in the Boca River varies from 1 to 45%, while contents in its tributaries are between 7 and 89% (the Dievčia voda Valley). Garnet's source rocks are located mostly in the upper course of the Boca River (crystalline rocks of the Tatric Unit). This is in agreement with the decreasing garnet content in the river towards its mouth (Fig. 5). Garnet is also present in sedimentary and/or volcano-sedimentary rocks of the Hronic Unit (Vozárová & Vozár, 1988).

Gold

Gold is a regular constituent of most samples (Fig. 6). Gold from the Boca River has typical gold-yellow color; often varying to orange, mustard-yellow, reddish or yellowish white.

Its surface is occasionally coated with Fe-oxyhydroxides and often shows marks (scratches, prints, dents) indicating mechanical damage during the transport. The surfaces of all gold grains studied by SEM and BSE methods are porous. In 88-100% of gold grains, the pores were distributed evenly, while in some cases, elevated concentrations of pores were detected in vicinity the grain's rim. Most pores are of isometric shape and are a maximum 2 μm in size.

A majority of gold grains are rounded to a various degree (Fig. 7, 8, 9). There is no distinct correlation between the roundness of grains and the length of transport. Depending on the sample, approximately 30-70% of gold

grains were overgrown with quartz (Fig. 10). The percentage of gold/quartz overgrowths does not decrease towards the mouth. Overgrowths with pyrite are rare.

The morphology of gold shows extensive variations. For the purpose of this study, all gold grains were assigned to one of three categories: flakes, nuggets or branching nuggets according to the ratio of the *a*, *b* or *c* dimensions. Flakes are the most frequent shape of gold particles (Fig. 11) and usually don't overgrow with quartz or pyrite. We didn't observe any distinct relationship between the gold particle shape and the distance of travel because the quantity of gold grains in samples from the headwaters (NB-Š14, 15) and from the mouth of the river (NB-Š6, 8, 9, 10) do not allow for a reliable statistical evaluation. However, a few trends can be established: a) the number of flake-shaped gold grains generally increases towards the mouth; and b) the number of nuggets and branching nuggets reaches its maximum in the middle course of the Boca River and then decreases gradually.

To assess features that indicate instability of Au-Ag alloys in an oxidizing aquatic environment, close attention was paid to compositionally different phases in the BSE images. The percentage of gold grains with "inclusions" (isolated, compositionally-different areas with higher/lower fineness) was observed to increase with the distance of travel. Gold-rich rims (Fig. 12) are abundant, generally 1 to 20 μm thick and may contain elevated concentration of pores or sponge-like structures. The percentages of gold-rich rims were also observed to increase with the travel distance, thus proving the time dependence of the Ag-leaching process.

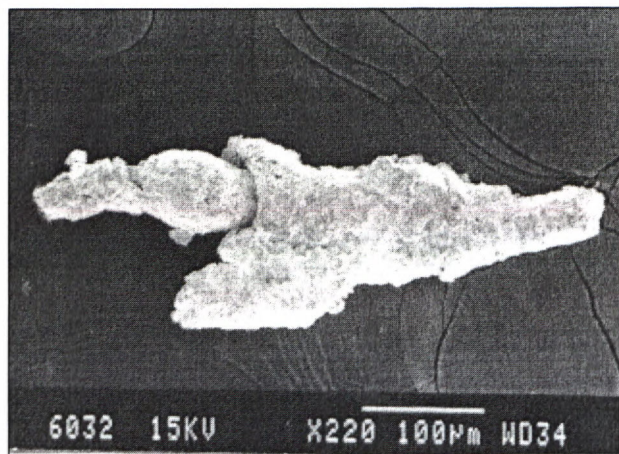


Fig. 7. Highly deformed (formerly flake-shaped) gold particle (NB-Š8).

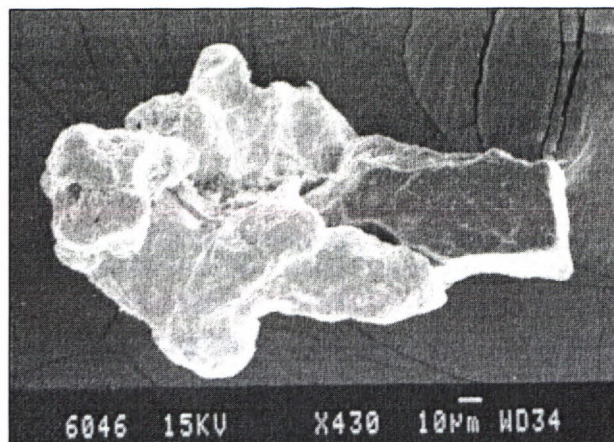


Fig. 10. Rounded gold grain overgrown with quartz. (NB-Š4).

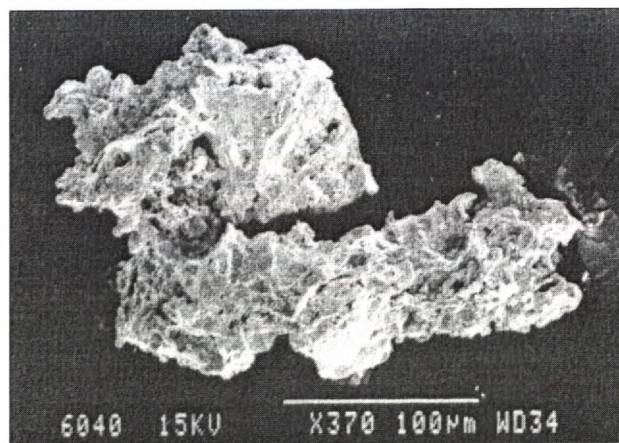


Fig. 8. Well-preserved gold particle, minimally rounded by the river transport (NB-Š2).

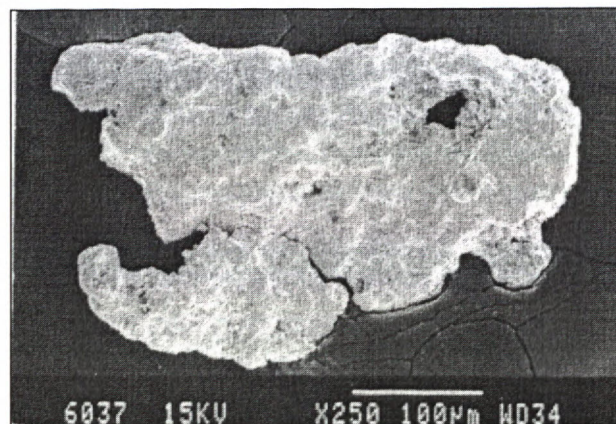


Fig. 11. Well-rounded, flake-shaped gold grain (NB-Š2).

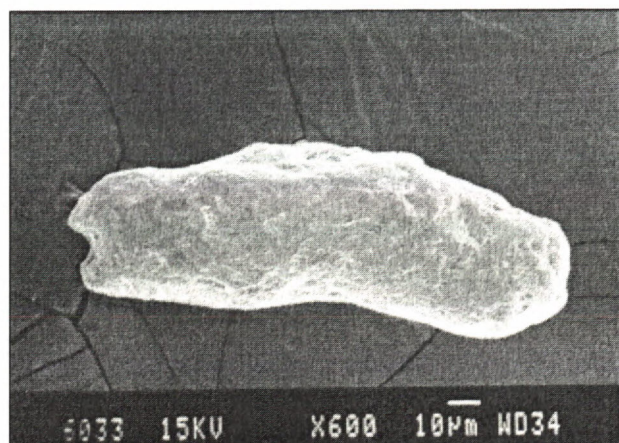


Fig. 9. Completely rounded wire-shaped gold grain (NB-Š7).

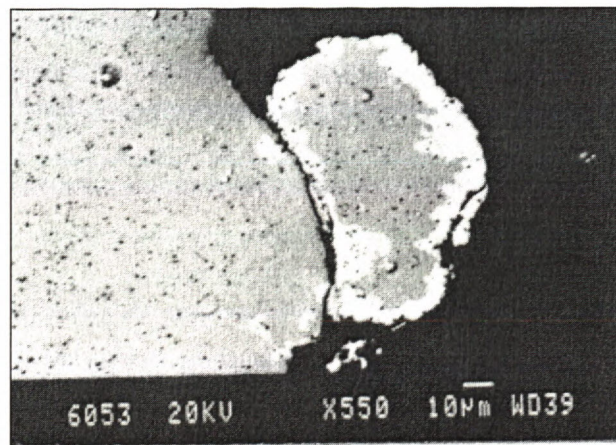


Fig. 12. Example of well-developed gold-rich rim on alluvial gold grain (NB-Š3).

Au:Ag ratio of gold grains varies between 2.1 (65.8:30.5 wt.%) and 70.6 (94.6:1.34 wt.%). The true fineness (F_T) values range between 683 and 986. As a consequence of similar lattice constants of gold and silver, a strong correlation exists between Au and Ag content. Hg content is slightly elevated (up to ~2.2 wt.%)

with the exception of one gold grain containing 22.83 wt.% of Hg. This anomalously high Hg concentration is a result of amalgamation process. The concentration of other analyzed elements (Fe, Sb, Bi, Te, Cu) does not exceed 0.95 wt.%. Representative WDS analyses of gold are in Tab. 1.

Tab. 1. Representative WDS analyses of gold from the Boca River. Analysis (1) represents gold grain with anomalous Hg content. Analyses (2a) and (2b) represent homogenous gold grain and analyses (3a) and (3b) gold grain with gold-rich rim sample No. NB-Š3??? (note the differences in F_T). * - because of the high Hg content, F_T calculated as $Au/(Au+Ag+Hg) \times 1000$.

Analysis Location	(1) rim	(2a) core	(2b) rim	(3a) core	(3b) rim
Fe	0.48	0.22	0.23	0.30	0.03
Te	0.25	0.01	0.01	0.15	0.07
Sb	0	0.14	0.16	0.17	0.10
Ag	6.93	2.67	3.09	28.29	1.34
Hg	22.83	2.13	2.22	0.95	1.04
Au	66.18	93.74	94.73	69.06	94.64
Cu	0.13	0.10	0.11	0.11	0.11
Bi	0.55	0.51	0.57	0	0.40
Σ	97.35	99.50	100.77	99.02	97.73
F_T	690*	952*	947*	709	986
Formula	Au _{0.51} Ag _{0.32} Hg _{0.17}	Au _{0.93} Ag _{0.05} Hg _{0.02}	Au _{0.92} Ag _{0.06} Hg _{0.02}	Au _{0.57} Ag _{0.43}	Au _{0.97} Ag _{0.03}

The gold distribution in the Boca River is uneven, primarily governed by the location and availability of primary sources. The second important influence is the morphology and profile of the Boca Valley (Fig. 2, 3). Low gold content in headwater samples is primary caused by a limited (or none) number of primary occurrences, as well as by unsuitable depositional conditions (high stream velocity, a narrow valley). The gold content in samples then generally increases from sample NB-Š13 to sample NB-Š3. This feature correlates well with valley morphology (the valley broadens and stream velocity decreases), as well as with more abundant primary sources: mine fields Chopec (SE of V. Boca) and Zach (E-NE of N. Boca) had both been exploited for gold (Bergfest, 1952) and recent studies confirm the presence of gold at these localities (Ozdín & Chovan, 2000; Smirnov, 2000). Low gold content in samples from the Boca River's lower course (NB-Š4 – 10) can be explained by a large distance from the gold's primary sources, even though the morphology would favor a sedimentation process. The gold content in the Boca River's tributaries is generally low, varying from 1 gold grain/sample (NB-KD1, NB-JO1, NB-JE1) up to 12 gold grains/sample (NB-SD1).

Ilmenite

Ilmenite is present in the paramagnetic fraction of all samples in the form of anhedral grains and fragments, usually with sharp edges. Euhedral tabular crystals are rare. Ilmenite possesses a characteristic black color with bluish tint and high metallic luster. The surface is often coated with the weathering product of ilmenite, leuc-xene, which is of white to grayish color. The ilmenite content in the Boca River samples varies from 1% to 48% and gradually increases towards the mouth (Fig. 5). The latter indicates the presence of the source rocks all along the Boca River. The paramagnetic fraction of the Kráľovská dolina Valley sample contains 78% of ilmenite. Ilmenite was found as an accessory mineral in both Kráľička- and Ďumbier-type granitoids (Biely & Bezák

(eds.), 1997). It is fairly abundant in sedimentary and/or volcanic rocks of the Hronic Unit (Vozárová & Vozár, 1988).

Magnetite

Magnetite is present in the ferro-magnetic fraction of every sample. It usually occurs as sub-rounded to rounded grains and rarely as euhedral cubic crystals. The Boca River's magnetite possesses a typical black color and high metallic luster. The surface is often covered with weathering products - Fe oxyhydroxides ("limonite") that can also fill the fissures and cracks on the magnetite surface. It occurs in the ferro-magnetic fraction along with magnetic anthropogenic material and it is distinguishable only with difficulty. Due to the negligible significance of magnetite, its content in samples wasn't evaluated.

Micas (undistinguished)

Micas are a very common admixture of both para- and diamagnetic fractions of all samples. Due to the Fe content and/or separation methods (tribromomethane quality, electric current setting during electromagnetic separation), mica content in samples varies greatly. Micas occur invariably as {001} basal plates (very good cleavage), usually with a round, rarely irregular or pseudo-hexagonal outline. They usually have white, gray or silver-white color with a green or brown tint (presumably due to the elevated Fe content) and vitreous to glassy luster. Overgrowths with quartz and chlorites are common. Maximal mica content of samples from the Boca River is 38% in the diamagnetic fraction and 12% in the paramagnetic fraction (sample NB-Š15). Generally all rock types (with the exception of sedimentary carbonates) in the drainage area of the Boca River can be considered source rocks of micas (Biely & Bezák (eds), 1997). Muscovite was also described from wall-rock hydrothermal alteration zones of siderite mineralization in the Vyšná Boca area (Ozdín & Chovan, 2000).

Monazite

Monazite is an accessory admixture of most samples. It's yellowish to yellow-brown (honey-like) grains are usually well rounded, egg-shaped or spherical. Anhedra to subhedral crystals are rare. Its identification is somewhat problematic, because its rounded grains can be mistaken for titanite. Broska & Siman (1998) and Biely & Bezák (eds.) (1997) described accessory monazite from granitoid and metamorphic rocks of the Tatric Unit. Monazite, probably hydrothermal in origin, was described from veporic tectonic unit (Hvožd'ara, 1980, 1999). The Hronic Unit (Vozárová & Vozár, 1988) can be considered a minor source of monazite.

Pyrite

Pyrite is a very common admixture of all samples. In diamagnetic fractions, pyrite usually forms euhedral to subhedral hexahedrons, pyritohedrons (a dodecahedron with pentagonal faces) and various crystals with combinations of these forms. Well-rounded grains and crystal fragments are also common. Cubic faces often show striation parallel with the edges. The surface of pyrite crystals is often affected by oxidation in aquatic environments - typically pale to dark brassy-yellow color is changed to a red, red-brownish color. Thin coatings of oxyhydroxides ("limonite") were often observed on the surface of the grains. It readily dissolves in hydrochloric and nitric acid. In paramagnetic fractions, pyrite forms predominantly anhedra, rounded grains, partly or entirely changed into "limonite".

Pyrite distribution in both fractions is generally equal. Both fractions show an elevated pyrite content in the headwaters of the Boca River. This correlates with numerous outcrops of ore veins (Sb-Au, siderite) and their wall-rock alteration zones in the area (Ozdín & Chovan, 2000, Smirnov, 2000), which are also predominant donors of pyrite. Other possible donors include: accessory pyrite in crystalline rocks of the Tatric unit and volcanic rocks of the Hronic unit (Biely & Bezák, 1997); barite mineralization (the Svídovo Quarry, Malužinská dolina Valley); and Pb-mineralization (Malužiná-Olovienka).

The Boca River's tributaries contain 3-30% of pyrite in both para- (Fig. 5) and diamagnetic fractions (samples from Dievčia voda Valley (NB-DV1) and Joachymstáhl-ska dolina Valley (NB-JO1), respectively).

Quartz

Quartz is a regular constituent of every sample. Euhedral crystals are scarce. It usually forms anhedra grains and variously rounded fragments of milky-white to grayish color. Fe-oxyhydroxide coatings on the surface may influence its color. Overgrowths with chlorites, micas, pyrite or gold are common. Quartz content in samples varies due to the separation methods - especially tribromomethane quality. Fe-oxyhydroxide coatings are also of considerable importance during the electromagnetic separation.

Rutile

Rutile is a regular accessory mineral in all samples. It occurs mostly as variously rounded grains and fragments; non-rounded grains are usually euhedral crystals with well-developed pyramidal terminations or slender prisms. "Knee shaped" twins (Fig. 13) were rarely encountered. Its color varies from deep-blood red and brownish-red to brownish-black and black. Adamantine to sub-metallic luster is typical.

The distribution of rutile in the Boca River is generally even. Samples from the Za Pavčovým Valley (NB-ZP1) and Sklepská dolina Valley (NB-SD1) contain 10% and 8% of rutile, respectively. Major donor rocks of rutile are igneous and/or metamorphic rocks of the Tatric crystalline basement.

Scheelite

Scheelite is very rare in the Boca River and occurs irregularly in quantities as low as a few grains per sample. No scheelite was found in the Boca River's tributaries. Its grains are well rounded; possess milky-white color and an adamantine to greasy luster. Characteristic blue fluorescence in UV light (Warren, 1969; Gleason, 1972) was observed.

Titanite

Titanite is an accessory mineral in most of samples. It forms irregular grains of yellow-brown to brown color, sometimes with observable cleavage. Color and luster of its rounded grains can be mistakenly identified as monazite or xenotime. The major sources of titanite are crystalline rocks of the Tatric Unit (Biely & Bezák (eds.), 1997).

Xenotime

Xenotime is very scarce, with only a few well-preserved euhedral crystals with tetragonal-dipyramidal habitus found. Its color is yellowish with vitreous to resinous luster. Its content in samples is presumably higher, since it can be mistakenly identified as monazite, or even zircon and titanite (Mange and Mauer, 1992). Accessory xenotime was described from granitoid and metamorphic rocks of the Tatric Unit (Biely & Bezák (eds.), 1997).

Zircon

Zircon is present in diamagnetic fraction of all samples. It typically occurs in a vast variety of well-defined, euhedral prismatic crystals with pyramidal termination (Fig. 14), owing to its hardness and high chemical stability (Nickel (ed.), 1973). The length of crystals (along *c*-axis) varies from <0.05 to ~1.5 mm. Fragments of euhedral crystals and sub- to well-rounded grains are rare. Generally, rounding is more advanced on larger grains. The color varies from deep red to pinkish to orange and even colorless varieties. Luster is adamantine. No luminescence in UV light was observed.

The zircon content in the Boca River varies between 1 to 14% and it gradually decreases towards the mouth (Fig. 5). Samples from some Boca River's tributaries, such as the Dievčia voda (NB-DV1) and Sklepská dolina (NB-SD1) Valleys contain 36% and 28% of zircon, respectively. Zircon is a common accessory mineral in granitoid and metamorphic rocks of the Tatric Unit (Broska & Uher, 1991). Vozárová & Vozár (1988) described accessory zircon from Late Paleozoic Hronic complexes present in middle and lower course of the Boca River.

Discussion and conclusions

Mineralogical research of heavy minerals in the Boca River showed the presence of 21 minerals and mineral groups. Cinnabar in a primary hydrothermal mineralization has never been described neither in the studied area nor in any other primary occurrence in the Nízke Tatry Mountains. However, it was described by Chovan et al., (1995) in alluvial sediments in the Magurka Deposit area with highest concentrations in the Rišianka Valley. Its primary occurrences can be presumably assigned to circulation of low-temperature fluids in areas of relatively young tectonic activity.

Scheelite, though never described in its host rock in the Boca River's drainage area, has been found at numerous localities in the Tatric and Veporic units (Hvožd'ara, 1985). Scheelite impregnations in paleobasalts and amphibolites and in quartz veins are present at W-Au deposit Jasenie - Kyslá (Pulec et al., 1983). Quartz-scheelite veins in metamorphic rocks of the Tatric unit are present at the Sb-Au Dúbrava Deposit (Čillík et al., 1979, Chovan et al., (ed.) 1994). Analogical source rocks are presumed in the studied area.

The find of cassiterite, identified by spectral and XRD analyses by Linkešová & Čillík (1979), remains speculative. Content of cassiterite in pan-samples varies between x and xx grains. Its possible source is unknown, nevertheless Linkešová & Čillík (1979) suspect its linkage to bodies of porphyric granites.

Content of micas and chlorites (a.k.a. layered silicates) is only orientational, because during the sample preparation, these tend to disintegrate into several daughter flakes (Dill, 1998) that introduce errors in the statistical evaluation.

We observed no carbonate and/or sulfide anomalies in our samples. This implies that siderite- and base metal mineralizations have virtually no effect on the mineral content of the alluvium compared to the influence of surrounding Mesozoic carbonate complexes.

Gold was actively mined in the Nižná and Vyšná Boca surroundings and also gleaned from the Boca River (Bergfest, 1952). Morphological evidence of mining of alluvial gold in the Boca Valley was found and documented. It was found that the highest concentration of remains after gold panning is at the confluence of the Boca River and the Michalovský potok Brook, between the villages of Malužiná and Kráľova Lehota. However, the highest gold counts were obtained from samples between Nižná Boca and Malužiná (samples NB-Š2,

NB-Š3). These results are in very good agreement with morphology of the Boca Valley. Gold grains from the Boca River exhibit signs of mechanical damage (scratches, deformations, indentations) and rounding processes. However, we observed neither distinct correlation between the roundness of gold grains and distance of transport, nor decreasing number of overgrown gold grains (quartz) with increasing transport distance. These correlations were observed at numerous localities (e.g., Groen et al., 1990; Bakos & Chovan, 1999, Knight et al., 1999, Bahna et al. 2001). Flakes (not overgrown with quartz or pyrite) were found to be the most frequent particle shape. Our results suggest that the percentage of flake-shaped gold grains increases and the percentage of nuggets and branching nuggets decreases with increasing distance of transport. It is important to point out that our results can be biased because of small quantities of gold grains in several samples from the Boca River (NB-Š15, 14, 6, 8, 9, 10).

Gold-rich rim formation was observed on gold grains from the Boca River and the number of gold grain with this feature was found to increase with transport distance. Models summarized by Groen et al., (1990) suggest the formation of gold-rich rims by hydrometallurgical, self-electrorefining processes driven by electromotive force (EMF) between two different metals in a solution whose Eh is higher than that in which the alloy is stable.

Elevated Hg content in some alluvial gold grains (up to ~2.2 wt.%) and one grain with 22.83 wt.% of Hg confirm historic reports (Bergfest, 1952) that mention the use of amalgamation process to extract gold from the ore.

Acknowledgements

Authors would like to thank Š. Ferenc (ŠGÚDŠ B. Bystrica) and R. Laffers (Comenius University) for their help with mapping and sample collection. We also appreciate the help of M. Gregorová and J. Stankovič (Comenius University) with sample separation and microprobe analysis, respectively. This work was supported by grants VEGA No.1/8318/01, 1/1027/04 and the Department of Environment, project No. 160. Brian Hahn (SUNY Stony Brook) is thanked for proofreading the manuscript.

References

- Abbot, P. L. (1999): *Natural Disasters*, 2nd Edition, WCB McGraw-Hill, 397.
- Bahna B., Smirnov A., Chovan M. & Bakos F. (2001): Changes of gold chemical composition during transport in alluvial sediments as documented on localities in the Western Carpathians, *Mineralia Slovaca*, 33, 514-515 [in Slovak].
- Bakos F., & Chovan, M. (1999): Genetic types of gold at the Magurka deposit, *Mineralia Slovaca*, 31, 3-4, 217-225 [in Slovak].
- Bergfest, A. (1952): Mining in Boca, Central Mining Archive B. Štiavnica, *Manuscript*, 76 [in Slovak].
- Biely, A., & Bezák V. (eds.) (1997): Geologic map of the Nízke Tatry Mts. 1:50000 - Explanations, *GSSR Bratislava*, 232 [in Slovak].
- Broska I. & Uher P. (1991): Regional typology of zircon and their relationship to allanite-monzonite antagonism (on example of Hercynian granitoids of the Western Carpathians), *Geologica Carpathica*, 42, 271-277.
- Broska I. & Siman P. (1998): The breakdown of monazite in the Western Carpathian Veporic Orthogneisses and Tatric granites, *Geologica Carpathica*, 49, 161-167.

- Cambel, B., Král, J. & Burchart, J. (1990): Isotopic geochronology of the Western Carpathians crystalline core, *VEDA Bratislava*, 183 [in Slovak].
- Chovan, M., Háber, M., Jeleň, S. and Rojkovič, I. (eds.) (1994): Ore textures in the Western Carpathians, *SAP, Bratislava*, 219.
- Chovan, M., Póč, I., Jancsy, P. a Krištín, J. (1995): Sb-Au (As-Pb) mineralization of the Magurka deposit, Nízke Tatry Mts., *Mineralia Slovaca* 27, 397 – 406 [in Slovak].
- Čillík, I., Hvožd'ara, P., Michálek, J. (1979): Scheelite in antimony deposit at Dúbrava, Nízke Tatry Mt. *Mineralia Slovaca*, 11, 4, 311-326 [in Slovak].
- Dill, H. G. (1998): A review of heavy minerals in clastic sediments with case studies from the alluvial-fan through the near shore-marine environments, *Earth-Science Reviews*, 45, 103-132.
- Ferenc, Š. & Rojkovič, I. (2001): Copper mineralizations in the Permian basalts of the Hronicum unit, *Geolines*, 13, 22-27.
- Friedl, I. (1987): Study of mineralizations in volcanic rocks of Permian age at the Malužiná – Svídovo locality (Nízke Tatry Mts.), *Manuscript – Diploma thesis*, Department of Mineralogy and Petrology, Comenius University, 76 [in Slovak].
- Gleason, S. (1972): Ultraviolet Guide to Minerals, *Ultra-Violet Products, Inc.*, 244.
- Groen, J. C., Craig, J. R. & Rimstidt, D. (1990): Gold-rich rim formation on electrum grains in placers, *Canadian Mineralogist*, 28, 207-228.
- Hvožd'ara, P., (1980): Prospection minerals at tatroveporicum basement. *Acta geol. geogr. Univ. Comen.*, 35, 5-43 [in Slovak].
- Hvožd'ara P. (1985): Results of panning prospecting in the veporic crystalline complex. *In: Accessory Minerals*, GÚDŠ Bratislava, 125 - 132. [in Slovak].
- Hvožd'ara, P., (1999): Gold placers in the Western Carpathian area. *Mineralia Slovaca*, 31, 241-248 [in Slovak].
- Knight, J. B., Morison, S. R. & Mortensen, J. K. (1999): The relationship between placer gold particle shape, rimming and distance of fluvial transport as exemplified by gold from the Klondike district, Yukon Territory, Canada, *Economic Geology*, 94, 635-648.
- Linkešová, M., & Čillík, I. (1979): Cassiterite in the Nízke Tatry Mts., *Mineralia Slovaca*, 11, 4, 354 [in Slovak].
- Mange, M. A. & Maurer, H. F. W. (1992): Heavy Minerals in Color, *Chapman & Hall*, 147.
- Matula, I., & Hvožd'ara, P. (1985): Current condition of regional prospecting works using the method of heavy minerals and alluvial sediments in Slovakia, *In: Accessory minerals*, GÚDŠ Bratislava, 27 – 37 [in Slovak].
- Nickel, E. (ed) (1973): Stability of Heavy Minerals, *Schweizerbart'sche, E. Verlagsbuchhandlung*, 125.
- Ozdín, D. & Chovan, M. (2000): New mineralogical and paragenetical knowledge about siderite veins in the vicinity of Vyšná Boca, Nízke Tatry Mts., *Slovak Geol. Mag.*, 5, 255 – 271.
- Petrík, I., Broska, I., Uher, P. & Král, J. (1993): Evolution of the Variscan granitoid magmatism in the Western Carpathian realm. *Geol. Carpath.*, 44, 4, 265-266.
- Pulec, M., Klinec, A. & Bezák, V. (1983): Geology and exploration of scheelite – gold ores at Kyslá near Jasenic. *In: Pecho, J.(ed.): Scheelitovo-zlatonosné zrudnenie v Nízkyh Tatráh. GÚDŠ*, 11 - 37 [in Slovak].
- Rost, R. (1956): Heavy Minerals, *Academia*, 238 [in Czech].
- Smirnov, A. (2000): Sb-Au mineralization in Nižná Boca (Nízke Tatry Mts.), *Manuscript – Diploma (MSc) thesis*, Department of Mineralogy and Petrology, Comenius University, 131 [in Slovak].
- Turan, J. (1962): Barites of the Nízke Tatry Mts. and adjacent areas, *Geologické Práce, Zošity* 62, 115 – 122 [in Slovak].
- Vozárová, A. & Vozár, J. (1988): Late Paleozoic in West Carpathians, *GÚDŠ Bratislava*, 314.
- Warren, S. T. (1969): Minerals That Fluoresce With Mineralight Lamps, *Ultra-Violet Products, Inc.*, 32.

The carbonate rocks of Kozani area (NW Greece) in regard to certain industrial applications

CONSTANTINA DAGOUNAKI*, ANNA KASSOLI-FOURNARAKI*, ANANIAS TSIRAMBIDES*
and CONSTANTINOS SIKALIDIS**

*School of Geology, Aristotle University of Thessaloniki, 541 24 Thessaloniki, Greece.

**School of Chemical Engineering, Aristotle University of Thessaloniki, 541 24 Thessaloniki, Greece.

Abstract. The suitability of Kozani's broader area carbonate rocks for use in industrial applications is examined on the basis of their mineralogical, chemical and technical features. The studied carbonate rocks belong to the Pelagonian zone and are represented mainly by pure limestones with minor dolomites and dolomitic limestones. Examination concerning their insoluble residue, organic matter and whiteness together with their mineralogical and chemical composition satisfy specific requirements for use in certain industrial applications. As it was resulted, nearly all carbonate formations, except some of the Siatista formations and the dolomitic or dolomite containing formations of Vermion, satisfy the requirements for paint industry. Three formations (one from Vermion, one from Kozani and one from Vourinos) are suitable for paper industry. Only the Siatista carbonate rocks can be used in rubber industry. The most suitable rocks for flue gas desulfurisation are one formation from Siatista and one from Vermion. Finally, all the dolomitic formations of the area meet the requirements for fertiliser industry.

Key words: Northwestern Greece, carbonate rocks, dolomite, industrial applications.

Introduction

General

Naturally occurring carbonate rocks, which include limestones, marbles and dolomites, are extremely important natural resources finding widespread applications and thus being placed among the most important raw materials. This is due to their application in many uses usually after mechanical and/or chemical treatment. The main use of limestone as crushed stone is in constructions, mainly as an aggregate and filler, providing strength and hardness, ideal particle shape and resistance to weathering. Limestones along with marbles are used as decorative stones because they show ideal colors and mechanical strength. In addition, significant amounts of limestone are used in the metal refining, in the flue gas desulfurisation and as inert fillers extending further in numerous industrial products (i. e. paper, paint, glass, plastic, etc), (Boynton, 1980, Pentarakis, 1981, Laskaridis, 1994, Oates, 1998, Tsirambides, 2001). Dolomite is the raw material for the production of MgO and it is necessary to alloys, paints and developed products. It is used in desulfurisation of iron and steel, in the manufacture of special cements, refractories, pharmaceuticals, glass industry, fertilizers, etc. Carbonate rocks are finally used in chemical industry for the production of Mg(OH)₂ and chemical MgCO₃ (Anani, 1984, Tsirambides, 1996). The carbonate rocks often contain impurities which depending on the frequency of their appearance and contribution into the rock, can affect their exploitation (Katerinopoulos & Stamatakis, 1995).

Greece is a country with many carbonate formations. Having marble production equal to 2,05 million tones possess the third place in the European Union and the eighth in the world. It is estimated that the deposits of dolomites in Greece are about 10 million tones while the deposits of limestones and marbles are virtually unlimited (Laskaridis, 1994, Tsirambides, 1996).

In this paper some of the most significant carbonate rock formations of Kozani area (NW Greece) are mineralogically, chemically and technologically studied in order to determine their suitability for several industrial applications, as in paper, paint and rubber industry, as well as in flue gas desulfurisation and in fertilizers industry. It must be mentioned that the carbonate rocks of Kozani broaded area have stimulated recently the strong interest of several researchers concerning their potential use in industry (Laskaridis, 1989, Laskaridis, 1994, Laskaridis, 1996, Laskaridis, 2000, Dagounaki, 2001).

Geological Setting

Geotectonically, the broader area belongs to the Pelagonian zone. The crystalline unit of the Pelagonian pre-Upper Carboniferous basement includes a series of metamorphic rocks intruded in several places by large masses of Upper Carboniferous granites. Two separate carbonate covers were deposited on the margins east and west of the Pelagonian zone during the Triassic-Jurassic. The cover of the eastern margin is a neritic carbonate sequence which thrust westward onto the Pelagonian crystalline basement in the Late Jurassic-Early Cretaceous. The autochthonous neritic carbonate cover of the western Pe-

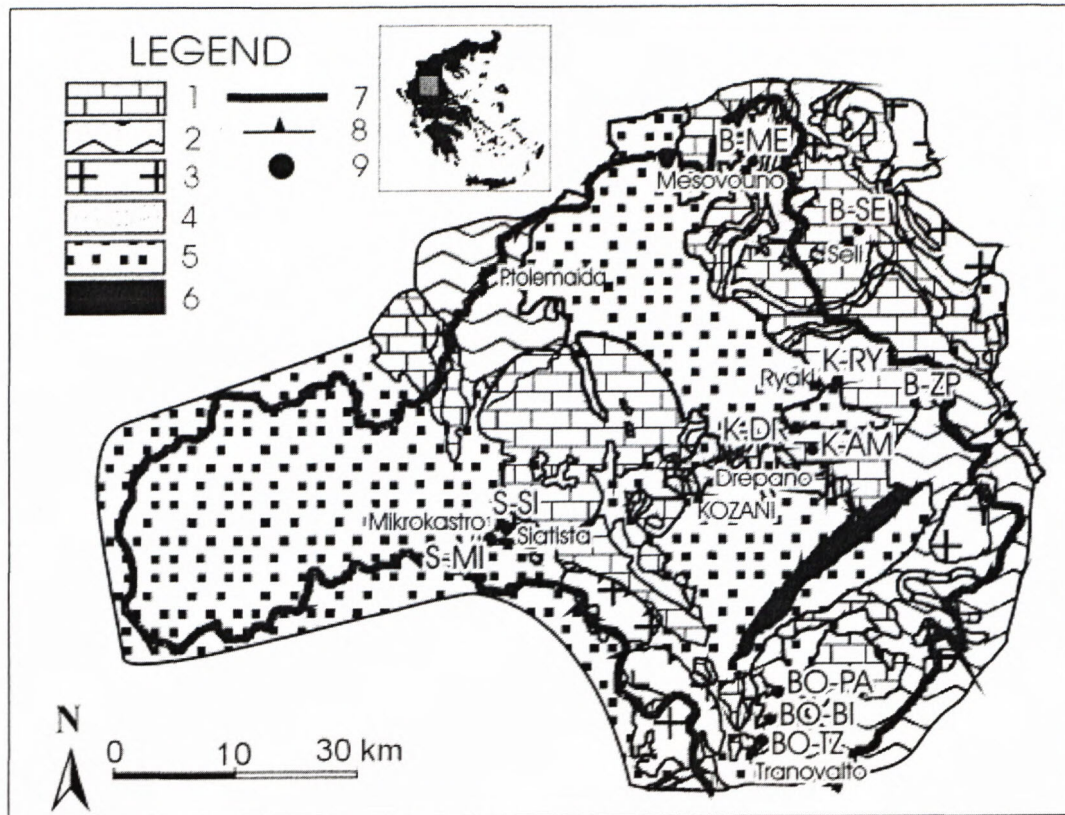


Figure 1. Geological sketch map of the Kozani broader area and sample locations.

1 = Limestones-marbles, 2 = Metamorphic rocks, 3 = Igneous rocks, 4 = Flysch, 5 = Alluvial deposits, 6 = Polyfytos lake, 7 = Kozani prefecture borders, 8 = Obduction, 9 = Sample locations.

lagonian margin was deposited on the Upper Paleozoic metaclastics (Mountrakis, 1984, Mountrakis, 1986). Big ophiolitic complexes were obducted on the Triassic-Jurassic carbonate formations of the Pelagonian zone. Ophiolites are overlain by Middle-Upper Cretaceous sediments and Early Paleocene flysch deposits (Mountrakis, 1985).

Two metamorphic events are inferred, a pre-Upper Carboniferous metamorphism of mainly upper greenschist facies which affected the crystalline basement and a post-Jurassic which resulted in a weak, low-grade greenschist fabric in the Upper Paleozoic and Mesozoic rocks (Mountrakis, 1984, Mountrakis, 1986, Nance, 1981).

Materials and methods

Representative carbonate samples were collected from the whole area of Kozani prefecture (Fig. 1). Samples S-MI and S-SI were collected from the formations near the town of Siatista. Samples B-SE, B-ME and B-ZP derive from carbonate formations of the Vermion mountain. Samples K-RY, K-DR and K-AM were collected from carbonate formations near the town of Kozani. Samples BO-BI, BO-TZ, BO-PA1 and BO-PA2 belong to the quarried limestone formations of Vourinos.

Thin sections were prepared for microscope examination in order to examine their texture and mineralogical composition. Part of each carbonate sample was ground

in an agate mortar for X-Ray Diffraction (XRD) analysis, as well as for chemical and whiteness determinations. XRD analyses were performed using a Phillips type diffractometer with Ni-filtered $\text{CuK}\alpha$ radiation. Randomly oriented samples were scanned over the interval $3-63^\circ$ of 2θ at a scanning speed of $1.2^\circ/\text{min}$. Semi-quantitative estimation of the abundances of the minerals was made from the XRD data.

Chemical analyses of the rock samples were performed by Atomic Absorption Spectrophotometry (AAS) using a PERKIN-ELMER 5000 apparatus. Ground samples were heated at 450°C for two hours in order to remove the organic matter and were treated by 1N HCl solution for the determination of the insoluble residue and its mineral content. Finally, pellets of 5 cm diameter and 0.5 cm thickness were prepared from the ground samples and their whiteness were measured using a DIFFUSION SYSTEMS, Model 99 spectrometer.

Results and discussion

Macroscopically, the studied carbonate samples display a distinctive variation in color and appearance. Samples S-MI, S-SI, B-SE, B-ME and K-DR are dark gray with white veinlets, samples K-RY and BO-PA2 are light gray and samples B-ZP, K-AM, BO-BI, BO-TZ and BO-PA1 are white in color. Microscopic examination of thin sections revealed a coarse-grained holocrystalline texture-

for B-ZP, K-AM, BO-BI, BO-TZ, BO-PA1 and BO-PA2 and a micritic texture for S-MI, B-ME, K-RY. Finally, the S-SI, B-SE, K-DR are consisted of medium and coarse grains, often tectonized.

The mineralogical composition (semi-quantitative determination by XRD) of the samples is shown in Table 1. The majority of the samples (S-MI, S-SI, B-SE, B-ZP, K-DR, BO-BI, BO-TZ, BO-PA1) are limestones with calcite content between 93-99% and only the B-ME, K-RY and K-AM are dolomitic rocks with dolomite content ranging between 92-96%. The sample BO-PA2 is characterized as dolomitic limestone with calcite content 83% and dolomite 17% (Harben 1992). The maximum percentage of impurities (minerals except of calcite and dolomite) was observed in sample B-ME (3%).

Table 1. Mineralogical composition (wt.%) of the Kozani carbonate rocks.

	Calcite	Dolomite	Quartz	Chlorite	Muscovite
S-MI	99		1		
S-SI	99		1		
B-SE	93	6	1		
B-ME	5	92		3	
B-ZP	99		1		
K-RY	4	96			
K-DR	99		1		
K-AM	5	95			
BO-BI	99		1		
BO-TZ	97	3			
BO-PA1	97		1		2
BO-PA2	83	17			

S-MI and S-SI=Statista (Upper Jurassic-Lower Cretaceous and Middle Triassic-Lower Liassic limestones, respectively)

B-SE, B-ME and B-ZP=Vermion (limestone from Axios zone, Upper Cretaceous dolomite and quarried limestone, respectively)

K-RY, K-AM and K-DR =Kozani (Triassic-Lower Jurassic dolomites and Middle-Upper Cretaceous limestone, respectively)

BO-BI, BO-TZ, BO-PA1 and BO-PA2=Vourinos (Middle Triassic-Jurassic quarried limestones)

The results of chemical analyses are consistent with the mineralogical composition (Table 2). The amount of impurities (oxides except of CaO and MgO) ranges between 1.14% and 3.22%, which is explained by the low grade of metamorphism (greenschist face) of the rocks. Chemical analyses for the amount of trace elements show that only two samples (B-SE and B-ME) present higher concentrations of Cr and all the samples except S-SI, B-ME, K-RY and K-AM present higher concentrations of Ni compared to average composition given for commercial limestones. K-DR presents higher concentration of Co compared to the other samples. These relatively higher concentrations of the above trace elements are attributed to the direct contact of the limestone formations with the ophiolitic complexes.

Table 3 shows the insoluble residue with the corresponding mineralogical composition for each sample, as well as the organic matter content and the values of

whiteness determined. The insoluble residue presents low values ranging between 0.09% wt. and 1.73% wt. and contains mainly quartz, chlorite and muscovite and less albite. The paragenesis quartz+chlorite+muscovite+albite confirms the greenschist metamorphic phase of the carbonate formations. The organic matter ranges between 0 and 1.07%, remaining thus within the limits given for carbonate rocks (Boynton, 1980).

Concerning the whiteness of the studied samples, it was found that the color of B-ZP, K-RY, K-AM, BO-TZ and BO-PA1 is approaching the 'pure white color', the color of S-SI, K-DR, BO-BI and BO-PA2 is in the wavelength of yellow, the color of B-ME and B-SE is in the wavelength of blue-green and the color of S-MI is in the wavelength of orange.

The main quality requirements for use of carbonate rocks on the basis of their chemical composition (wt.%) and values of their whiteness are (Boynton, 1980, Power, 1985, Harben, 1992, Oates, 1998):

- Paper industry: for limestones: >96% CaCO₃, for dolomites: >53% CaCO₃, >44.5% MgCO₃.
- Paint industry: (CaCO₃ + MgCO₃) >95%, MgCO₃ >3%, brightness 80% (putty) to 96% (paper coating).
- Rubber industry: Cu < 40 ppm, MnO < 0.02%, (CaCO₃ + MgCO₃) > 98%.
- Flue gas desulfurisation: CaO >53.2%, MgO >0.5%, SiO₂ >0.65%, CO₂ >41.8% whiteness > 80%, insoluble residue < 1%.
- Fertilisers: Coarsely pulverised dolomitic limestone and dolomite are frequently added to fertilisers. High-calcium limestone is rarely used in fertiliser formulations, because it can release ammonia from nitrogenous compounds.

According to the experimental results and the established standards the studied carbonate rocks can be used for the following industrial applications:

- The samples K-RY, B-ZP and BO-TZ are suitable for the paper industry. Comparing the chemical composition of these samples to the requirements, it is shown that they are very close to the necessary standards. The sample K-RY contains up to 96.9% (CaCO₃ + MgCO₃) and this is above the established limit of 53% CaCO₃ and 44.5% MgCO₃. The sample B-ZP is a pure limestone containing more than 96% CaCO₃, therefore, it is suitable for the manufacture of paper. The sample BO-TZ has a content of CaCO₃ almost 96%, a fact which is not forbidding for its use to the paper industry.
- Furthermore, the samples S-SI, B-ZP, K-RY, K-DR, K-AM, BO-BI, BO-PA1 and BO-PA2 can be used in the paint industry, since they fulfil the chemical specifications and the whiteness limits. The content of (CaCO₃ + MgCO₃) of these samples exceeds the limit of 95%, the lowest value is observed in BO-PA1 (96.76%) and the highest one in S-SI (98.71%). Their whiteness values are also within the limits, as the lowest one is 82.2% (K-DR) and the highest one is 95.1% (B-ZP).

Table 2. Chemical composition of the Kozani carbonate rocks.

(wt. %)	S-MI	S-SI	B-SE	B-ME	B-ZP	K-RY	K-DR	K-AM	BO-BI	BO-TZ	BO-PA1	BO-PA2	(Mason & Moore 1982)*
SiO ₂	0.54	0.70	2.41	2.14	2.14	2.41	1.88	2.41	2.94	2.67	2.67	2.14	5.19
Al ₂ O ₃	0.10	0.00	0.12	0.15	0.00	0.00	0.00	0.00	0.00	0.00	0.17	0.00	0.81
TiO ₂	0.016	0.290	0.016	0.000	0.000	0.000	0.016	0.100	0.000	0.000	0.000	0.000	0.060
MnO	0.010	0.002	0.010	0.004	0.005	0.002	0.007	0.002	0.007	0.002	0.002	0.004	
Fe ₂ O _{3t}	0.15	0.07	0.13	0.07	0.00	0.00	0.06	0.00	0.04	0.00	0.07	0.00	0.54
CaO	54.30	55.20	51.25	31.15	54.60	31.85	53.03	30.45	52.58	53.90	52.80	49.80	42.57
MgO	0.56	0.29	2.08	21.33	0.40	20.00	0.62	21.75	1.38	0.92	0.82	4.62	7.89
K ₂ O	0.03	0.03	0.19	0.06	0.14	0.10	0.11	0.09	0.05	0.09	0.11	0.05	0.33
Na ₂ O	0.16	0.22	0.30	0.09	0.23	0.21	0.26	0.19	0.10	0.07	0.08	0.12	0.05
P ₂ O ₅	0.14	0.19	0.04	0.03	0.045	0.02	0.03	0.03	0.03	0.02	0.02	0.025	0.04
CO ₂	43.52	43.22	43.36	44.88	42.34	45.06	43.60	44.86	42.81	42.14	43.14	42.85	
(ppm)													(Oates 1998)**
Co	28	22	16	b.d.l.	b.d.l.	16	46	b.d.l.	b.d.l.	b.d.l.	19	b.d.l.	
Cr	11	12	23	27	15	13	17	15	15	15	15	12	3-15
Ni	21	b.d.l.	28	b.d.l.	17	b.d.l.	21	b.d.l.	21	21	21	17	0.5-15
Rb	58	60	84	28	64	54	36	24	29	38	38	26	
Sr	213	185	358	168	228	153	518	102	440	210	213	250	
Zn	17	6	7	13	14	16	5	8	7	6	7	7	3-500

b.d.l.=below detection limit, *Average limestone composition (Mason & Moore, 1982), **Typical ranges of trace elements in commercial limestones (Oates, 1998)

Table 3. Insoluble residue (wt.%), mineralogical composition of insoluble residue (wt.%), organic matter (wt.%) and hiteness values (%) of the Kozani carbonate rocks.

	Insoluble residue	Mineralogical composition of the insoluble residue				Organic matter	Whiteness*
		Quartz	Chlorite	Muscovite	Albite		
S-MI	0.52	100				0.29	75.3
S-SI	0.16	100				0.20	84.5
B-SE	0.96	61	9	8	22	0.28	58.0
B-ME	1.22		100			0.61	67.2
B-ZP	0.20	1		99		0.19	95.1
K-RY	1.73	11	37	52		1.07	90.0
K-DR	0.09	100				0.20	82.2
K-AM	0.76		52	48		1.00	93.0
BO-BI	1.23	36		64		0.20	82.4
BO-TZ	0.26			97	3	0.00	90.0
BO-PA1	0.94	18	16	66		0.15	93.0
BO-PA2	1.03			100		0.19	85.3

*percentage reflectance value of sample

- The samples S-SI and S-MI are suitable for the rubber industry, as their content in CaO, MnO and Cu fulfil the requirements. The values are 54.3-55.2% for the CaO, 0.002-0.01% for the MnO and their concentration in Cu is below the detection limit (9 ppm) of the spectrophotometer for Cu. Their content in (CaCO₃ + MgCO₃) is ranging between 93.38% and 98.71%, values that are higher than the established ones.
- The samples S-SI and B-ZP can be used in the flue gas desulfurisation as their content in CaO is 55.2% and 54.6%, respectively, quantities much higher than the lowest limits. Their whiteness values (84.5% for S-SI and 95.1% for B-ZP) are above the limit of 80%. Their content in MgO is for S-SI 0.29% and for B-ZP 0.40%. They contain more SiO₂ than the established

value and their content in CO₂ is above 41.8% (43.22% for S-SI and 42.34% for B-ZP). Finally, their insoluble residue is below 1%, (0.2% for S-SI and 0.19% for B-ZP).

- Finally, the samples B-ME, K-RY, K-AM and BO-PA2 are suitable as raw materials in fertilisers. The first three samples are dolomitic rocks with MgO content ranging between 20% and 21.75%, while the sample BO-PA2 is a dolomitic limestone containing 4.62% of MgO.

Conclusions

The carbonate rocks at the Kozani broader area represent a variety of carbonate formations ranging from pure limestones (which is the majority of the rock formations)

to dolomitic limestones and dolomites. Mineral impurities, such as quartz and other silicates, participate in minor or trace amounts, remaining in the majority of the samples below 0.5%.

Measurements concerning their insoluble residue, organic matter and whiteness together with their mineralogical and chemical composition satisfy special requirements for use in certain industrial applications. Thus, nearly all carbonate formations, except some of the Siatista formations and the dolomitic or dolomite containing formations of Vermion, are suitable for paint industry. On the contrary, only three formations (one from Vermion, one from Kozani and one from Vourinos) can be used in paper industry. Furthermore, only the Siatista carbonate rocks can be used in rubber industry while for flue gas desulfurisation the most proper rocks are one formation from Siatista and one from Vermion. Finally, all the dolomitic formations of the area are suitable for the fertiliser industry.

References

- Anani, A., 1984: Applications of dolomite. *Industrial Minerals* 206, 45-55.
- Boynton, S.R., 1980: Chemistry and Technology of Limestone, 2nd edition. *Wiley & Sons*, New York, 1-578.
- Dagounaki, C., 2001: Mineralogical and geochemical characteristics of carbonate rocks from Kozani areas, Macedonia, Greece, and investigation of their capability for application in industry. MSc Thesis, *Aristotle University of Thessaloniki*, Thessaloniki, 1-108 (in Greek).
- Harben, P.W., 1992: The industrial minerals handybook. *Ind. Miner. Div., Metal Bull. PLC*, London, 17-19.
- Katerinopoulos, A. & Stamatakis, M. 1995: Applied mineralogy-petrology. Industrial minerals and rocks and their uses. *National and Kapodistrian University*, Athens, 1-311 (in Greek).
- Laskaridis, K., 1989: Examination and appraisal of Greek white limestones and dolomites for their use in industry (e.g. paper industry). *Bull. Geol. Soc. Greece*. 13, 2, 295-304 (in Greek).
- Laskaridis, K., 1994: Greek white calcitic marbles. Examination and appraisal for industry. *Industrial Minerals* 319, 53-57.
- Laskaridis, K., 1996: Quality valuation of white carbonate of Macedonia for industrial uses. *Mineral Wealth* 100, 45-54.
- Laskaridis, K., 2000: Applicability of marble wastes from the Tranovaltos-Kozani area for use as fillers in industry. *Proceedings of 1st congress of the Committee of Economical Geology, Mineralogy and Geochemistry*, Kozani, 288-298.
- Mason, B. & Moore, C.B., 1982: Principles of geochemistry. *J. Wiley & Sons*, New York, 152-155.
- Mountrakis, D., 1984: Structural evolution of the Pelagonian Zone in Northwestern Macedonia, Greece. In: The geological evolution of the eastern Mediterranean, Special Publications of the Geological Society No. 17. *Blackwell Scientific Publications*, Oxford, 581-590.
- Mountrakis, D., 1985: Geology of Greece. *University Studio Press*, Thessaloniki, (in Greek).
- Mountrakis, D., 1986: The Pelagonian zone in Greece: a polyphase-deformed fragment of the Cimmerian continent and its role in the geotectonic evolution of the eastern Mediterranean. *J. Geology* 94, 335-347.
- Nance, D., 1981: Tectonic history of a segment of the Pelagonian zone, northeastern Greece. *Can. J. Earth Sci.* 18, 1111-1126.
- Oates, J.A.H., 1998: Lime and limestone. Chemistry and technology, production and uses. *Wiley VCH*, Weinheim, 1-455.
- Pentarakis, E., 1981: A brief review of capabilities and applications of limestone and lime. The recent situation and the potentials for Greece. *Mineral Wealth* 11, 23-44 (in Greek).
- Power, T., 1985: Limestone specifications. Limiting constraints on the market. *Ind. Minerals* 212, 65-91.
- Tsirambides, A., 1996: Greek marbles and other decorative stones. *University Studio Press*, Thessaloniki, 1-310 (in Greek).
- Tsirambides, A., 2001: Industrial applications of the dolomite from Potamia, Thassos Island, N. Aegean Sea, Greece. *Materials and Structures* 34, 110-113.

Faint, illegible text in the top left quadrant, possibly bleed-through from the reverse side of the page.

Faint, illegible text in the top right quadrant, possibly bleed-through from the reverse side of the page.

Small, faint markings or text fragments located on the right side of the page.

A small, faint red mark or smudge located in the lower right area of the page.

Thrust fault geometry of Southern Elburz Mountains in the Northern Iran

ABAS KANGI

Department of Geology, Islamic Azad University, Shahrod, Iran
E-Mail: abkangi@hotmail.com

Abstract. A three-dimensional analysis of the geometrical position of thrust faults in the Gorg-Dare area in the south of the Elburz Mountains indicates the dominance of the thrust sheets in that area. The function of thrust sheets has resulted in the disorganization of stratigraphy and consequently in the intricacies of geology in this area. On the whole, the geometry of thrust fault in this area is based on the Imbricat design. However, each thrust fault consists of smaller geometrical forms inside it. Accurate desert measurements for drawing the geological map of this area showed that each thrust sheet is made up of certain Cylindrical structures. These Cylinder-shaped structures which are surrounded with faults have placed masses of rocks adjacent to each other. Considering the large variety of ages of the Cylindrical masses adjacent to each other, it is possible that the establishment of each Cylinder-shaped structures took place during different periods of thrust fault activities. Altogether, such systems in the southern parts of the Elburz Mountains have had a major role in the evolution of geological structures and brought about fascinating geological appearance.

Key words: Elburz Mountains., Thrust Tectonics, Structural Analysis., Fault Geometry

1. Introduction

The Elburz mountains system in northern Iran (Fig.1), extending in a sinuous manner for about 2000 km from the Lesser Caucasus of Armenia and Azerbaijan in the northwest to the mountains of northern Afghanistan to the east forms a composite poly-orogenic belt. The tectonic history of southern Elburz mountains is poorly understood, since from the upper Triassic time the area was affected by the Cimmeride and the Alpine tectonic events. Attempts to synthesize regional stratigraphy and structural features of this mountains system have been restricted to what Stocklin (1960, 1968, 1974a,b) and Stampfli (1978) presented on the basis of data which were meagre and scanty at the time, and by workers (Berberian and King, 1981; Davoudzadeh et al., 1986; Davoudzadeh and Weber-Diefenbach, 1987; Boulin, 1988; Sengor, 1990; Stampfli et al., 1991) who based their analyses almost entirely on the same data and interpretations already presented by Stocklin and Stampfli. Detailed structural and lithostratigraphic analyses in some specific critical parts of the Elburz, as well as systematic paleontological studies along certain stratigraphic sections have resulted in a better understanding of the stratigraphy and structural geometry of this mountains system (Seyed-Emami et al., 1971; Bozorgnia, 1973; Seger, 1977; Stampfli, 1978; Hamdi and Janvier, 1981; Ahmadzadeh-Heravi, 1983; Hamdi et al., 1989; Seyed-Emami and Alavi-Naini, 1990; Golshani, 1990; Alavi, 1996).

Our work is concentrated on a relatively small (25km) part of the Gorg-Dare near Shahrod city. The fault geometry there were studied during approximately

six months of field works. The principal product of which, a geologic map (Fig. 2), was constructed using a 1: 20000 aerial photographic base. This detailed map and attendant structural geology work, gave us the new pattern of thrust faulting geometry in this area.

2. Lithostratigraphy

Based stratigraphic analyses several formations may be distinguished in this area (Fig.2) each formation formed in a tectonically controlled environment and in the following paragraphs I present a brief and general description of these formations, ranging from the oldest to the youngest.

The most characteristic constituents the upper Cambrian Mila Formation are nodular limestones, in part strongly glauconitic and containing abundant trilobites, brachiopods, and hyolithids. These limestones are associated with dolomitic, marly, shaly and sandy beds. This unit is considered to represent deposits of an epicontinental platform sedimentary basin that was influenced by the initial stages of extensional tectonics (Alavi, 1996). The upper Devonian-Carboniferous Geirud Formation consists of sandstones, shales, fossiliferous sandy limestones and several phosphatic layers, followed by sandstones, shales and fossiliferous limestone.

The lower Triassic to middle Triassic Elikah Formation consists of an association of limestone, partly marly, rarely dolomitic, yellow to pinkish. Many beds are crowded with worm-tracks, calcaires vermicules (Stocklin, 1977).

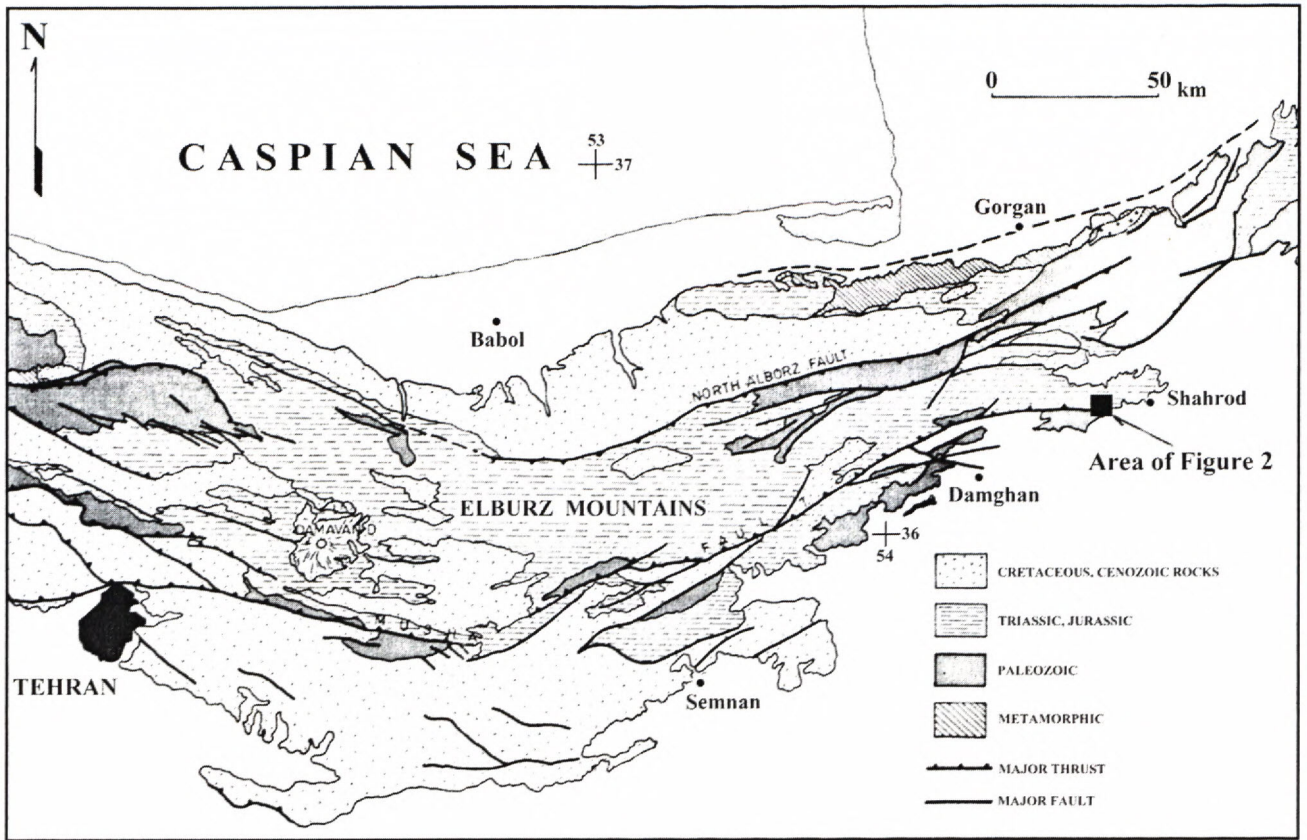


Fig. 1. Tectonic map of the Elburz system with major lithotectonic units and main structural features (Adapted from Geological map of Iran 1:1000,000 NIOC 1973-1978; 6 sheets).

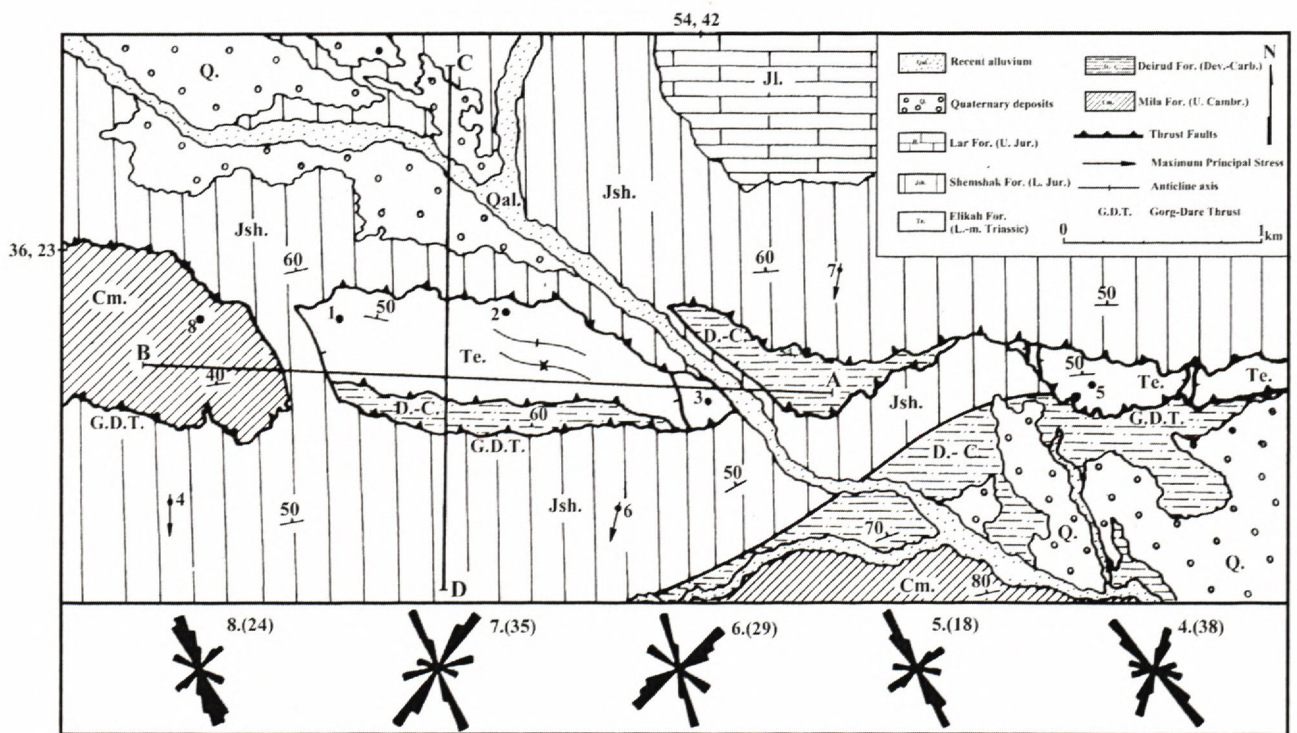


Fig. 2. Geologic map of Gorg-Dare area in southern Elburz Mountain, showing the characteristic joint patterns, illustrated by rose diagrams, and the maximum principal stress.

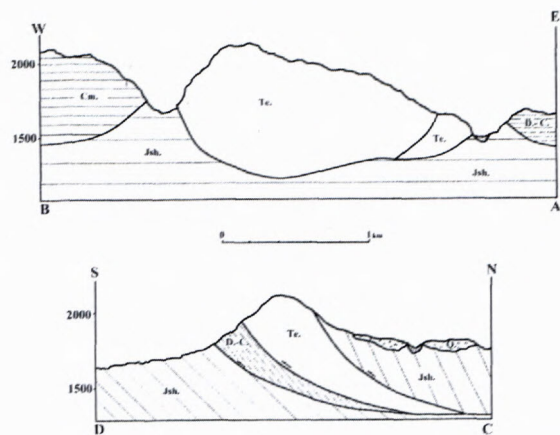


Fig. 3 Cross-section the Gorg-Dare area with major structural features. Localities shown in Figure 2.

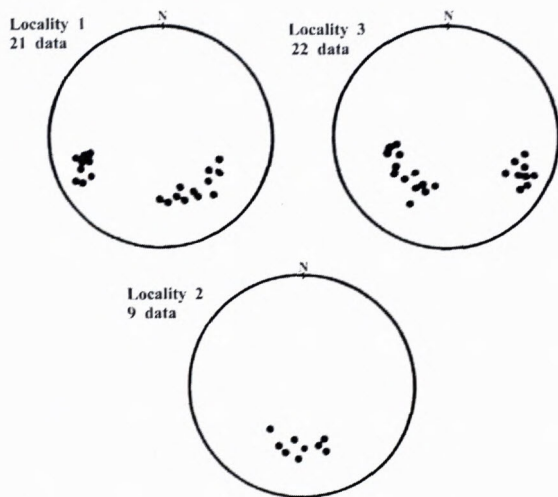


Fig. 4 The measurements conducted on the surrounding faults of a cylinder-shaped structure. Localities shown in Figure 2.

The lower Jurassic Shemshak Formation consists of an association of sandstones, siltstones, shales and claystones, that have coal seams up to 1.5m thick as a characteristic feature (Assereto, 1966). The lower part of the Shemshak Formation is characterized by cross-bedding and ripple marks are numerous and indicate a very shallow-water to lagoonal environment of sedimentation. The upper parts contain features characteristic of deltaic environment (Stocklin, 1968, 1977). The lower part of rocks may have formed the Shemshak Formation is characterized by plant fragments which are of central Asiatic type. Cross-bedding and ripple-marks are numerous and indicate a very shallow water to lagoonal environment of sedimentation. The upper parts contain features characteristic of deltaic environment. Regional structural considerations coupled with the sedimentary characteristics of this unit, with distinctive lateral variations, strongly suggest that these in a foreland basin in front of the tectonically active, south-verging, blocks uplifted during the Cimmeride orogeny, which later became covered by marine transgression strata (Alavi, 1996).

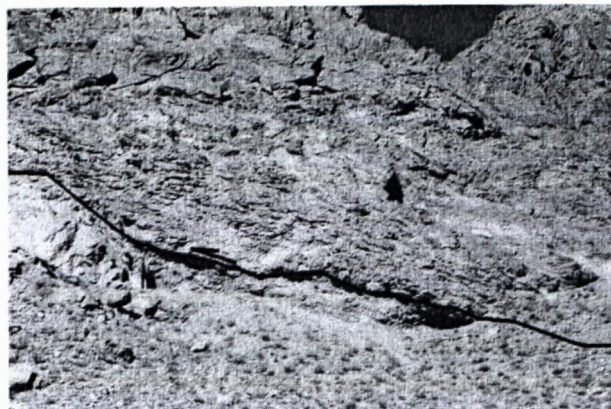


Fig. 5 Development mylonites at surface Gorg-Dare Thrust fault.



Fig. 6. C-type shear band cleavage in surface Gorg-Dare thrust fault.

The upper Jurassic Lar Formation is composed of light gray, compact and thin bedded to massive partly reef limestone 250 to 350 meters thick and containing characters-tic nodules and bands of white or violet chert. The limestone overlies conformably the Shemshak Formation.

3. Structural Geology

The tectonics of the Elburz system are dominated by thrust faults. Stocklin (1968), synthesized a generalized tectonic framework for the Elburz Mountains as a large, E-w trending, deep-seated synclinal structure whose southern and northern limbs were imbricated by several south-verging and north-verging thrust faults.

3.1. The Gorg-Dare Region

The Gorg-Dare region, north west of shahrod (Fig. 2), studied in this area, thrusts are the dominant structural features. They are all north dipping and mostly associated with mylonites (Fig. 5). Mylonites can be recognized in the field by their small grain size and strongly developed, unusually regular and planar folia-

tion and straight lineation. Mylonites commonly contain two or even three foliations, inclined to each other at small angles, that is thought to have developed contemporaneously (Passchier and Trouw, 1998). Foliation in mylonite is locally subject to tight or isoclinal folding. In most cases, the axial planar foliation in these folds cannot be distinguished from the main foliation in the mylonite. Some of these folds are sheath folds, that is they have a tubular shape parallel to the mylonite lineation. Study C-type shear bands in this mylonites display a north-to-south movement direction (Fig. 6). Thrusting was propagated sequentially southward from the interior of the Elburz mountains toward its southern foreland.

The Gorg-Dare area is affected by thin-skinned tectonics. The thrust sheets comprising various stratigraphic units, including, Mila Formation, Geirud Formation, Elikah Formation and Shemshak Formation. Fig. 2 and the cross-section in Fig. 3 reveal the general geometry of the thrust faults exposed in the Gorg-Dare area. Geometrically, generations of thrusts, all south-verging, from imbricate fans, composed of several single sheets and a number of internal thrust sheets Cylinder form. These are restricted to the structural sheets and are bounded by the thrust boundaries (Fig. 7). It is clear that the Cylinder forms are genetically related to the thrust movements.

The measurements of the position of the three-dimensional geometry of thrust faults in this area indicates that there are certain forms of Cylinder-shaped geometry in thrust sheets. These Cylinder-shaped structures, which make up a thrust sheet altogether have unnaturally placed different formations adjacent to each other. In appearance a mass of Cylinder-shaped rock is surrounded with a group of thrusts in all directions. Moreover, the existing lineations with a radial design on these thrusts can be observed in different parts of the Cylindrical structure. The most appropriate place for the observation of such a structure is where there are two Cylinder-shaped connections. Here, the geometrical form of Cylinder-shaped thrusts are easily observable. Based on desert measurements and observations, attempts are made to display the three-dimensional geometry of such structures in Figures 7 and 8. Among the other interesting structures present in each of the Cylinder-shaped masses are the existence of conjugate thrusts (Fig. 9). Such thrusts can be observed as a group of parallel thrusts with a slope of 90 degrees in every Cylinder-shaped mass. These thrusts are usually formed crisscross along with the displacement of strike slip. The collection of crisscross thrusts was formed in the course of the displacement and establishment of thrust sheets in the masses of Cylinder-shaped rocks.

3.2. Structural Analysis

In order to describe the three-dimensional geometry of cylinder-shaped structures, structural parameters such as faults and fractures found in the region under study have been extensively measured. These measured data have been the main foundation of detailed interpretation on the structural model of the region. Statistical analyses

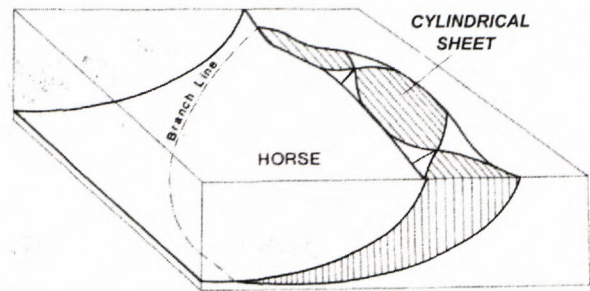


Fig. 7. Block diagram showing horse in a volume of rock surrounded by fault surfaces, formed three cylindrical sheets.

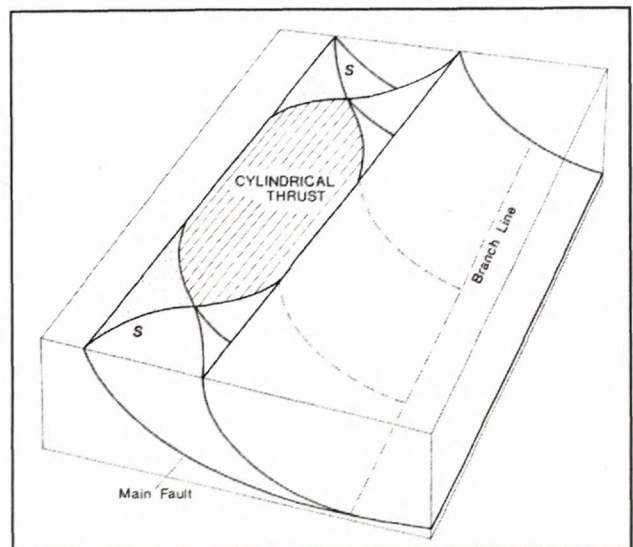


Fig. 8. Block diagram showing cylindrical sheet, which has two major faults, with connecting splay (S) and one branch line depth.

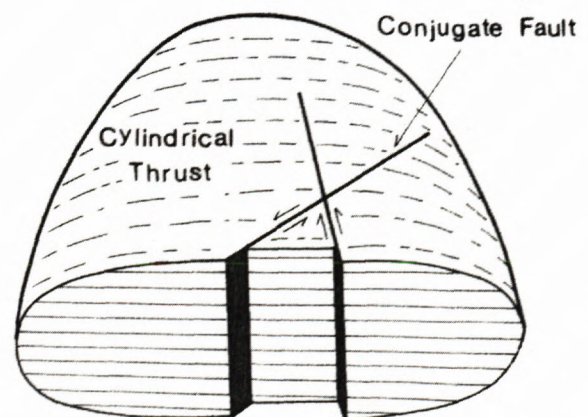


Fig. 9. Three-dimensional view of conjugate fault system, internal cylindrical sheet.

carried out on the conjugate faults indicate that direction of maximum principal stress generally has on N10E orientation. The measurements conducted on the surrounding faults of a cylinder-shaped structure indicate that every section of this structure follows a particular geometrical pattern. In Figure 4, geometrical situation of fa-

ults in various parts of a cylinder-shaped structure has been illustrated by the stereonet. This set of measured faults shows this structure in a three-dimensional pattern. Striations on the surface of faults covering a cylinder-shaped structure have a radial pattern. Therefore, by approaching the end of this structure, the angle of striation pitch will be smaller.

4. Conclusions

According to the geometrical indices of thrust faults in the Gorg-Dare area in the south of the Elburz Mountains the following results are presented.

1. As a major system, the thrust faults dominate the changes of forms in the southern part of the Elburz.

2. The results of the study of C-type shear bands on the surface of thrust faults indicates the displacement of thrust sheets from the north to the south.

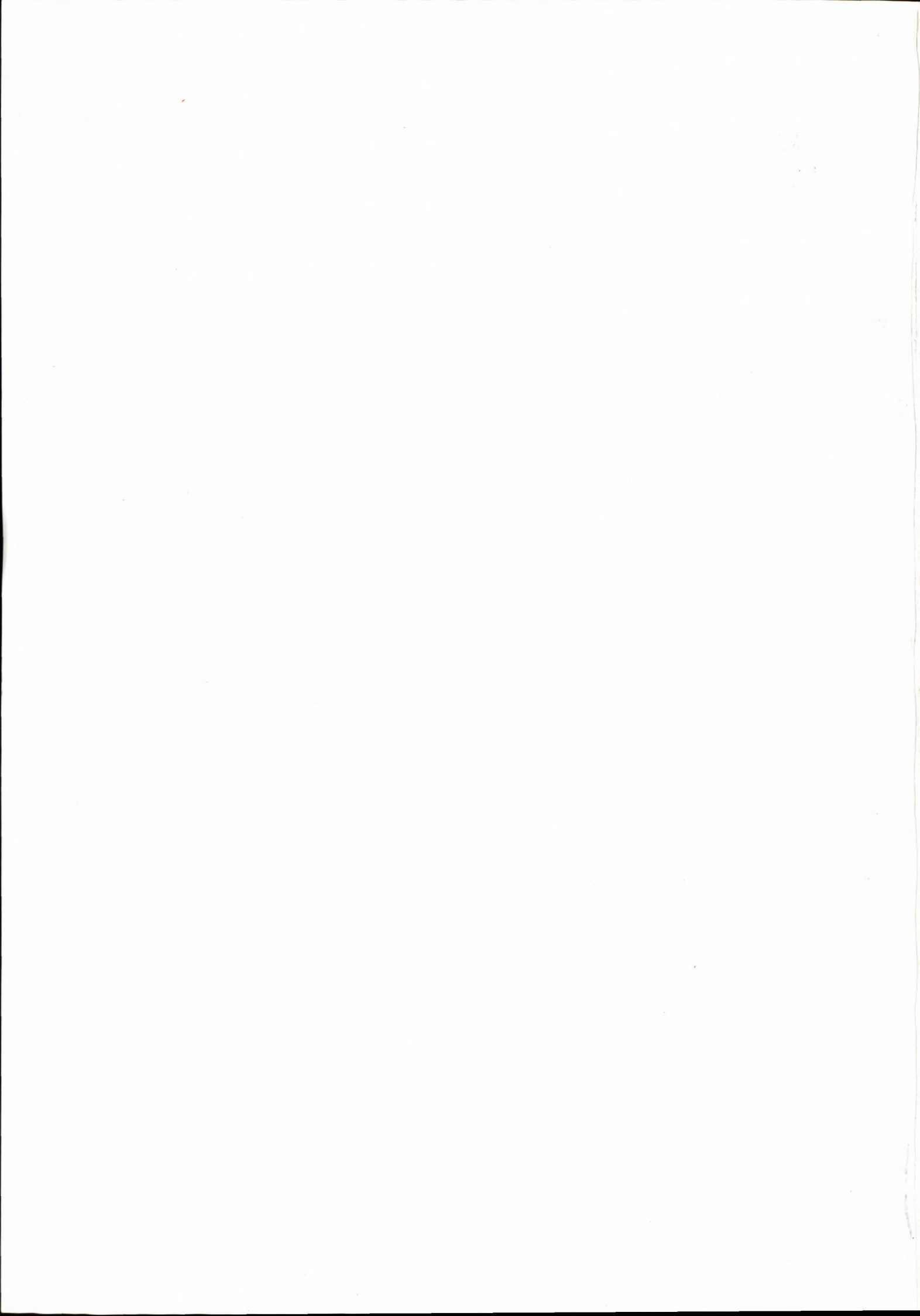
3. The position of the three-dimensional geometry of thrust faults in this area is redolent of the existence of Cylindrical forms in thrust sheets.

4. Cylinder-shaped masses have placed stratigraphic units adjacent to each other and have caused structural intricacies.

5. During the displacement and establishment of Cylinder-shaped masses, conjugate thrusts were formed as a collection of parallel thrusts with a slope of 90 degrees in the masses of rocks.

References

- Ahmadzadeh-Heravi, M. (1983): Brachiopoda and conodonts of the sedimentary rocks of The south Bojnourd area, and their stratigraphic implications (in farsi). Bull. Fac.Engng, Tehran University, 45,32-45.
- Alavi, M. (1996): Tectonostratigraphic synthesis and structural style of the Alborz mountain System in northern Iran, Geodynamic, V. 21 , No. 1, PP. 1-33.
- Assereto, R. (1966): The Jurassic Shemshak Formation in central Elburz (Iran): Riv. Ital. Paleont. Stratigr. 72,1133-1182.
- Berberian, M. and King (1981): Towards a paleogeography and tectonic evolution of Iran: Can.J.Earth Sci.18,210-265.
- Boulin, J. (1988): Hercynian and Eocimmerian events in Afghanistan and adjoining regions. Tectonophysics 148, 253-278.
- Boyer, S. E. and Elliott, D. (1982): Thrust systems: Am. Ass. Petrol. Geol. Bull. 66, 1196-1230.
- Bozorgnia, F. (1973): Paleozoic foraminiferal biostratigraphy of central and eastern Alborz Mountains, Iran. National Iranian Oil Company, Geological Laboratories Publication No. 4, pp. 185.
- Davoudzadeh, M., Lensch, G. and Weber-Diefenbach, K. (1986): Contribution to the paleogeography, stratigraphy, and tectonics of the Infrecambrian and Lower Paleozoic of Iran. Neu. J. Geol. Palaont. Abh. 172,245-269.
- Davoudzadeh, M. and Weber-Diefenbach, K. (1987): Contribution to the paleogeography, stratigraphy, and tectonics of the Upper Paleozoic of Iran. Neu. J. Geol. Palaont. Abh. 175, 121-146.
- Golshani, F. (1990): The upper Proterozoic-lower Paleozoic stratigraphy of Iran with remarks on tectonics, magmatism and metamorphism (Ph. D.thesis): Hokaido University, Hokaido, Japan, pp. 272.
- Hamdi, B. and Janvier, Ph. (1981): Some conodonts and fish remains from lower Devonian lower part of the Khoshyelaqe Formation), northeast Shahrud, Iran: Tehran, Iran. (Geological Survey of Iran, Report No. 49, 195-213.
- Hamdi, B., Brasier, M.D. and Jiang, Z. (1989): Earliest skeletal fossils from precambrian-Cambrian boundary strata, Elburz Mountains, Iran. Geo.Mag. 126, 253-286.
- Passchier, C. W. and Trouw, R. A. J. (1998): Microtectonics: Springer Publication P. 283
- Ramsay, J. G. (1987): Modern Structural Geology, Vol. 2, Academic press, Ed, London P.700.
- Seeger, F. E. (1977): Zur Geologie des Nord-Alamut Gebietes (Zentral-Elburz) (Ph.D. Thesis): Eidgenossische Technische Hochschule, Zurich, PP. 161.
- Sengor, A. M. C. (1990): A new model for the late Paleozoic-Mesozoic tectonic evolution Of Iran and implications for Oman; In The Geology and Tectonics of the Oman Region (Robertson A. H. F., Searl M. P. and Ries A .P.and Ries A .C., eds.). Special Publication no. 49, 797-831.
- Seyed-Emami, K., Brants, A. and Bozorgnia, F. (1971): Stratigraphy of the Cretaceous rocks southeast of Esfahan; In Contributions to Paleontology and Stratigraphy of Iran. Part 2. Geological Survey of Iran Report no. 20, 5-11.
- Seyed-Emami, K. and Alavi-Naini, M. (1990): Bajocian stage in Iran: Memorie Descrittive della carta Geologica d' Italia 40,215-222.
- Stampfli, G. M. (1978): Etude geologique generale de I, Elburz oriental au S de Gonbad-e-Qabus (Iran, N-E): These de Doctur des Sciences, no. 1868, Universite de Geneve, P. 328.
- Stampfli, G., Marcoux, J. and Baud, A. (1991): Tethyan margins in space and time: Palaeogeog. Palaeoclimat. Palaeoecol. 87, 373-409.
- Stocklin, J. (1960): Ein Querschnitt durch den Ost Elburz: Eclogae Geol. Helv. 72,681-694.
- Stocklin, J. (1968): Structural history and tectonics of Iran: A review. Am. Ass. Petrol. Geol. Bull. 52,1229-1258.
- Stocklin, J. (1974a): Northern Iran: Alborz Mountains: Geol. Soc. Special Publication no. 4, 213-234.
- Stocklin, J. (1974b): Possible ancient continental margins in Iran. In the geology of continental margins. Edited New York, P. 873-887.
- Stocklin, J. (1977): Structural correlation of the Alpine ranges between Iran and central Asia. Mem. Soc. Geol. Fr. Hors P. 145-353.



Instructions for authors

Slovak Geological Magazine – periodical of the Geological Survey of Slovak Republic is quarterly presenting the results of investigation and researches in wide range of topics: regional geology and geological maps, lithology and stratigraphy, petrology and mineralogy, paleontology, geochemistry and isotope geology, geophysics and deep structure, geology of deposits and metallogeny, tectonics and structural geology, hydrogeology and geothermal energy, environmental geochemistry, engineering geology and geotechnology, geological factors of the environment, petroarcheology.

The journal is focused on problems of the Alpine-Carpathian-Balkan region

General instructions

The Editorial Board of the Geological Survey of Slovak Republic – Dionýz Štúr Publishers accepts manuscripts in correct English. The papers that do not have sufficient accuracy in language level will be submitted back for language correction.

The manuscript should be addressed to the Chief Editor or the Managing Editor.

Contact address:

Geological Survey of Slovak Republic – Dionýz Štúr Publishers,
Mlynská dolina 1, 817 04 Bratislava, Slovak Republic
e-mail addresses: hok@gssr.sk
siposova@gssr.sk
http://www:gssr.sk

The Editorial Board accepts or refuses a manuscript with regard to the reviewer's opinion. The author is informed of the refusal within 14 days from the decision of the Editorial Board. Accepted manuscript is prepared for publication in an appropriate issue of the Magazine. The author(s) and the publishers enter a contract establishing the rights and duties of both parties during editorial preparation and printing, until the time of publishing of the paper.

Text layout

The manuscript should be arranged as follows: TITLE OF THE PAPER, FULL NAME OF THE AUTHOR(S); NUMBER OF SUPPLEMENTS (in brackets below the title, e.g. 5 figs., 4 tabs.), ABSTRACT (max. 30 lines presenting principal results) – KEY WORDS – INTRODUCTION – TEXT – CONCLUSION – ACKNOWLEDGEMENTS – APPENDIX – REFERENCES – TABLE AND FIGURE CAPTIONS – TABLES – FIGURES. The editorial board recommends to show a localisation scheme at the beginning of the article.

The title should be as short as possible, but informative, compendious and concise. In a footnote on the first page, name of the author(s), as well as his (their) professional or private address.

The text of the paper should be logically divided. For the purpose of typography, the author may use a hierarchic division of chapters and sub-chapters, using numbers with their titles. The editorial board reserves the right to adjust the type according to generally accepted rules even if the author has not done this.

Names of cited authors in the text are written without first names or initials (e.g. Štúr, 1868), the names of co-authors are divided (e.g. Andrusov & Bystrický, 1973). The name(s) is followed by a comma before the publication year. If there are more authors, the first one, or the first two only are cited, adding et al. and publication year.

Mathematical and physical symbols of units, such as %, ‰, °C should be preceded by a space, e.g. 60 %, 105 °C etc. Abbreviations of the units such as second, litre etc. should be written with a gap. Only SI units are accepted. Points of the compass may be substituted by the abbreviations E, W, NW, SSE etc. Brackets (parentheses) are to be indicated as should be printed, i.e. square brackets, parentheses or compound. Dashes should be typed as double hyphens.

If a manuscript is typed, 2 copies are required, including figures. The author should mark those parts of a text that should be printed in different type with a vertical line on the left side of the manuscript. Paragraphs are marked with 1 tab space from the left margin, or by a typographic symbol. Words to be emphasized, physical symbols and Greek letters to be set in other type (e.g. *italics*) should be marked. Greek letters have to be written in the margin in full (e.g. *sigma*). Hyphens should be carefully distinguished from dashes.

Tables and figures

Tables will be accepted in a size of up to A4, numbered in the same way as in a text.

Tables should be typed on separate sheets of the same size as text, with normal type. The author is asked to mark in the text where the table should be inserted. Short explanations attached to a table should be included on the same sheet. If the text is longer, it should be typed on a separate sheet.

Figures should be presented in black-and-white, in exceptional cases also in colour which must be paid approx. 100 EUR per 1 side A 4. Figures are to be presented by the author simultaneously with the text of the paper, in two copies, or on a diskette + one hard copy. Graphs, sketches, profiles and maps must be always drawn separately. High-quality copies are accepted as well. Captions should be typed outside the figure. The graphic supplements should be numbered on the reverse side, along with the orientation of the figures. Large-size supplements are accepted only exceptionally. Photographs intended for publishing should be sharp, contrast, on shiny paper. High quality colour photographs will only be accepted depending on the judgement of the technical editors.

If a picture is delivered in a digital form, the following formats will be accepted: *.cdr, *.dxf, *.bmp, *.tiff, *.wpg, *.fga., *.jpg *.gif, *.pcx. Other formats are to be consulted with the editors.

References

Should be listed in alphabetical and chronological order **according to annotation in the text** and consist of all references cited.

Standard form is as follows: 1. Family name and initials of author(s), 2. Publication year, 3. Title of paper, 4. Editor(s), 5. Title of proceedings, 6. Publishers or Publishing house and place of publishing, 7. Unpublished report – manuscript should be denoted MS. Unpublished paper can appear as personal communications only. 8. Page range

Quotations of papers published in non-Latin alphabet or in languages other than English, French, Italian, Spain or German ought to be translated into English with an indication of the original language in parentheses, e.g.: (in Slovak).

Example:

Andrusov, D., Bystrický, J. & Fusán, O., 1973: *Outline of the Structure of the West Carpathians*. Guide-book for geol. exc. of Xth Congr. CBGA. Bratislava: Geol. Úst. D. Štúra, 44 p.

Beránek, B., Leško, B. & Mayerová, M., 1979: Interpretation of seismic measurements along the trans-Carpathian profile K III. In: Babuška, V. & Plančár, J. (Eds.): *Geodynamic investigations in Czechoslovakia*. Bratislava: VEDA, p. 201-205.

Lucido, O., 1993: A new theory of the Earth's continental crust: The colloidal origin. *Geol. Carpathica*, vol. 44, no. 2, p. 67-74.

Pitoňák, P. & Spišiak, J., 1989: Mineralogy, petrology and geochemistry of the main rock types of the crystalline complex of the Nízke Tatry Mts. MS – Archiv GS SR, Bratislava, 232 p. (in Slovak).

Proofs

The translator as well as the author(s) are obliged to correct the errors which are due to typing and technical arrangements. The first proofs are sent to author(s) as well as to the translator. The second proof is provided only to the editorial office. It will be sent to authors upon request.

The proofs must be marked clearly and intelligibly, to avoid further errors and doubts. Common typographic symbols are to be used, the list and meaning of which will be provided by the editorial office. Each used symbol must also appear on the margin of the text, if possible on the same line where the error occurred. The deadlines and conditions for proof-reading shall be stated in the contract.

Final remarks

These instructions are obligatory to all authors. Exceptions may be permitted by the Editorial Board or the managing editor. Manuscripts not complying with these instructions shall be returned to the authors.

1. Editorial Board reserves the right to publish preferentially invited manuscript and to assemble thematic volumes.
2. Sessions of Editorial Board – four times a year and closing dates for individual volumes will be on every 31th day of March, June, September and December.
3. To refer to one Magazine please use the following abbreviations: *Slovak Geol. Mag.*, vol. xx, no. xx. Bratislava: D. Štúr. Publ. ISSN 1335-096X.

Contents

<i>Mikuš, T., Chovan, M., Pršek, J. and Šlepecký, T.:</i> Hydrothermal siderite – basemetals vein mineralization in the vicinity of Čavoj, Suchý Mts. _____	207
<i>Kollárová, V. and Ivan, P.:</i> Zoned clinopyroxenes from Miocene basanite, Banská Štiavnica – Kalvária (Central Slovakia): Indicators of complex magma evolution _____	217
<i>Hudáčková, N., Halásová, E., Fordinál, K., Sabol, M., Joniak, P. and Král, J.:</i> Biostratigraphy and radiometric dating in the Vienna Basin Neogene (Slovak part) _____	233
<i>Baráth, I., Hlavatý, I., Kováč, M. and Hudáčková, N.:</i> Depositional Systems of the Northern Vienna Basin _____	237
<i>Höck, G. D.:</i> Continental biostratigraphy and correlations of the Korneuburg Basin (Karpatian) and the Grund Beds / Molasse Basin (Early Badenian) _____	241
<i>Tempfer, P. M. and Höck, G. D.:</i> Indicators of terrestrial ecosystems in the Karpatian Korneuburg Basin and the Badenian Grund Beds _____	243
<i>Cicha, I. and Lízal, P.:</i> Stratigraphy of the Grund Fm., based on the Foraminifera _____	245
<i>Harzhauser, M.:</i> Distributional patterns and shifts of early Middle Miocene Gastropod Faunas in the Central Paratethys _____	247
<i>Hohenegger, J.:</i> A simple method of depth estimation based on presence/absence data using benthic foraminifera _____	249
<i>Petrová, P.:</i> Palaeoecological evaluation of the Karpatian sediments in the southern part of the Carpathian Foredeep using trend analysis _____	251
<i>Mandic, O., Harzhauser, M., Spezzaferri, S. and Zuschin, M.:</i> The palaeoenvironment of an early Middle Miocene Paratethys sequence in NE Austria with special emphasis on paleoecology of mollusks and foraminifera _____	253
<i>Stráník, Z.:</i> Lower Miocene of the Hustopeče Gate _____	255
<i>Švábenická, L.:</i> Middle Miocene nannofossils in the Carpathian Foredeep, Czech Republic (state-of-the-art) _____	257
<i>Coric, S., Hohenegger, J., Pervesler, P., Roetzel, R., Rögl, F., Scholger, R., Spezzaferri, S. and Stingl, K.:</i> Around the Early/Middle Miocene (Karpatian/Badenian) Boundary in the Austrian Neogene Basins. A Story of Gaps. _____	259
<i>Zuschin, M., Harzhauser, M. and Mandic, O.:</i> The molluscan composition of the tempestitic shell beds of the Grund Formation (Lower Badenian, Middle Miocene) in Lower Austria _____	261
<i>Hlavatý, I., Šály, B., Kováč, M. and Hudáčková, N.:</i> Paleogeography and sequence stratigraphy of the Northern Vienna Basin _____	263
<i>Kováč, M., Hohenegger, J., Pervesler, P. and Hudáčková, N.:</i> Neogene of the Vienna Basin and Alpine - Carpathian Foredeep _____	267
<i>Smirnov, A. and Chovan, M.:</i> Heavy Minerals in Alluvial Sediments of the Boca River (Nízke Tatry Mts., Slovakia) _____	269
<i>Dagounaki, C., Kassoli-Fournaraki, A., Tsirambides, A. and Sikalidis, C.:</i> The carbonate rocks of Kozani area (NW Greece) in regard to certain industrial applications _____	281
<i>Kangí, A.:</i> Thrust fault geometry of Southern Elburz Mountains in the Northern Iran _____	287